NASA CR-183453

Computer Sciences Corporation

CSC/TM-77/6236

EVALUATION OF EPHEMERIS REPRESENTATIONS FOR TRACKING AND DATA RELAY SATELLITE SYSTEM (TDRSS) SPACECRAFT

(NASA-CR-183453) EVALUATION OF EPHEMERIS REPRESENTATIONS FOR TRACKING AND DATA RELAY SATELLITE SYSTEM (TDRSS) SPACECRAFT (Computer Sciences Corp.) 66 p

N90-70266

Unclas

00/13 0253122

CSC

Prepared For

NATIONAL AERONAUTICS AND SPACE ADMINISTRATION

Goddard Space Flight Center

Greenbelt, Maryland

CONTRACT NAS 5-11999

Task Assignment 882

SEPTEMBER 1977

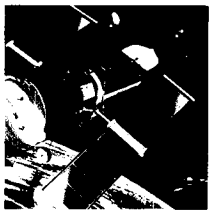

CSC/TM-77/6236

EVALUATION OF EPHEMERIS REPRESENTATIONS FOR TRACKING AND DATA RELAY SATELLITE SYSTEM (TDRSS) SPACECRAFT

Prepared for

GODDARD SPACE FLIGHT CENTER

By

COMPUTER SCIENCES CORPORATION

Under

Contract NAS 5-11999
Task Assignment 882

Prepared by:

Narendra Kumar 9/19/77
N. Kumar Date

Reviewed by:

Wayne D. McClain 9/19/77
W. McClain Date
Task Leader

Approved by:

Anne C. Long 9/19/77
A. Long Date
Section Manager

ABSTRACT

Several ephemeris representations for the Tracking and Data Relay Satellite System (TDRSS) are discussed in this document. Representations employing Hermite or Lagrange interpolation on mean equinoctial elements and a trigonometric series fit to Cartesian coordinates are compared with a high-precision ephemeris to estimate their accuracy. Estimates of onboard computer core and time requirements are also presented.

TABLE OF CONTENTS

Section 1 - Introduction 1-1

Section 2 - Evaluation of Mean Element Ephemeris Representations . . . 2-1

2.1 Summary of Algorithms 2-1
2.1.1 Lagrange Five-Point Interpolator 2-1
2.1.2 Hermite Two-Point Interpolator 2-2
2.1.3 Hermite Three-Point Interpolator 2-3
2.2 Interpolation Accuracy of Mean Element Representation . . . 2-4
2.2.1 Adams Sixth-Order Interpolation 2-4
2.2.2 Hermite and Lagrange Interpolation 2-7

Section 3 - Fourier Series Cartesian Coordinate Representation 3-1

Section 4 - Conclusions 4-1

4.1 Summary of Representation Accuracy Results 4-1
4.2 Comparison of OBC Time and Core Requirements 4-1

References

LIST OF ILLUSTRATIONS

Figure

2-1 Difference Between the High-Precision and Mean Element Representations of the Radial Component of Position Using a Sixth-Order Interpolator 2-9

2-2 Difference Between the High-Precision and Mean Element Representations of the Radial Component of Velocity Using a Sixth-Order Interpolator 2-10

2-3 Difference Between the High-Precision and Mean Element Representations of the Cross-Track Component of Position Using a Sixth-Order Interpolator 2-11

2-4 Difference Between the High-Precision and Mean Element Representations of the Cross-Track Component of Velocity Using a Sixth-Order Interpolator 2-12

2-5 Difference Between the High-Precision and Mean Element Representations of the Along-Track Component of Position Using a Sixth-Order Interpolator 2-13

2-6 Difference Between the High-Precision and Mean Element Representations of the Along-Track Component of Velocity Using a Sixth-Order Interpolator 2-14

2-7 Difference Between the High-Precision and Mean Element Representations of the Radial Component of Position Using a Two-Point Hermite Interpolator 2-15

2-8 Difference Between the High-Precision and Mean Element Representations of the Radial Component of Velocity Using a Two-Point Hermite Interpolator 2-16

2-9 Difference Between the High-Precision and Mean Element Representations of the Cross-Track Component of Position Using a Two-Point Hermite Interpolator 2-17

2-10 Difference Between the High-Precision and Mean Element Representations of the Cross-Track Component of Velocity Using a Two-Point Hermite Interpolator 2-18

2-11 Difference Between the High-Precision and Mean Element Representations of the Along-Track Component of Position Using a Two-Point Hermite Interpolator 2-19

2-12 Difference Between the High-Precision and Mean Element Representations of the Along-Track Component of Velocity Using a Two-Point Hermite Interpolator 2-20

2-13 Difference Between the High-Precision and Mean Element Representations of the Radial Component of Position Using A Three-Point Hermite Interpolator. 2-21

LIST OF ILLUSTRATIONS (continued)

Figure

2-14 Difference Between the High-Precision and Mean Element Representations of the Radial Component of Velocity Using A Three-Point Hermite Interpolator 2-22

2-15 Difference Between the High-Precision and Mean Element Representations of the Cross-Track Component of Position Using a Three-Point Hermite Interpolator. 2-23

2-16 Difference Between the High-Precision and Mean Element Representations of the Cross-Track Component of Velocity Using a Three-Point Hermite Interpolator. 2-24

2-17 Difference Between the High-Precision and Mean Element Representations of the Along-Track Component of Position Using a Three-Point Hermite Interpolator. 2-25

2-18 Difference Between the High-Precision and Mean Element Representations of the Along-Track of Velocity Using a Three-Point Hermite Interpolator. 2-26

2-19 Difference Between the High-Precision and Mean Element Representations of the Radial Component of Position Using A Five-Point Lagrange Interpolator. 2-27

2-20 Difference Between the High-Precision and Mean Element Representations of the Radial Component of Velocity Using A Five-Point Lagrange Interpolator 2-28

2-21 Difference Between the High-Precision and Mean Element Representations of the Cross-Track Component of Position Using a Five-Point Lagrange Interpolator. 2-29

2-22 Difference Between the High-Precision and Mean Element Representations of the Cross-Track Component of Velocity Using a Five-Point Lagrange Interpolator. 2-30

2-23 Difference Between the High-Precision and Mean Element Representations of the Along-Track Component of Velocity Using a Five-Point Lagrange Interpolator. 2-31

2-24 Difference Between the High-Precision and Mean Element Representations of the Along-Track Component of Position Using a Five-Point Lagrange Interpolator. 2-32

3-1 Difference Between the High-Precision and Cartesian/ Fourier Representations of the Radial Component of Position Using a 50-Minute Grid Spacing 3-4

3-2 Difference Between the High-Precision and Cartesian/ Fourier Representations of the Radial Component of Velocity Using a 50-Minute Grid Spacing 3-5

LIST OF ILLUSTRATIONS (continued)

Figure

3-3 Difference Between the High-Precision and Cartesian/ Fourier Representations of the Cross-Track Component of Position Using a 50-Minute Grid Spacing 3-6

3-4 Difference Between the High-Precision and Cartesian/ Fourier Representations of the Cross-Track Component of Velocity Using a 50-Minute Grid Spacing 3-7

3-5 Difference Between the High-Precision and Cartesian/ Fourier Representations of the Along-Track Component of Position Using a 50-Minute Grid Spacing 3-8

3-6 Difference Between the High-Precision and Cartesian/ Fourier Representations of the Along-Track Component of Velocity Using a 50-Minute Grid Spacing 3-9

3-7 Difference Between the High-Precision and Cartesian/ Fourier Representations of the Radial Component of Position Using a 100-Minute Grid Spacing 3-10

3-8 Difference Between the High-Precision and Cartesian/ Fourier Representations of the Radial Component of Velocity Using a 100-Minute Grid Spacing 3-11

3-9 Difference Between the High-Precision and Cartesian/ Fourier Representations of the Cross-Track Component of Position Using a 100-Minute Grid Spacing. 3-12

3-10 Difference Between the High-Precision and Cartesian/ Fourier Representations of the Cross-Track Component of Velocity Using a 100-Minute Grid Spacing. 3-13

3-11 Difference Between the High-Precision and Cartesian/ Fourier Representations of the Along-Track Component of Position Using a 100-Minute Grid Spacing. 3-14

3-12 Difference Between the High-Precision and Cartesian/ Fourier Representations of the Along-Track Component of Velocity Using a 100-Minute Grid Spacing 3-15

3-13 Difference Between the High-Precision and Cartesian/ Fourier Representations of the Radial Component of Position Using a 150-Minute Grid Spacing 3-16

3-14 Difference Between the High-Precision and Cartesian/ Fourier Representations of the Radial Component of Velocity Using a 150-Minute Grid Spacing 3-17

3-15 Difference Between the High-Precision and Cartesian/ Fourier Representations of the Cross-Track Component of Position Using a 150-Minute Grid Spacing 3-18

LIST OF ILLUSTRATIONS (continued)

Figure

3-16 Difference Between the High-Precision and Cartesian/ Fourier Representations of the Cross-Track Component of Velocity Using a 150-Minute Grid Spacing 3-19

3-17 Difference Between the High-Precision and Cartesian/ Fourier Representations of the Along-Track Component of Position Using a 150-Minute Grid Spacing 3-20

3-18 Difference Between the High-Precision and Cartesian/ Fourier Representations of the Along-Track Component of Velocity Using a 150-Minute Grid Spacing 3-21

LIST OF TABLES

Table

2-1 State Vectors for the TDRSS 2-5

2-2 Summary of TDRSS Representation Accuracies 2-6

4-1 Comparison of Uplink Data Set Length and Onboard Computer (OBC) Timing Requirements 4-3

SECTION 1 - INTRODUCTION

This memorandum presents an evaluation of ephemeris representations for the Tracking and Data Relay Satellite System (TDRSS). The primary evaluation criteria are accuracy and computational cost. The algorithm selection was based on a preliminary evaluation, carried out by Desai and Long (Reference 1). This work was performed on the IBM System/360-95 computer.

The goal of this evaluation is to determine an optimal ephemeris representation for the geosynchronous TDRSS orbits. The representation is to be used by the Solar Maximum Mission (SMM) Onboard Computer (OBC) to compute the line-of-sight vector from SMM to a TDRSS satellite. This information is required for pointing the High Gain Antenna System (HGAS) at the TDRSS.

Section 2 of this document is devoted to an examination of the various mean element ephemeris representations. A description is given of the different interpolation algorithms which were used. The results are presented in tabular form. A graphical representation of these results obtained using the Goddard Trajectory Determination System (GTDS) Ephemeris Comparison (COMPARE) Program is also presented.

In Section 3, the trigonometric series Cartesian coordinate representation is examined. The results of this analysis are presented, along with plots from the GTDS COMPARE Program.

Section 4 is devoted to a comparison of the results obtained from the mean element and trigonometric series representations. Estimates of comparative OBC time and core requirements are also presented. A direct evaluation of a trigonometric series representation of the Cartesian coordinates for TDRSS is recommended for use on SMM.

SECTION 2 - EVALUATION OF MEAN ELEMENT EPHEMERIS REPRESENTATIONS

In view of the low precision requirements for TDRSS position accuracy (i.e., about 10 kilometers) for the SMM mission, a mean orbital element representation was investigated. The mean equinoctial elements and element rates required for this representation were obtained using the Goddard Trajectory Determination System (GTDS) variation of parameters (VOP) averaged orbit generator. The interpolation on mean elements was performed using the Lagrange and Hermite interpolation algorithms given below:

- Hermite two-point interpolator, using two sets of elements and element rates
- Hermite three-point interpolator, using three sets of elements and element rates
- Lagrange five-point interpolator, using five sets of elements

The grid spacings were chosen such that a minimum number of grid points spanned the entire 3-day comparison arc.

2.1 SUMMARY OF ALGORITHMS

This section presents a summary of the three interpolators used.

2.1.1 Lagrange Five-Point Interpolator

At each interpolation time, the following computations are made for each element:

$$E = e_1 \tag{2-1a}$$

$$D = \frac{(e_1 - 8e_2 + 8e_4 - e_5)}{12} \tag{2-1b}$$

$$C = \frac{(-e_1 + 16e_2 - 30e_3 + 16e_4 - e_5)}{24} \tag{2-1c}$$

$$B = \frac{(-e_1 + 2e_2 - 2e_4 + e_5)}{12} \tag{2-1d}$$

$$A = \frac{(e_1 - 4e_2 + 6e_3 - 4e_4 + e_5)}{24} \tag{2-1e}$$

where e_i denotes the value of a given element at the ith grid point.

At each interpolation point associated with time t, the quantity $p = (t - t_3)/g$ is computed, where g is the grid interval in time and t_3 is the time associated with the third grid point. Then the interpolated element is obtained as

$$e(t) = E + p\left\{D + p\left[C + p(B + pA)\right]\right\} \tag{2-2}$$

2.1.2 Hermite Two-Point Interpolator

The required expressions for this interpolator are the following:

$$D = e_1 \tag{2-3a}$$

$$C = g\dot{e}_1 \tag{2-3b}$$

$$B = 3(e_2 - e_1) - g(2\dot{e}_1 + \dot{e}_2) \tag{2-3c}$$

$$A = 2(e_1 - e_2) + g(\dot{e}_1 + \dot{e}_2) \tag{2-3d}$$

where $\dot{e}_i$ are the element rates of the grid points.

At each interpolation point, the quantity $p = (t-t_1)/g$ is computed. Then, the following expression is evaluated for each element:

$$e(t) = D + p\left[C + p(B + pA)\right] \tag{2-4}$$

2.1.3 Hermite Three-Point Interpolator

For this interpolator, the required expressions are:

$$F = e_2 \tag{2-5a}$$

$$E = g\dot{e}_2 \tag{2-5b}$$

$$D = e_1 - 2e_2 + e_3 + \frac{g(\dot{e}_1 - \dot{e}_2)}{4} \tag{2-5c}$$

$$C = 5(e_3 - e_1) - \frac{g(\dot{e}_1 + \dot{e}_3 + 2\dot{e}_2)}{4} \tag{2-5d}$$

$$B = -\frac{e_1}{2} + e_2 - \frac{e_3}{2} + \frac{g(\dot{e}_3 - \dot{e}_1)}{4} \tag{2-5e}$$

$$A = \frac{3(e_1 - e_3) + g(\dot{e}_1 + 4\dot{e}_2 + \dot{e}_3)}{4} \tag{2-5f}$$

At each interpolation point, the quantity $p = (t - t_2)/q$ is computed. Then, the following expression is evaluated for each element:

$$e(t) = F + p\left\{E + p\left[D + p\left(C + p(B + pA)\right)\right]\right\} \qquad (2\text{-}6)$$

2.2 INTERPOLATION ACCURACY OF MEAN ELEMENT REPRESENTATION

The accuracy of a TDRSS trajectory computed by interpolation on mean elements was evaluated by comparison with a 3-day, high-precision trajectory. The results from these comparisons are presented below.

2.2.1 Adams Sixth-Order Interpolation

Comparisons of trajectories were made at 20-minute intervals over a 3-day duration. These trajectories were generated independently using the averaged VOP orbit generator with various interpolators and the high-precision Cowell orbit generator. Solar radiation pressure, a 4 x 4 geopotential, and solar and lunar gravitational effects were included in the force model. The nominal state vector for the TDRSS mission is given in Table 2-1.

To isolate error contributions inherent in the mean element representation from interpolation errors, a mean element trajectory was generated using the standard GTDS Adams integrator/interpolator. This interpolator is compatible with the integrator, producing results consistent with the accuracy of the integrated trajectory. This mean trajectory was compared with the high-precision trajectory. The statistics from this comparison are given in Table 2-2. The root-mean-square (rms) position errors are 1.21 kilometers for the radial (H) component, 0.19 kilometers for the cross-track (C) component, and 0.62 kilometers for the along-track (L) component. The rms velocity errors are 0.307×10^{-4} kilometers/second, 0.122×10^{-4} kilometers/second, and 0.931×10^{-4} kilometers/second, respectively, for the radial, cross-track, and along-track components. The minimum and maximum position differences for the radial,

Table 2-1. State Vector for the TDRSS
TDRS East

Parameter	Value
Epoch	740228.
Semimajor axis (kilometers)	42163.79344
Eccentricity	0.25304×10^{-3}
Inclination (degrees)	2.0
Longitude of ascending node (degrees)	133.63074
Argument of perigee (degrees)	301.633
Mean anomaly (degrees)	351.633
Latitude (degrees)	1.8 South
Longitude (degrees)	91 West
Period (approximate) (minutes)	1440.00
Spacecraft area (kilometers^2)	0.3×10^{-4}
Spacecraft mass (kilograms)	1402.00

Table 2-2. Summary of TDRSS Representation Accuracies

Representation	Interpolator	Grid Spacing (min)	RMS Position Error				RMS Velocity Error				Maximum Position Error			
			H (km)	C (km)	L (km)	Total (km)	H (m/s)	C (m/s)	L (m/s)	Total (m/s)	H (km)	C (km)	L (km)	Total (km)
Mean element	6th order Adams	1440	1.2162	0.1906	0.6257	1.3809	0.03074	0.01225	0.09313	0.09883	1.7727	0.2810	1.3337	1.9090
Mean element	2-point Hermite	5760	1.2151	0.2284	0.6416	1.3929	0.03276	0.01040	0.09304	0.09919	1.7578	0.3596	1.3327	1.9086
Mean element	3-point Hermite	2880	1.2162	0.1906	0.6255	1.3808	0.03071	0.01225	0.09313	0.09883	1.7729	0.2808	1.3332	1.9086
Mean element	5-point Lagrange	1440	1.2163	0.1904	0.6249	1.3810	0.03075	0.01227	0.09313	0.09884	1.7730	0.2808	1.1333	1.9086
Cartesian/ Fourier (7 coefficients)	none	50	0.1407	0.1630	0.3392	0.4017	0.02103	0.01065	0.01761	0.02942	0.4158	0.4839	0.6281	0.6453
Cartesian/ Fourier (7 coefficients)	none	100	0.1407	0.1636	0.3395	0.4022	0.02108	0.01065	0.01757	0.02943	0.3892	0.4572	0.6300	0.6482
Cartesian/ Fourier (7 coefficients)	none	150	0.1401	0.1666	0.3406	0.4042	0.02083	0.01066	0.01794	0.02949	0.3749	0.5659	0.6306	0.6844

cross-track, and along-track components are 0.58 and 1.77 kilometers, 0.0037 and 0.28 kilometers, and 0.0031 and 1.33 kilometers, respectively.

2.2.2 Hermite and Lagrange Interpolation

TDRSS mean element trajectories were generated using Hermite and Lagrange interpolators on the integrated mean elements and rates. The interpolated results were compared with a high-precision ORB1 File at intervals of 20 minutes. The high-precision file, unless otherwise stated, was always generated by a Cowell-type orbit generator. The statistics from such comparisons are given in Table 2-2. These estimates are discussed below.

In the case of two-point Hermite interpolation, with a grid spacing of 4 days, the total representation errors (as shown in Table 2-2) are the following: (1) the rms position errors are 1.21 kilometers for the radial component, 0.23 kilometers for the cross-track component, and 0.64 kilometers for the along-track component; (2) the rms velocity errors are 0.33×10^{-4} kilometers/second for the radial component, 0.10×10^{-4} kilometers/second for the cross-track component, and 0.93×10^{-4} kilometers/second for the along-track component; and (3) the minimum and maximum position differences are 0.58 kilometers and 1.76 kilometers for the radial component, 0.0039 kilometers and 0.36 kilometers for the cross-track component, and 0.0045 kilometers and 1.33 kilometers for the along-track component.

For the three-point Hermite interpolation (with a grid spacing of 2 days) the total representation errors (as given in Table 2-2) are as follows: (1) the rms position errors are 1.22 kilometers for the radial component, 0.19 kilometers for the cross-track component, and 0.62 kilometers for the along-track component; (2) the rms velocity errors are 0.31×10^{-4} kilometers/second for the radial component, 0.12×10^{-4} kilometers/second for the cross-track component, and 0.93×10^{-4} kilometers/second for the along-track component; and (3) the minimum and maximum position differences are 0.58 and 1.77 kilometers for the radial component, 0.0040 and 0.28 kilometers

for the cross-track component, and 0.0038 and 1.33 kilometers for the along-track component.

The representation errors in the case of five-point Lagrange interpolation (with a 1-day grid spacing) are as follows: (1) the rms poosition errors are 1.22 kilometers for the radial component, 0.19 kilometers for the cross-track component, and 0.62 for the along-track component; (2) the rms velocity errors are 0.31×10^{-4} kilometers/second for the radial component, 0.12×10^{-4} kilometers/second for the cross-track component, and 0.93×10^{-4} kilometers/second for the along-track component; and (3) the minimum and maximum position differences are 0.58 and 1.77 kilometers for the radial component, 0.0033 and 0.28 kilometers for the cross-track component, and 0.0035 and 1.13 kilometers for the along-track component.

The differences between the high-precision and the interpolated mean element trajectories are plotted in Figures 2-1 through 2-24.

This evaluation of interpolation accuracy using a mean element representation indicates that all interpolators produced about the same results, with root-sum-square (rms) position errors of about 1.5 kilometers and maximum errors of 2.2 kilometers.

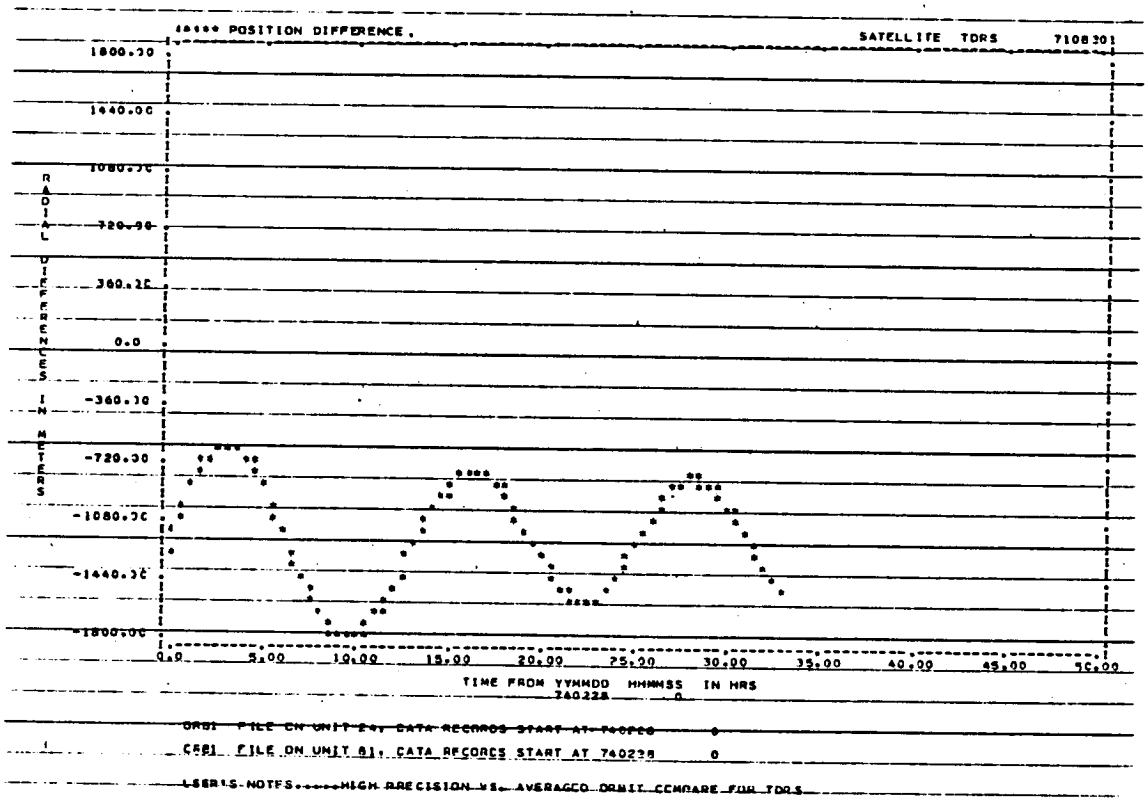

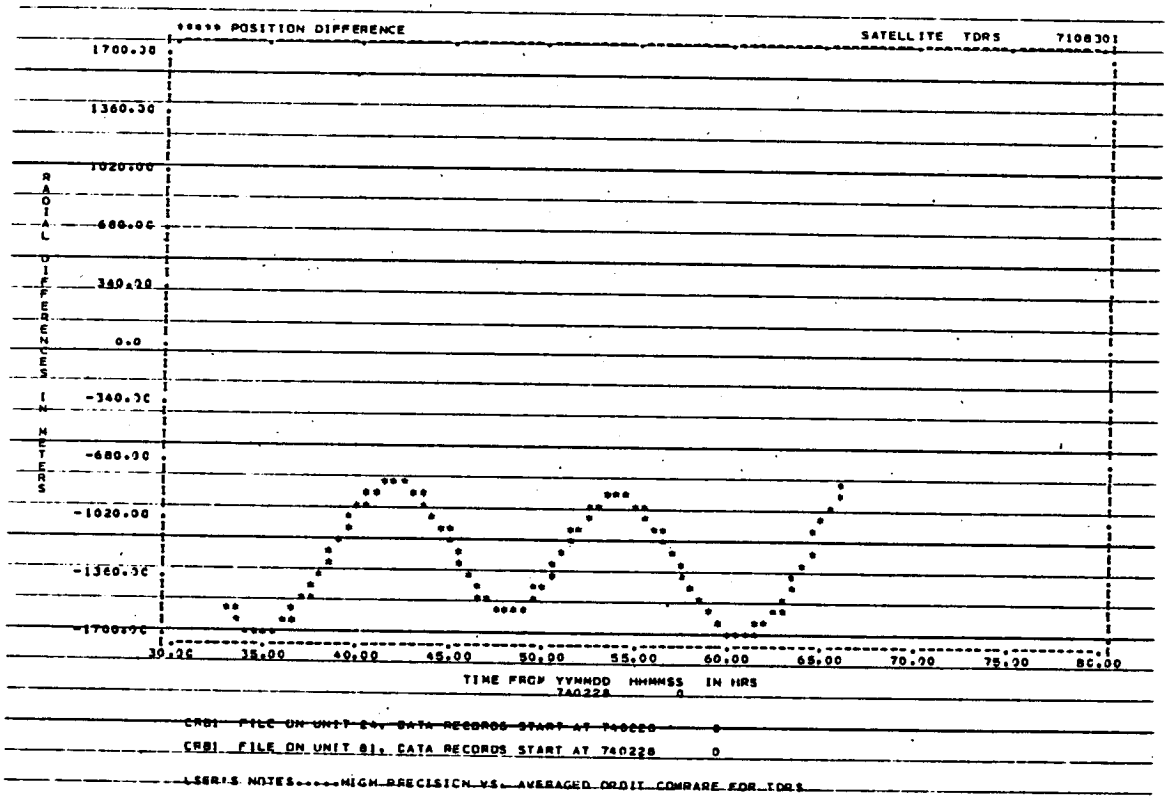

Figure 2-1. Difference Between the High-Precision and Mean Element Representations of the Radial Component of Position Using a Sixth-Order Interpolator

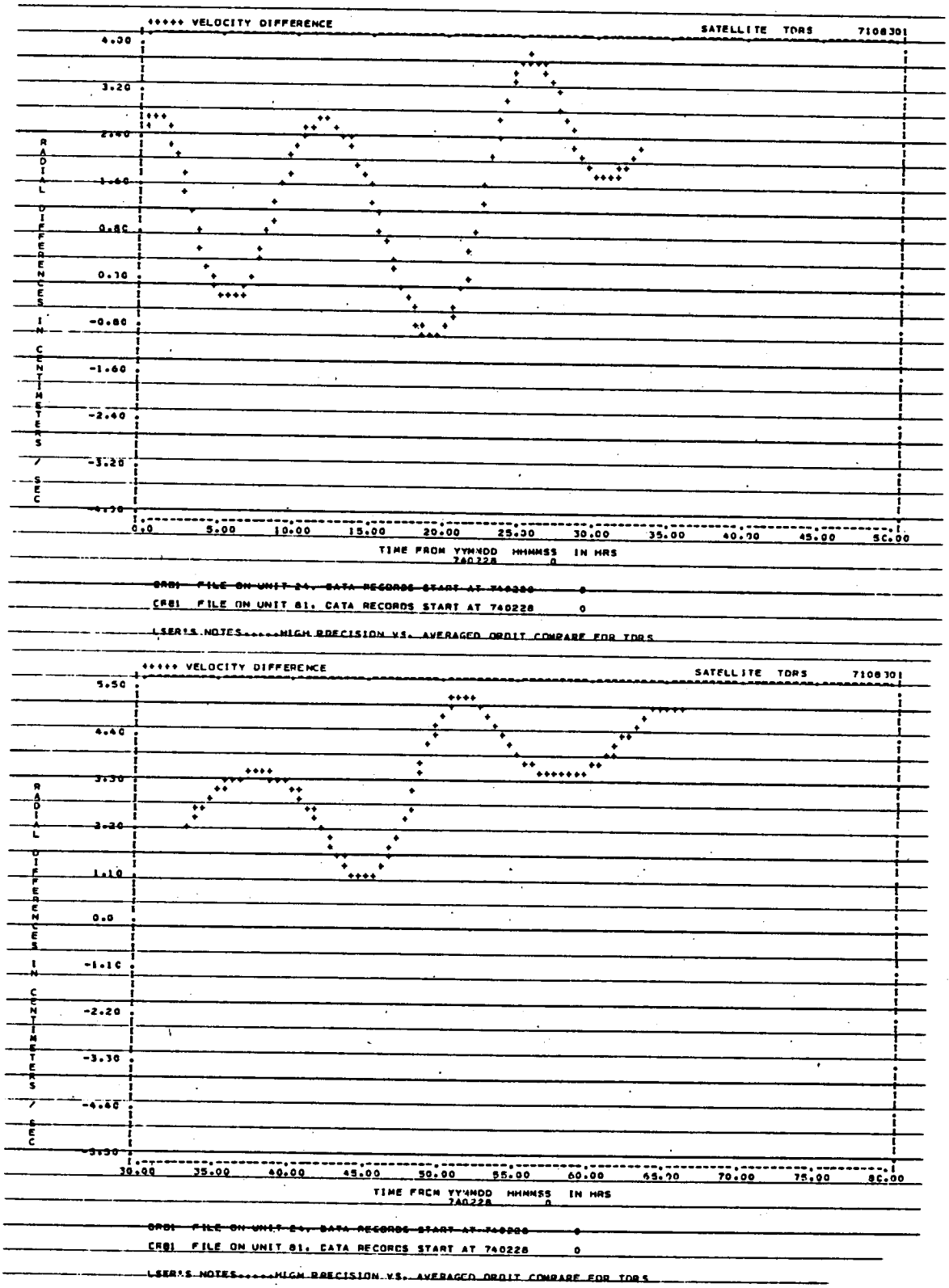

Figure 2-2. Difference Between the High-Precision and Mean Element Representations of the Radial Component of Velocity Using a Sixth-Order Interpolator

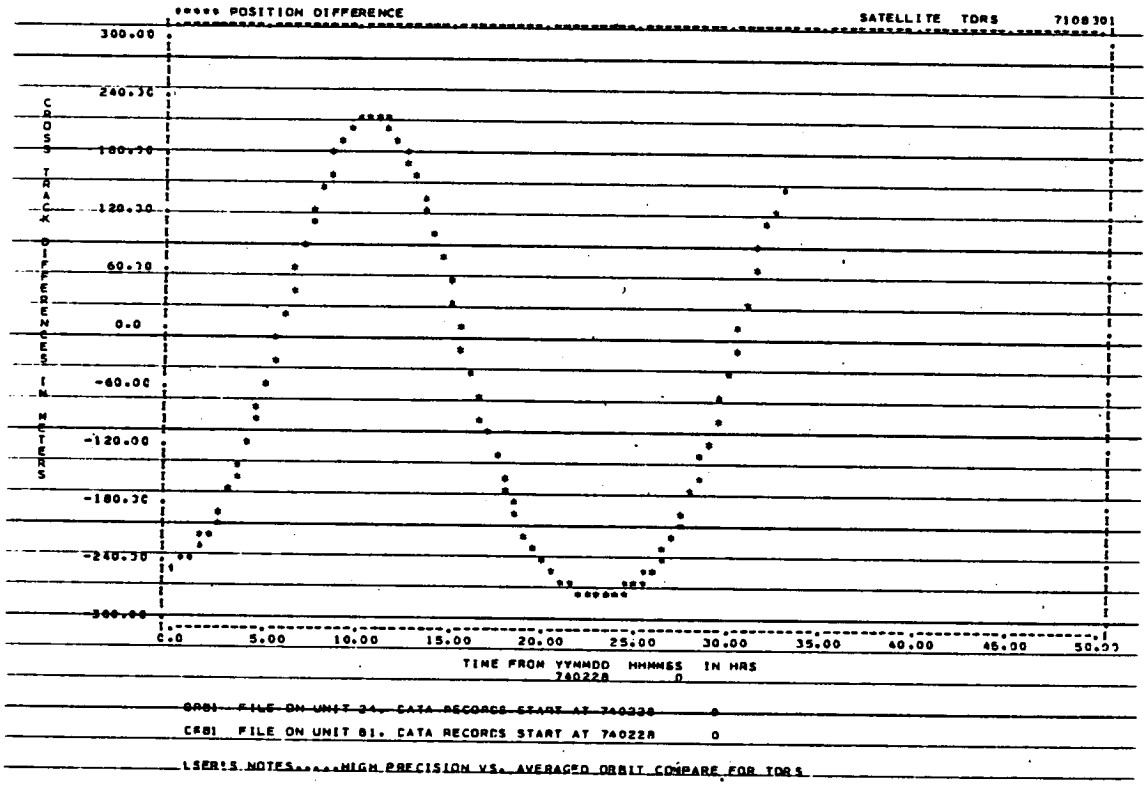

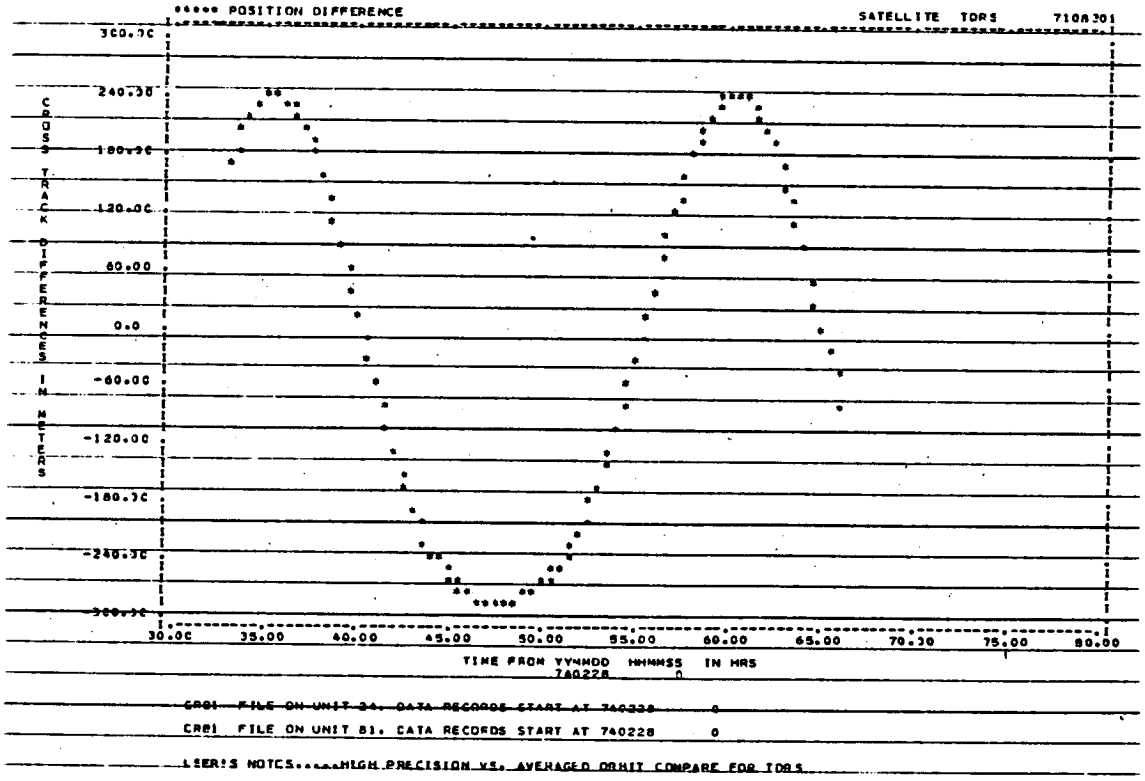

Figure 2-3. Difference Between the High-Precision and Mean Element Representations of the Cross-Track Component of Position Using a Sixth-Order Interpolator

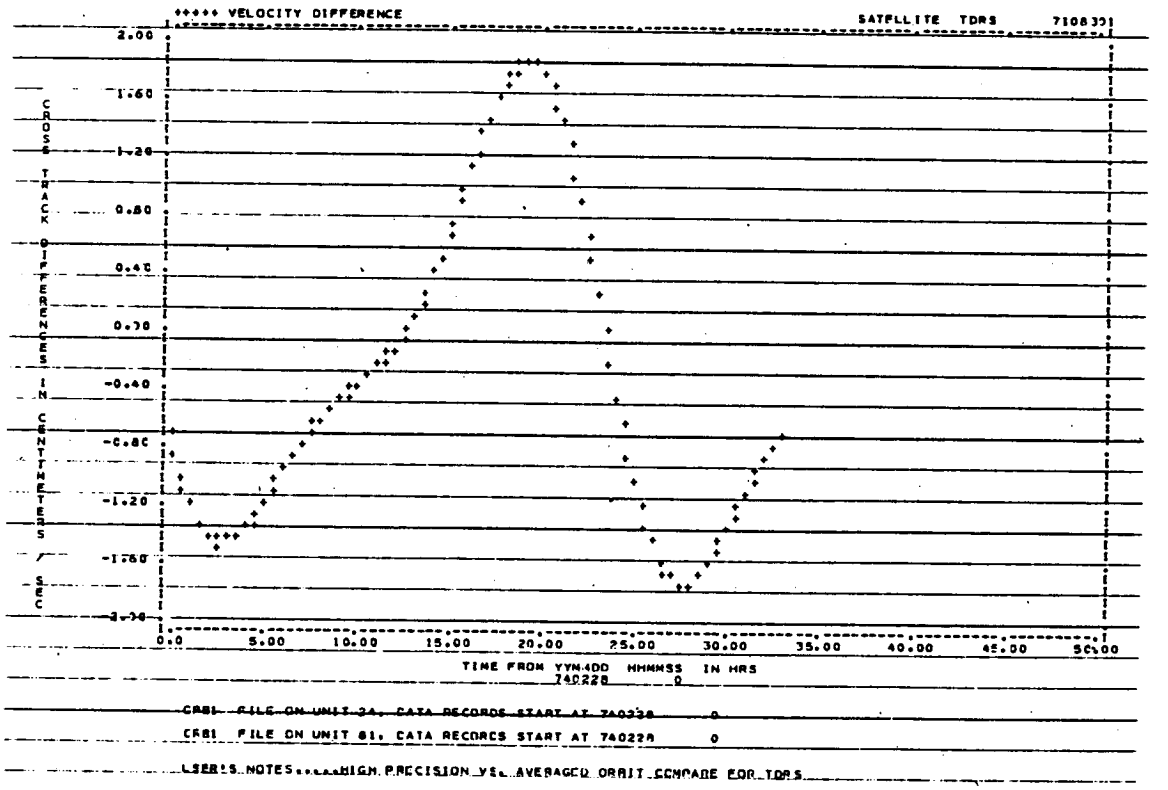

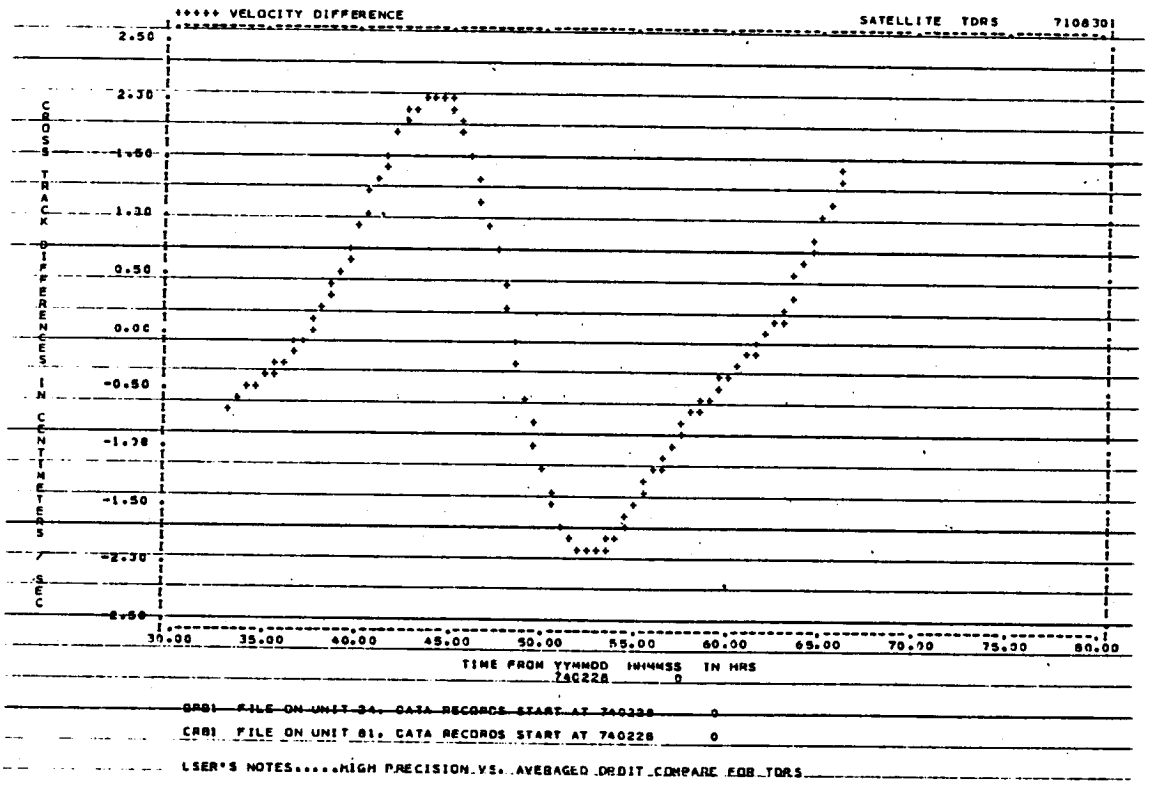

Figure 2-4. Difference Between the High-Precision and Mean Element Representations of the Cross-Track Component of Velocity Using a Sixth-Order Interpolator

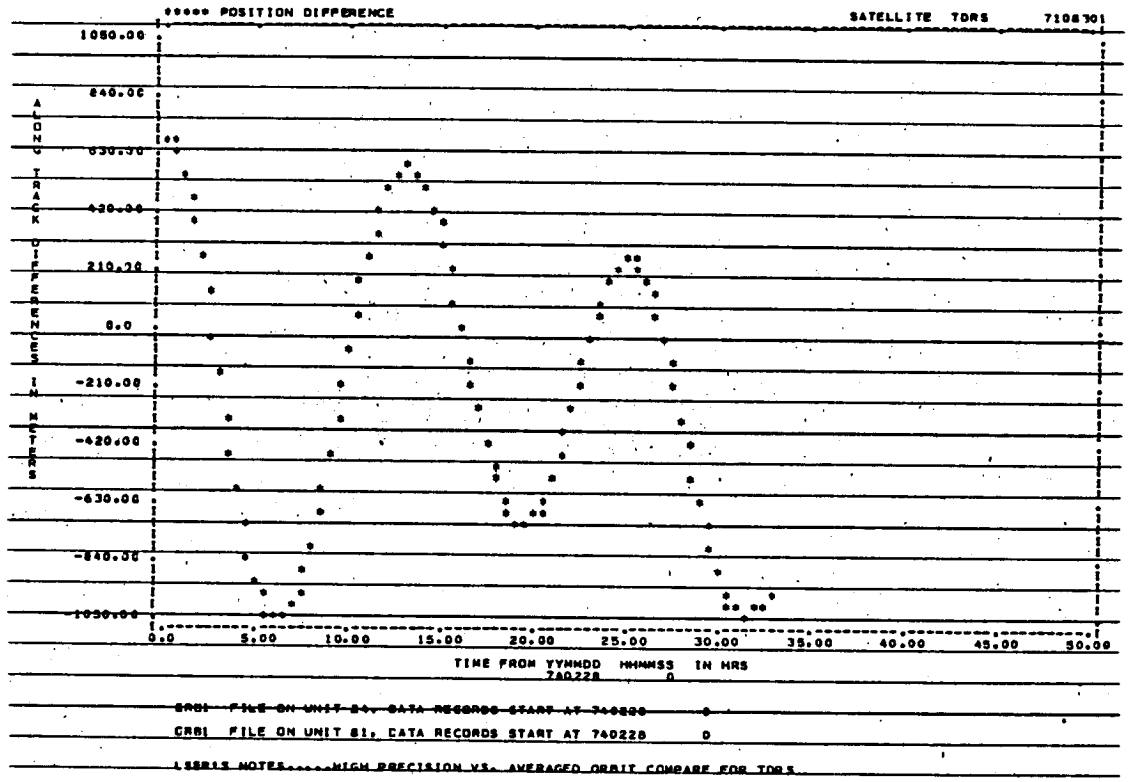

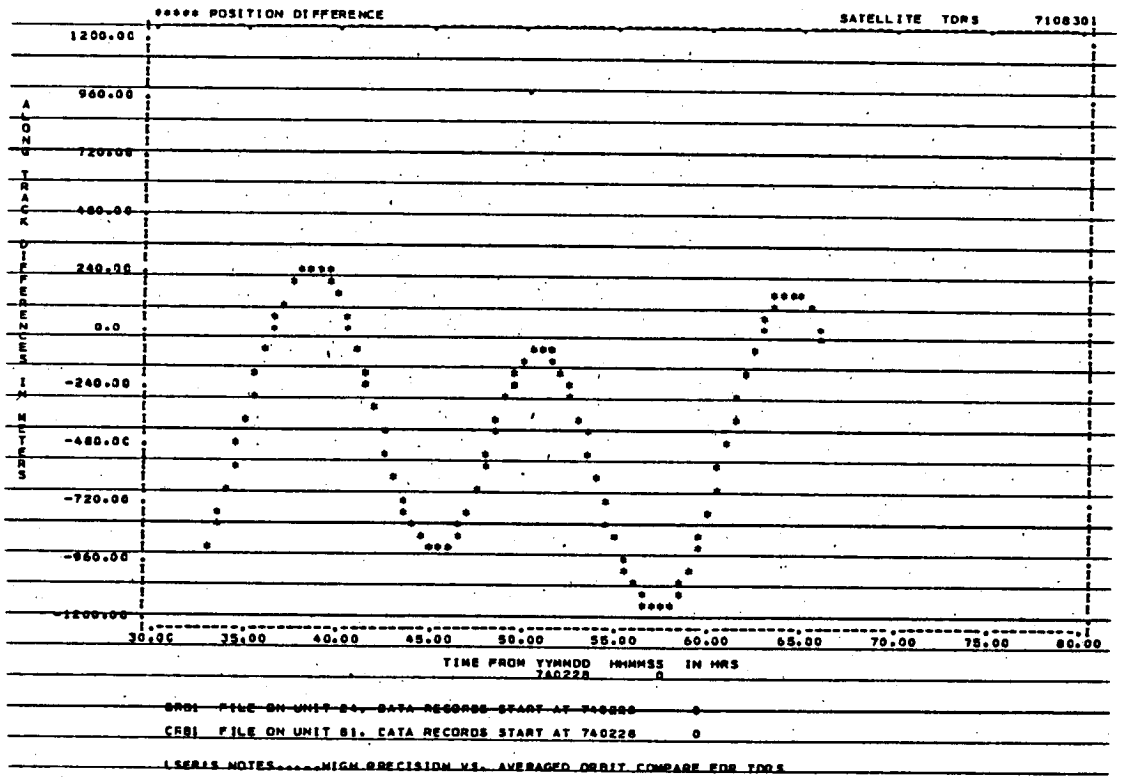

Figure 2-5. Difference Between the High-Precision and Mean Element Representations of the Along-Track Component of Position Using a Sixth-Order Interpolator

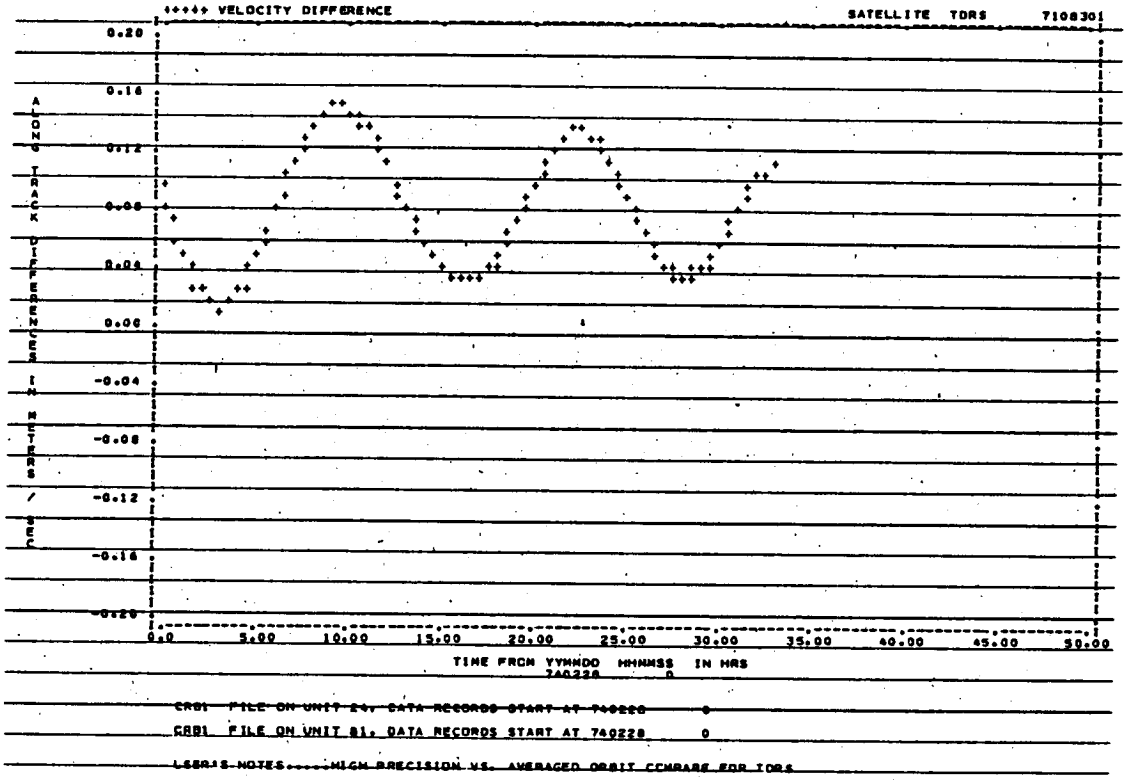

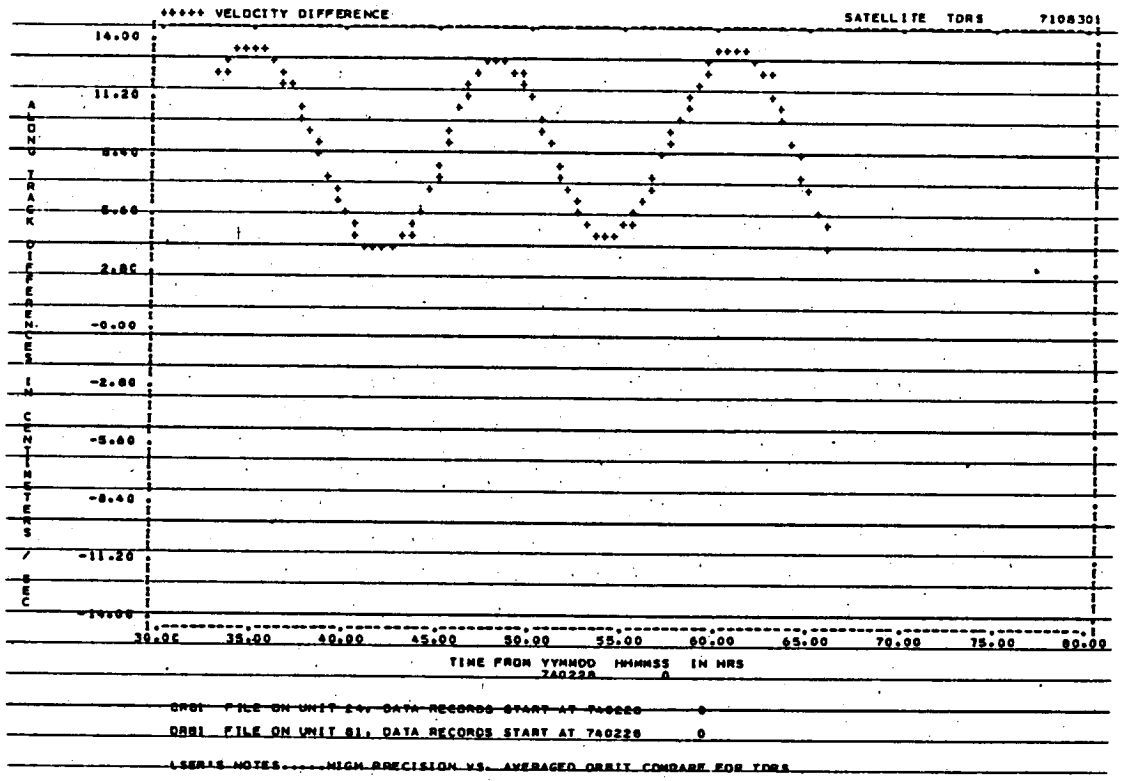

Figure 2-6. Difference Between the High-Precision and Mean Element Representations of the Along-Track Component of Velocity Using a Sixth-Order Interpolator

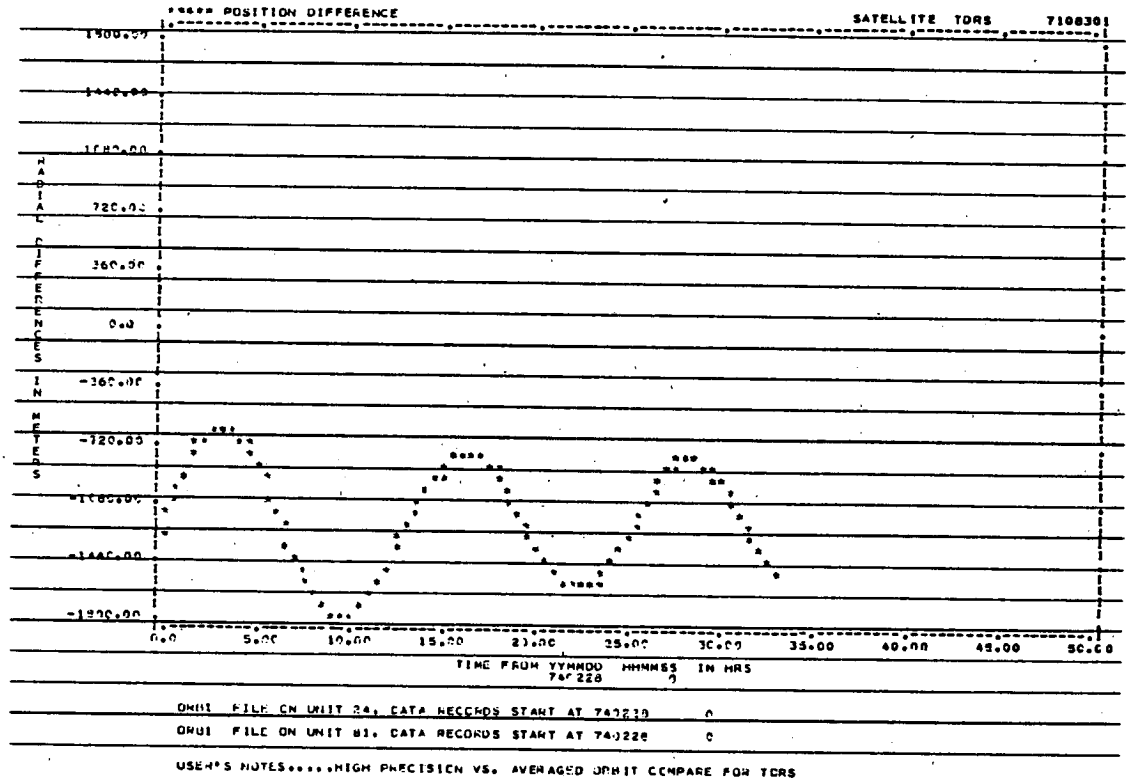

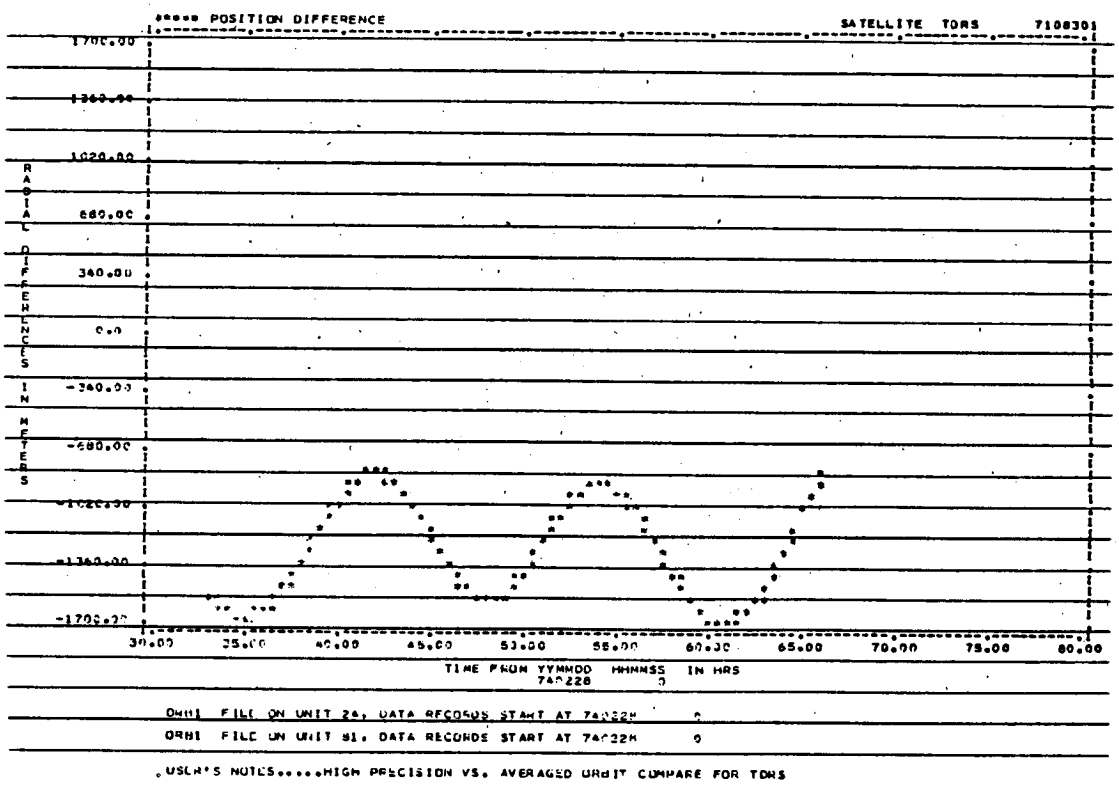

Figure 2-7. Difference Between the High-Precision and Mean Element Representations of the Radial Component of Position Using A Two-Point Hermite Interpolator

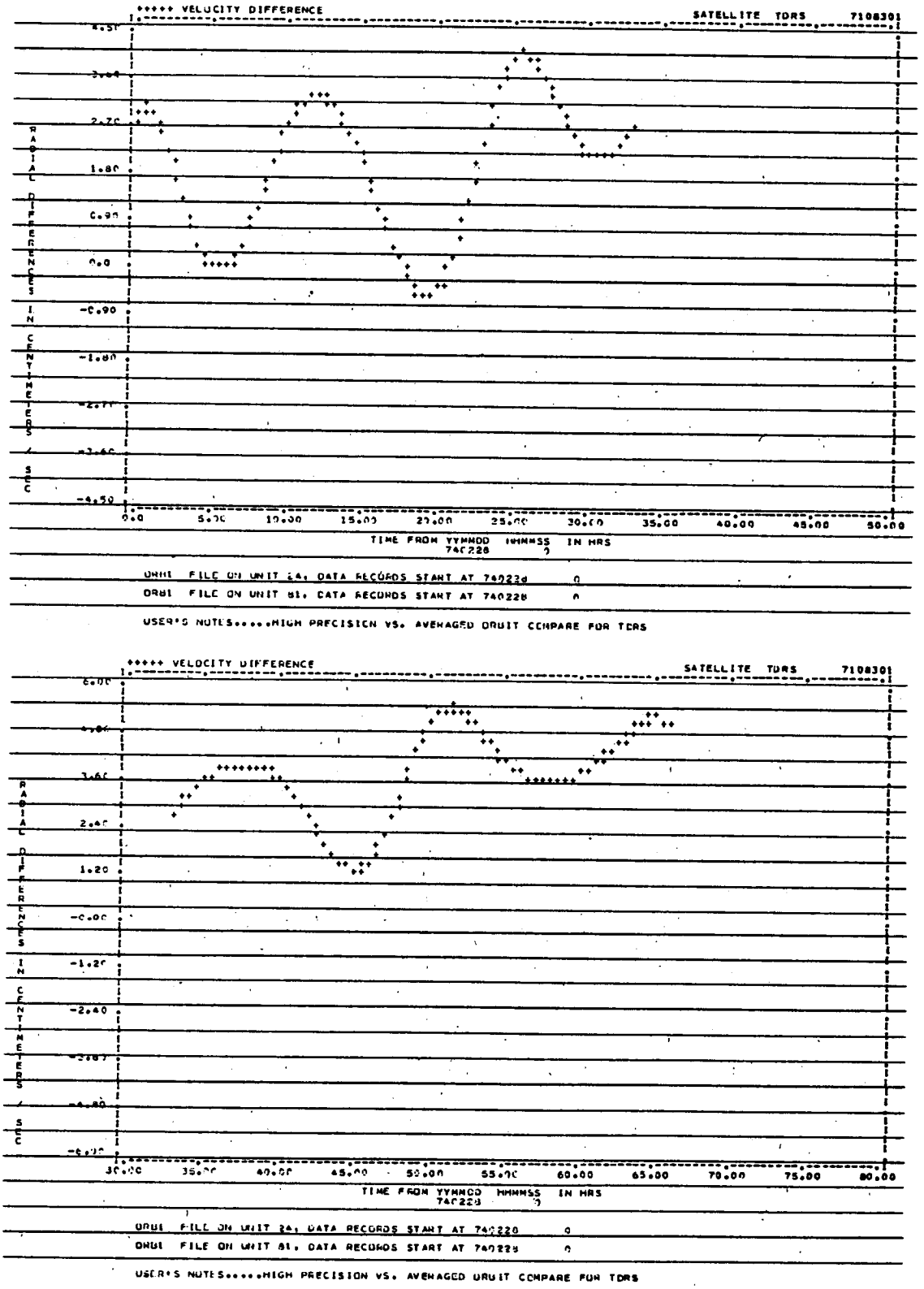

Figure 2-8. Difference Between the High-Precision and Mean Element Representations of the Radial Component of Velocity Using A Two-Point Hermite Interpolator

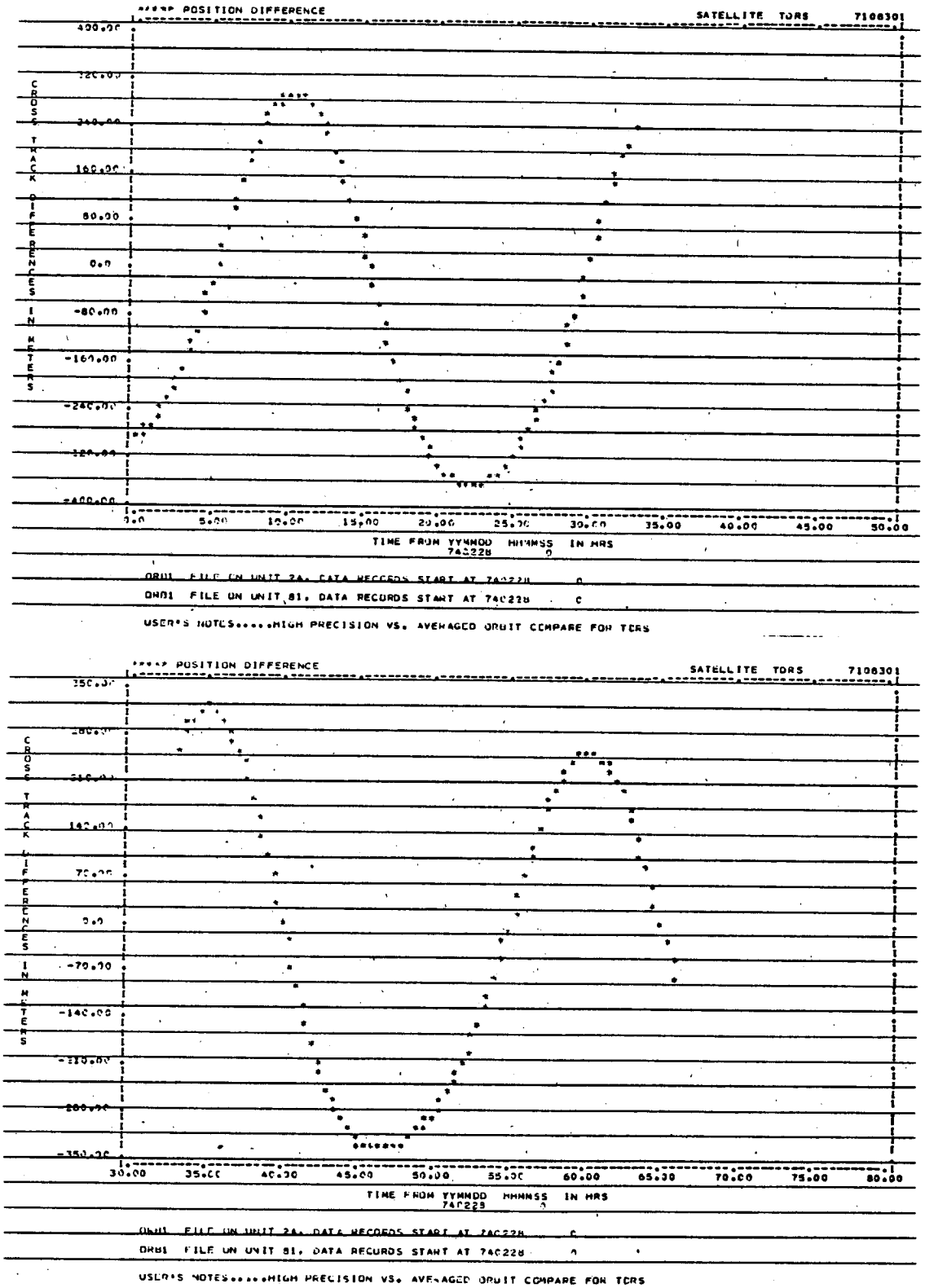

Figure 2-9. Difference Between the High-Precision and Mean Element Representations of the Cross-Track Component of Position Using a Two-Point Hermite Interpolator

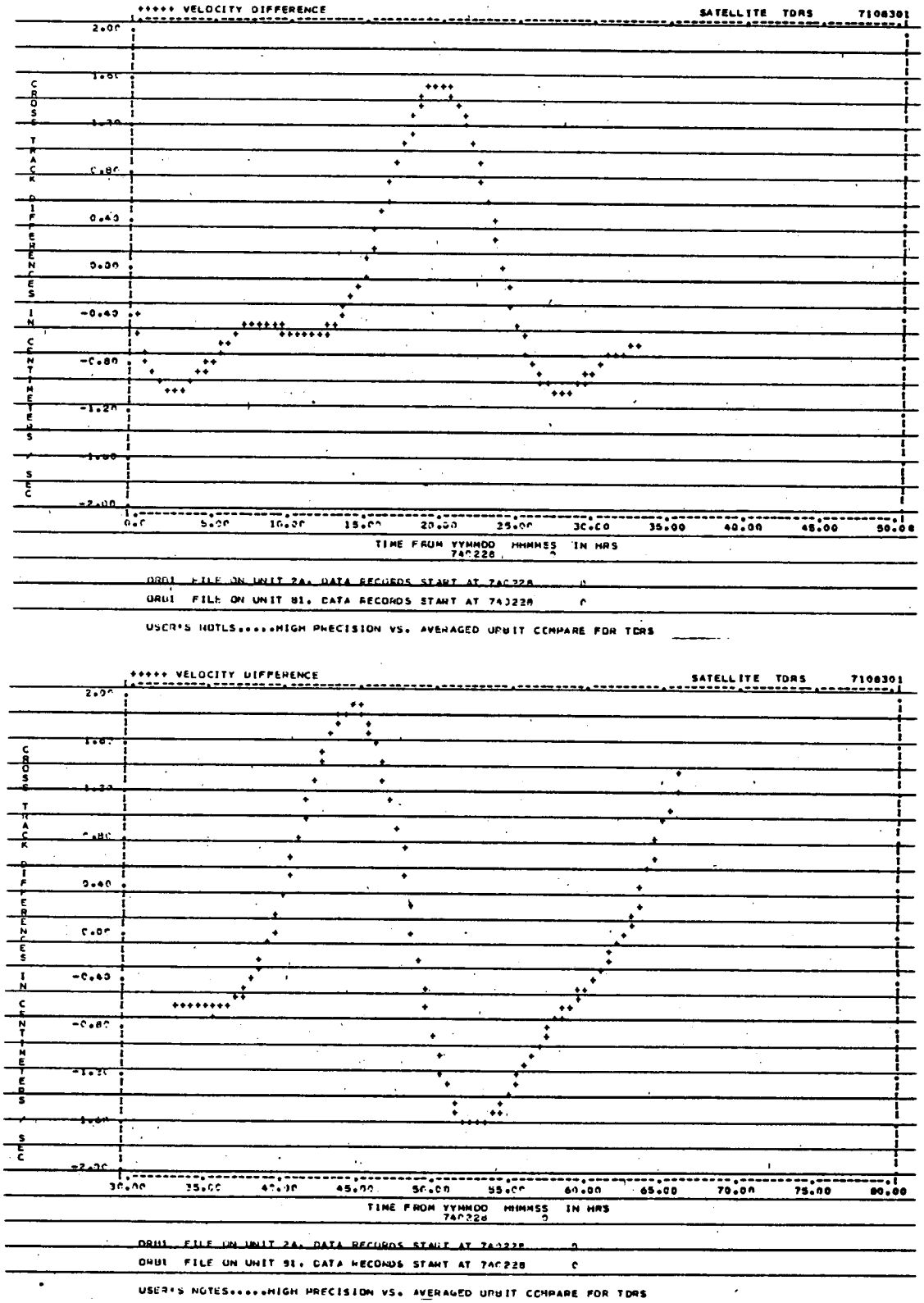

Figure 2-10. Difference Between the High-Precision and Mean Element Representations of the Cross-Track Component of Velocity Using a Two-Point Hermite Interpolator

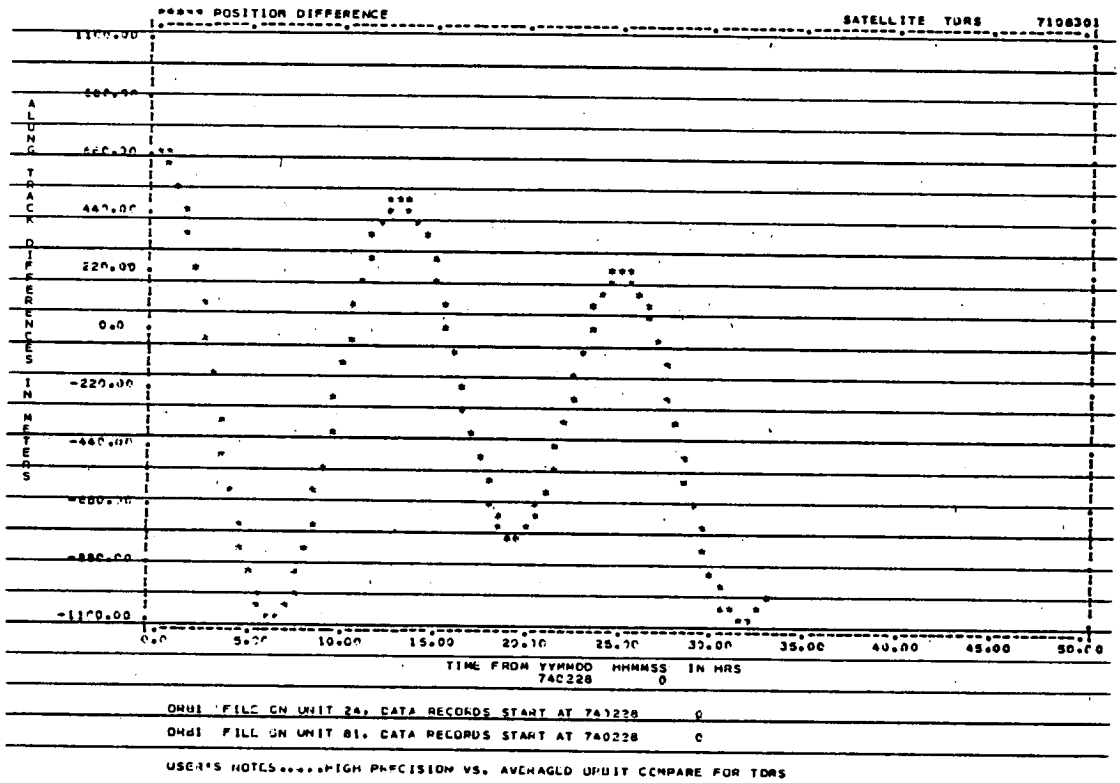

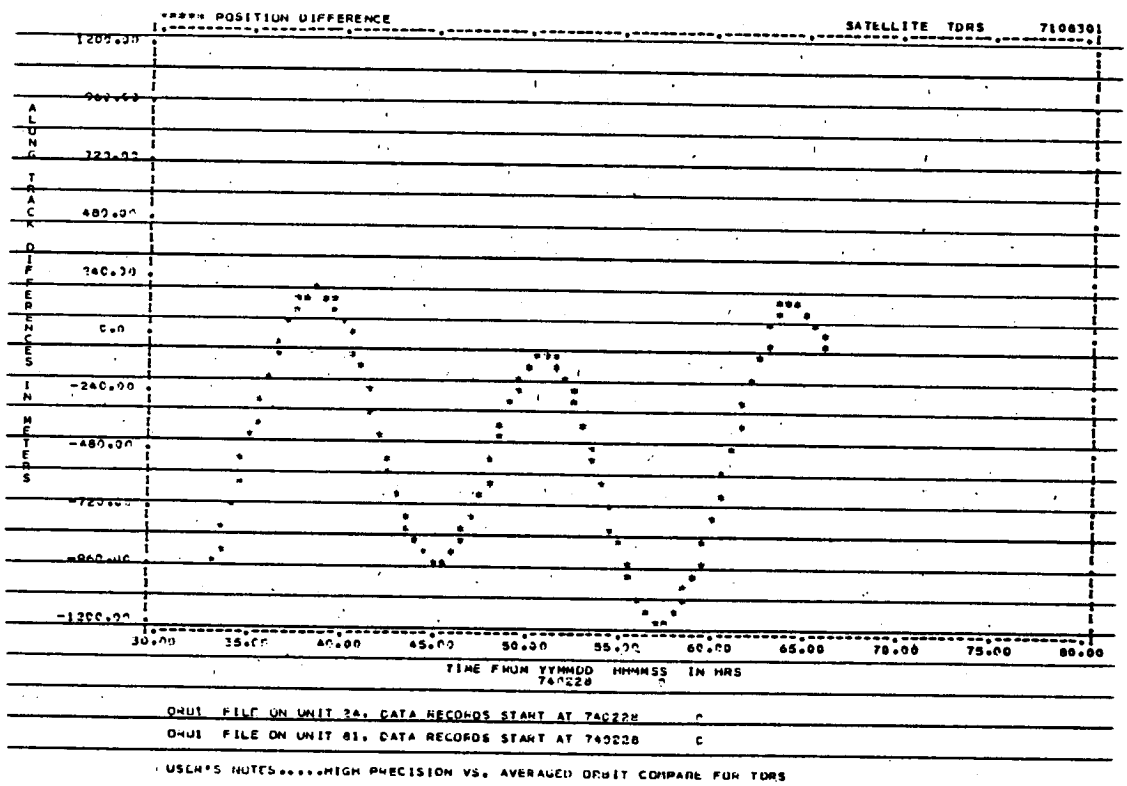

Figure 2-11. Difference Between the High-Precision and Mean Element Representations of the Along-Track Component of Position Using a Two-Point Hermite Interpolator

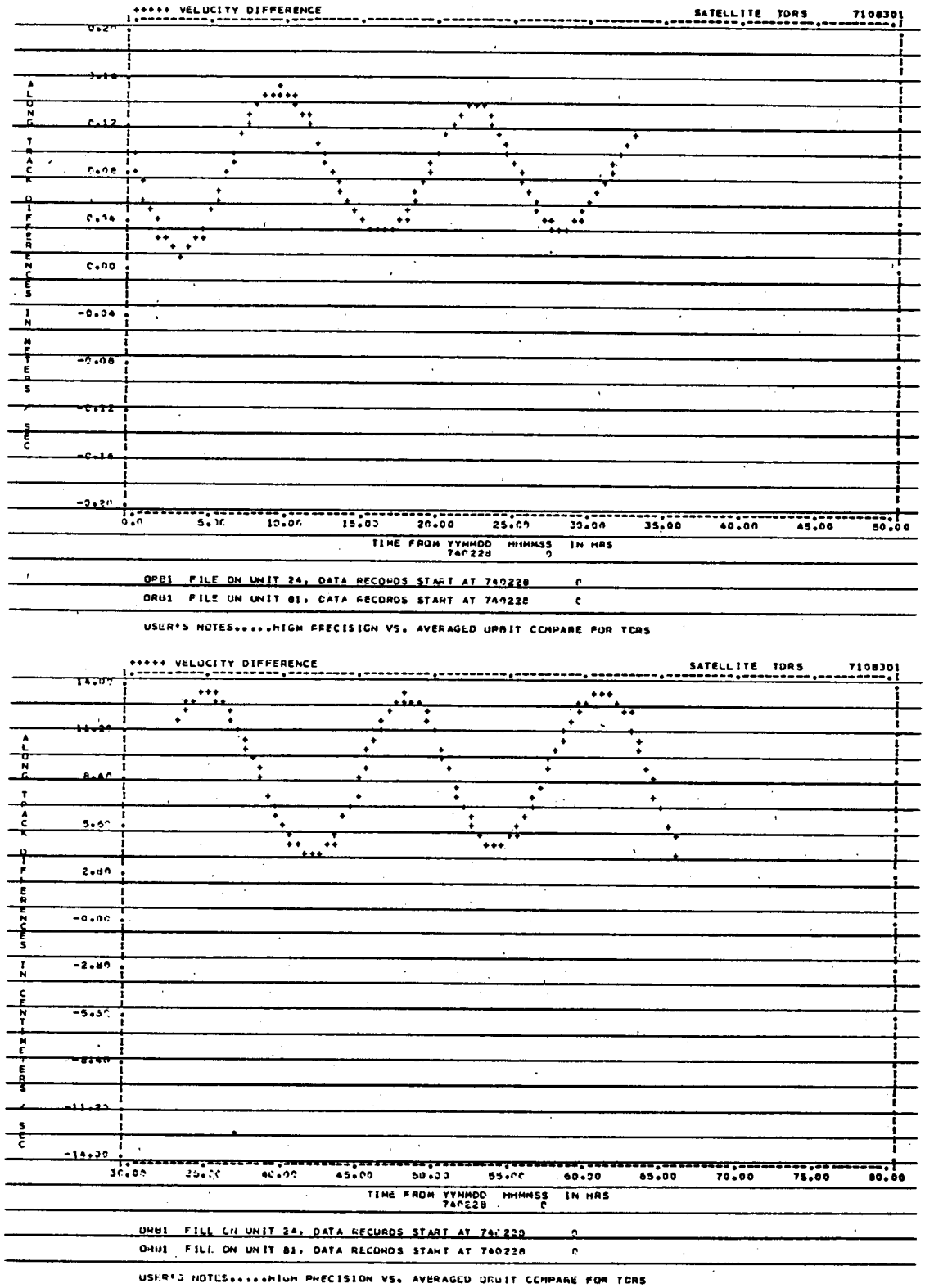

Figure 2-12. Difference Between the High-Precision and Mean Element Representations of the Along-Track Component of Velocity Using a Two-Point Hermite Interpolator

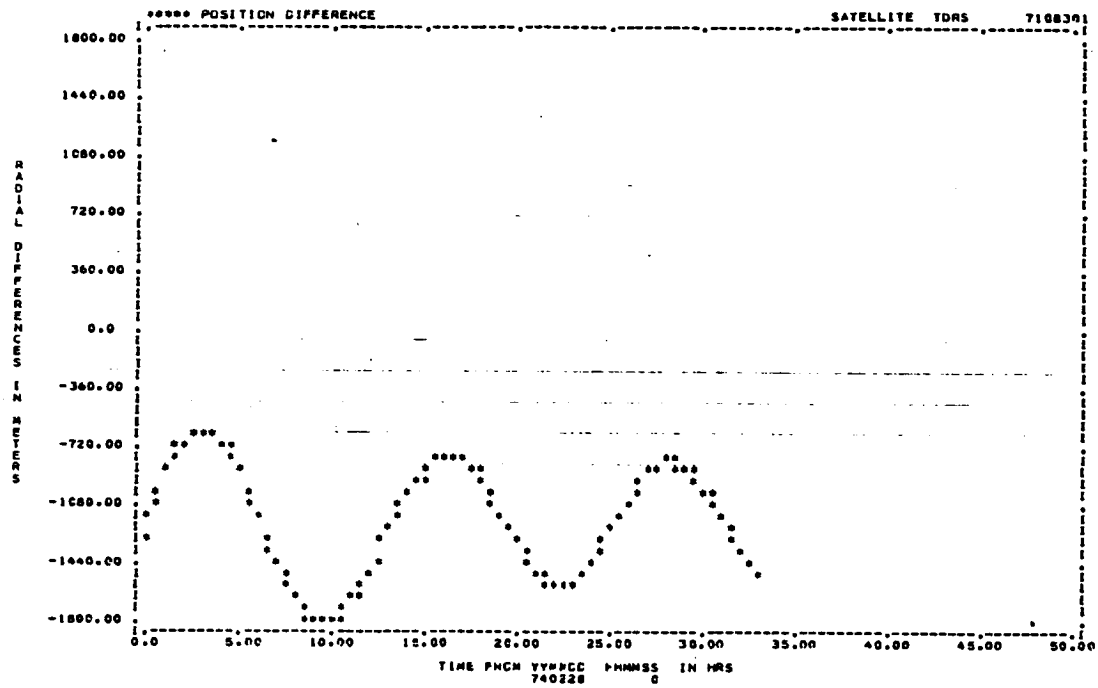

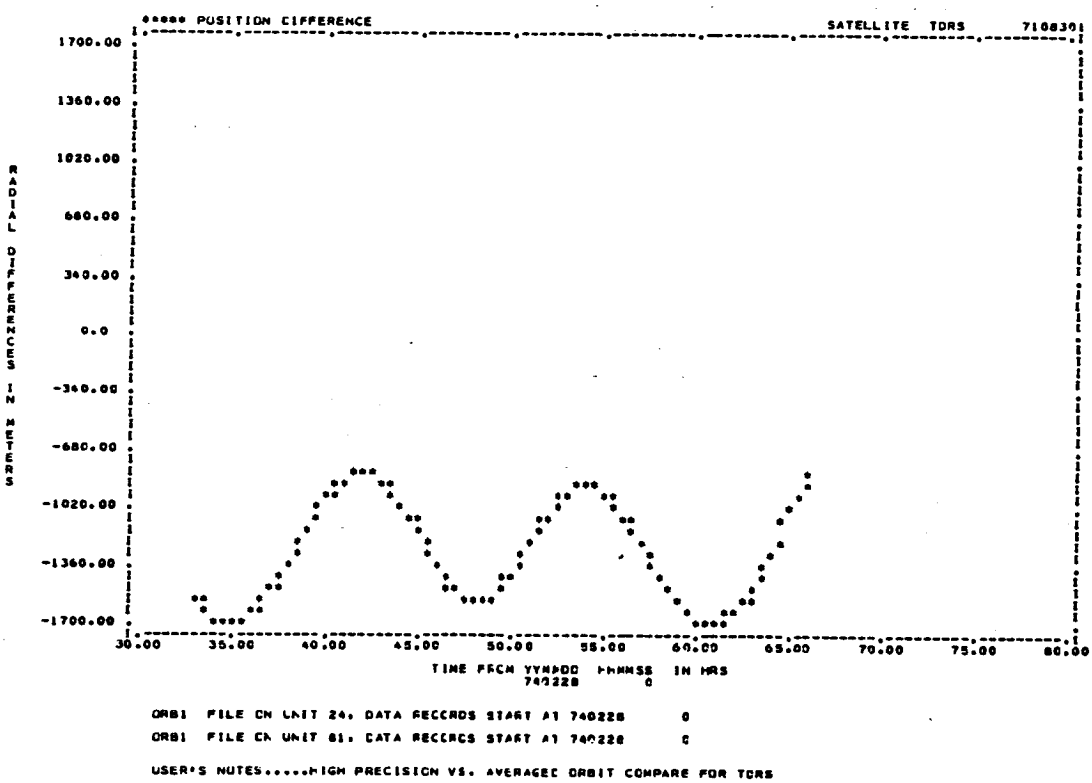

Figure 2-13. Difference Between the High-Precision and Mean Element Representations of the Radial Component of Position Using A Three-Point Hermite Interpolator

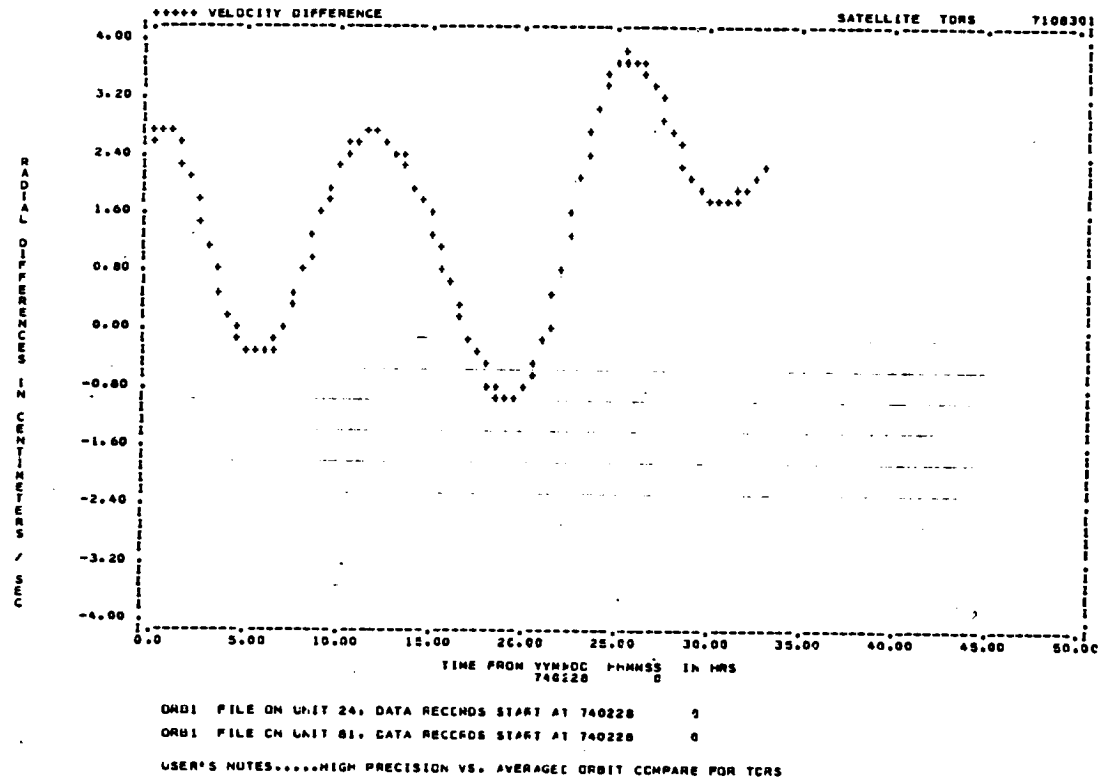

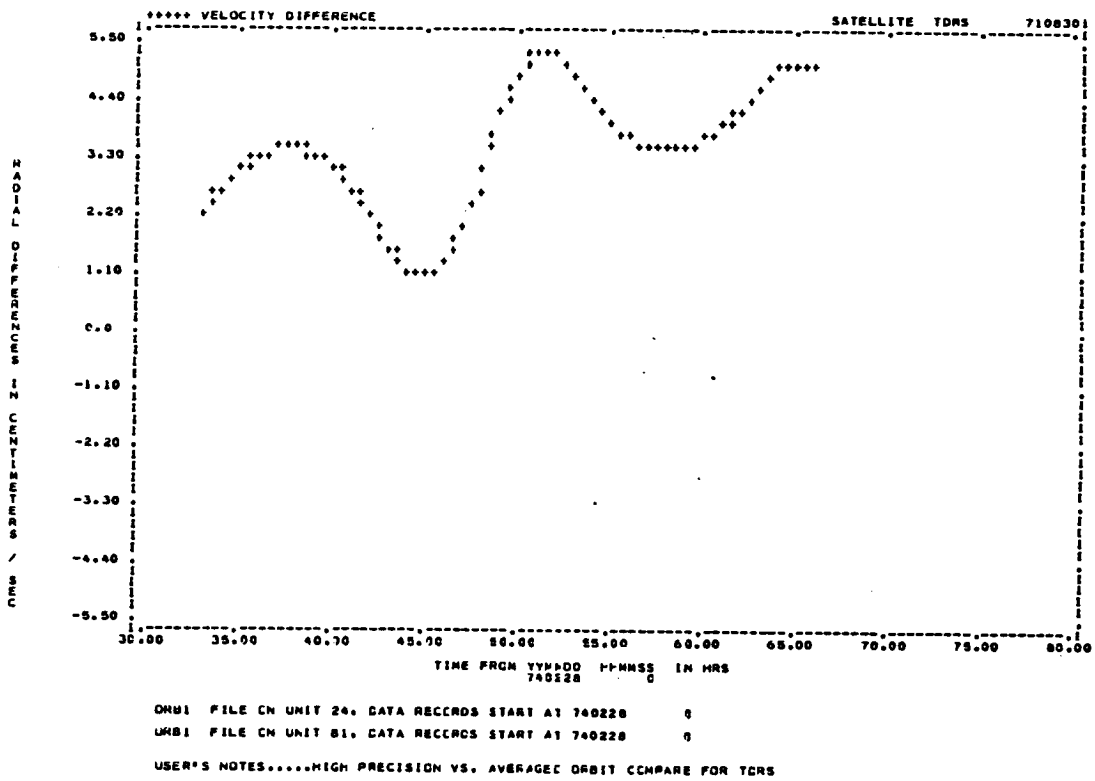

Figure 2-14. Difference Between the High-Precision and Mean Element Representations of the Radial Component of Velocity Using A Three-Point Hermite Interpolator

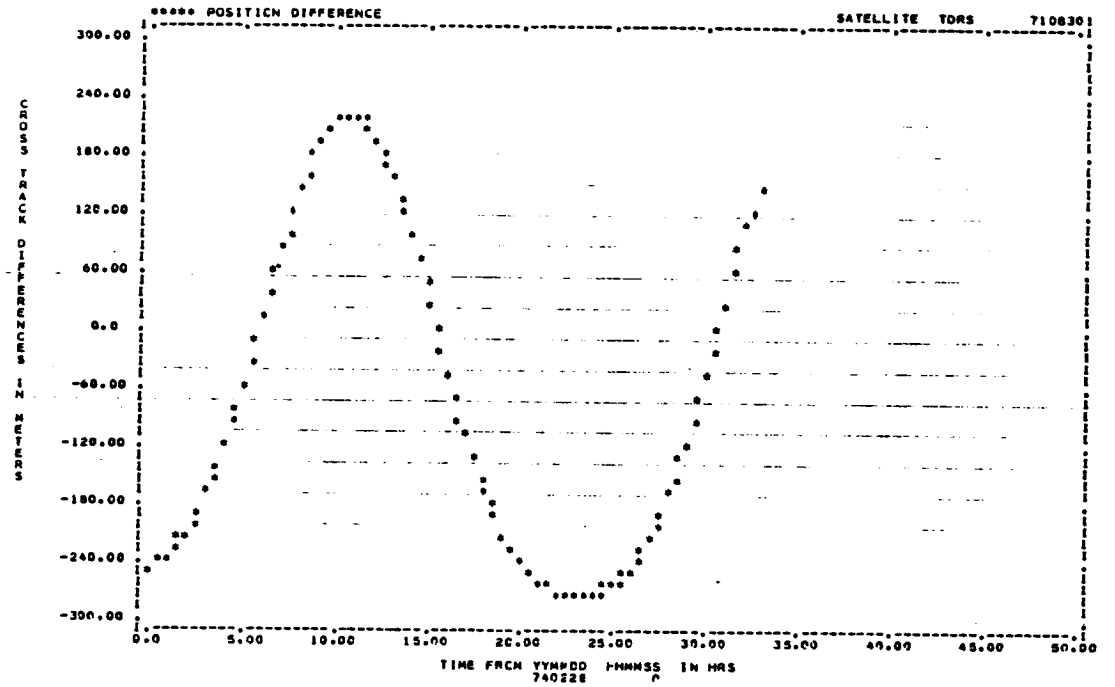

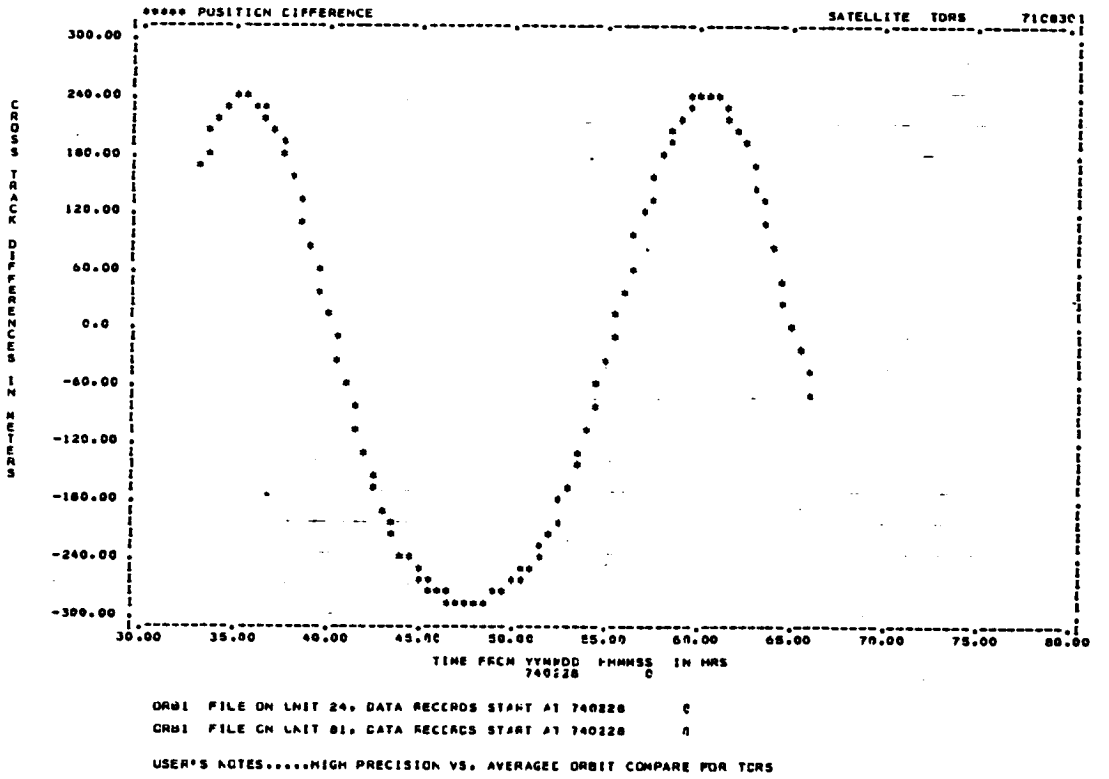

Figure 2-15. Difference Between the High-Precision and Mean Element Representations of the Cross-Track Component of Position Using a Three-Point Hermite Interpolator

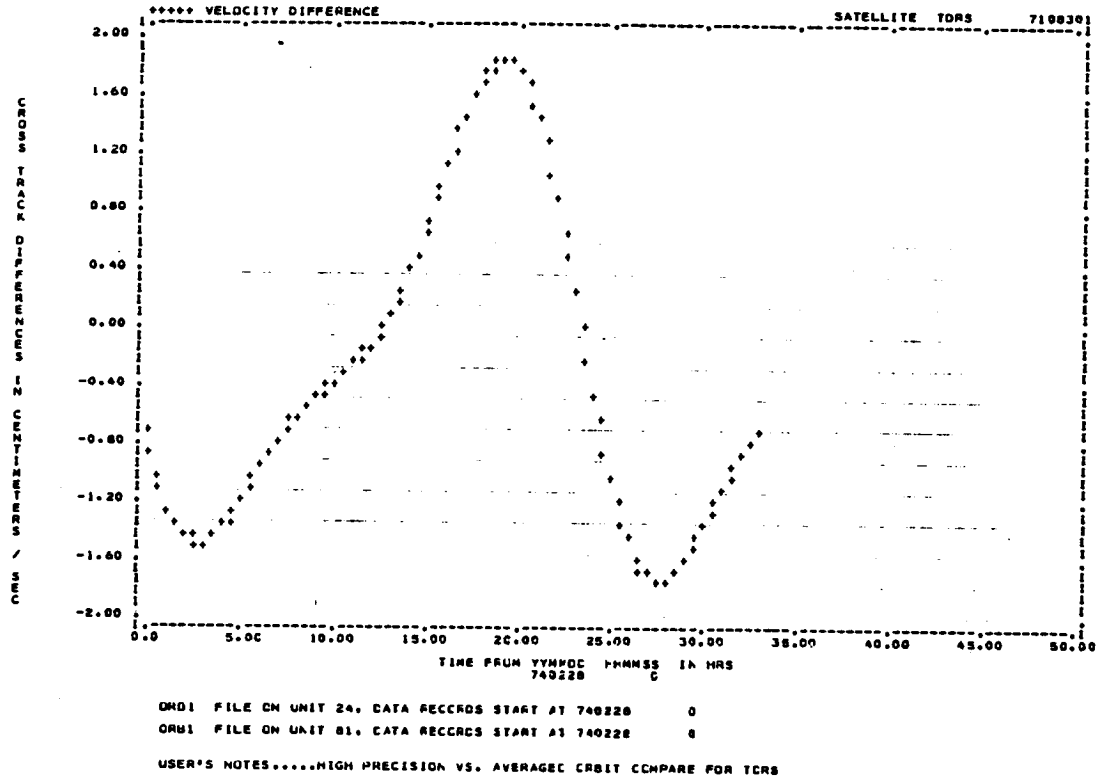

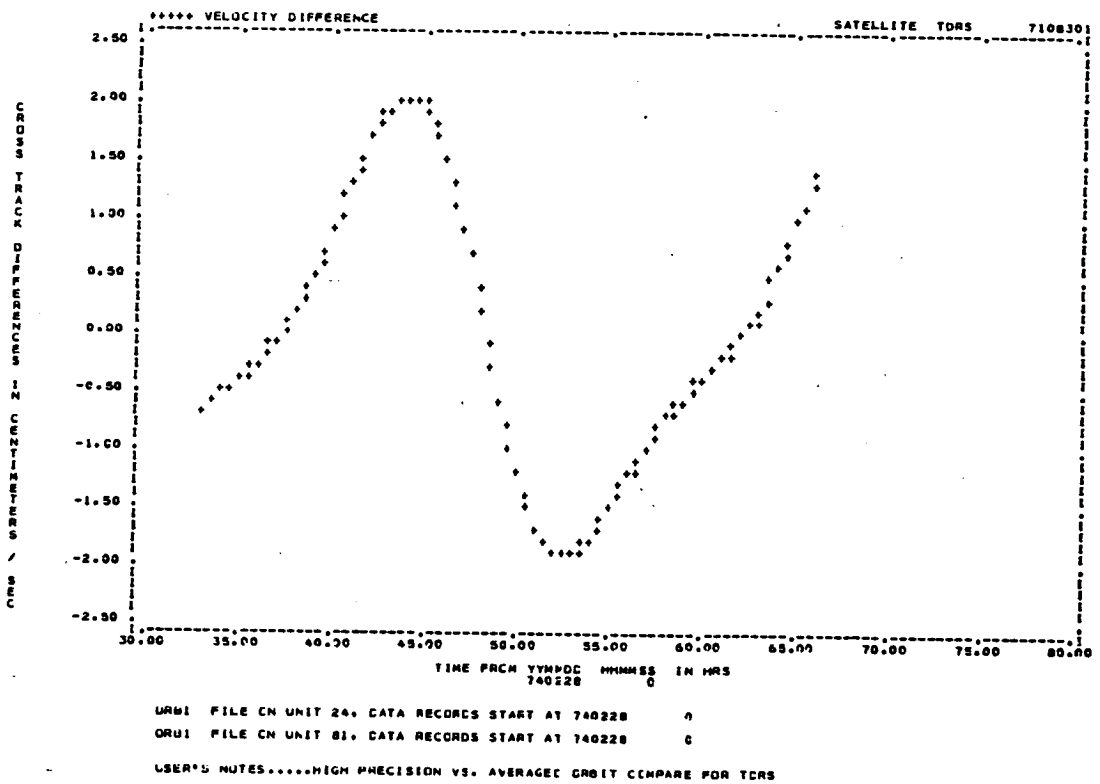

Figure 2-16. Difference Between the High-Precision and Mean Element Representations of the Cross-Track Component of Velocity Using a Three-Point Hermite Interpolator

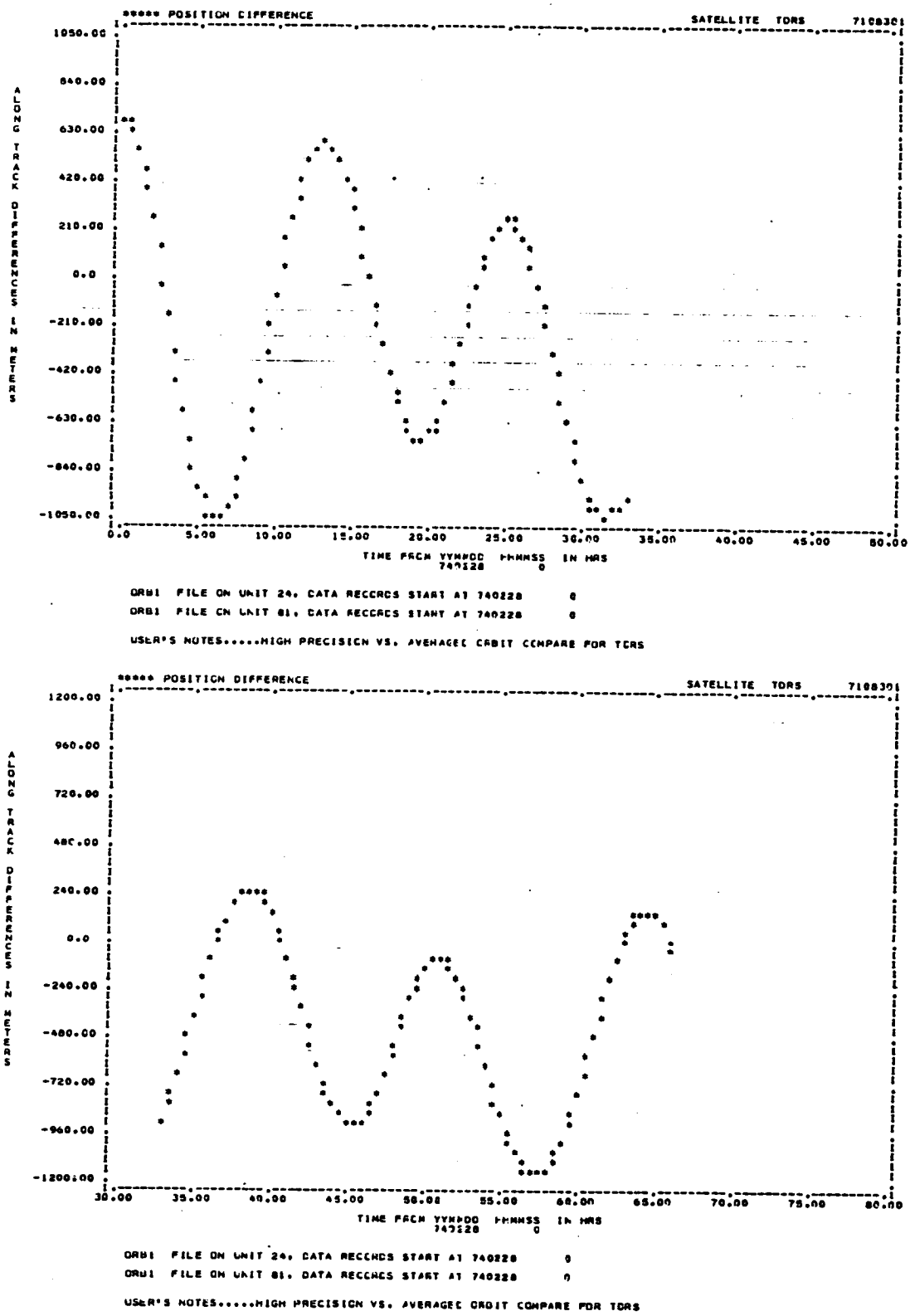

Figure 2-17. Difference Between the High-Precision and Mean Element Representations of the Along-Track Component of Position Using a Three-Point Hermite Interpolator

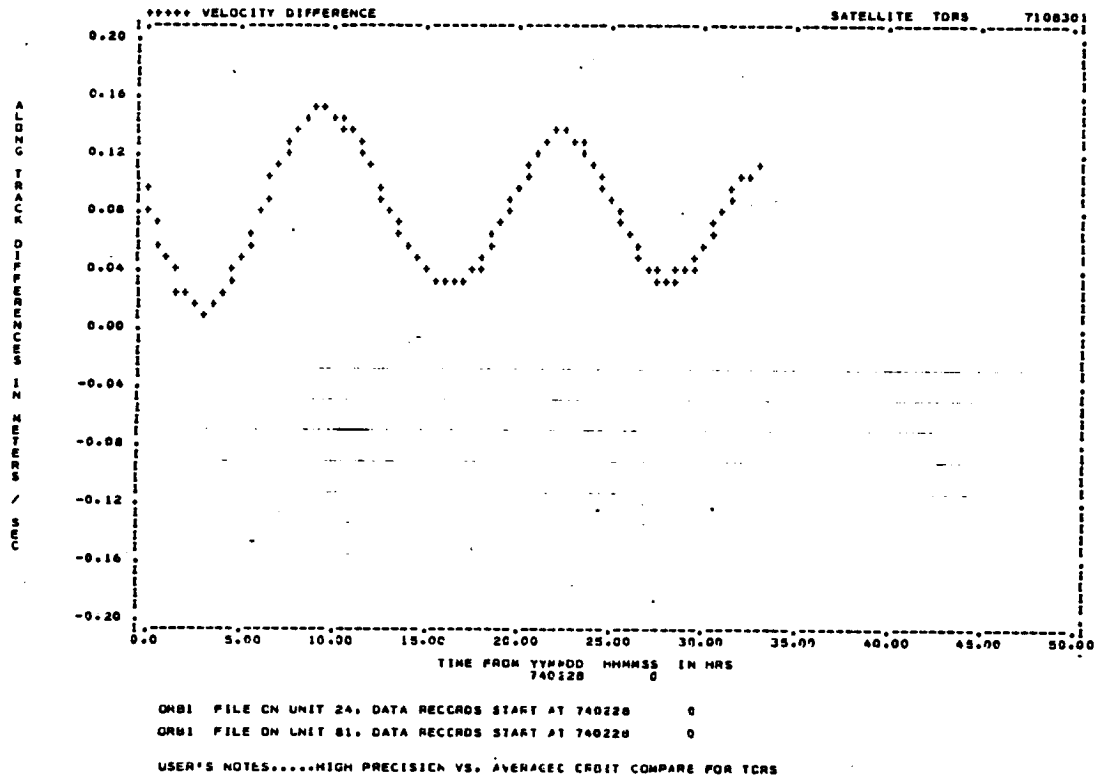

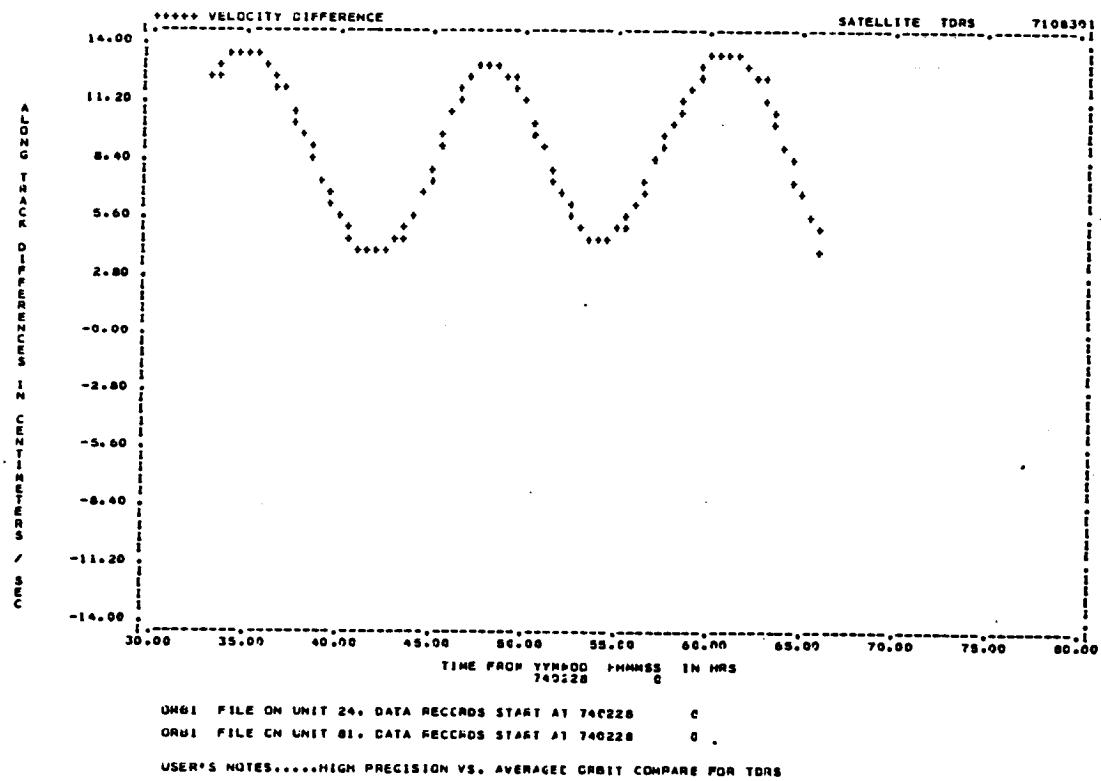

Figure 2-18. Difference Between the High-Precision and Mean Element Representations of the Along-Track Component of Velocity Using a Three-Point Hermite Interpolator

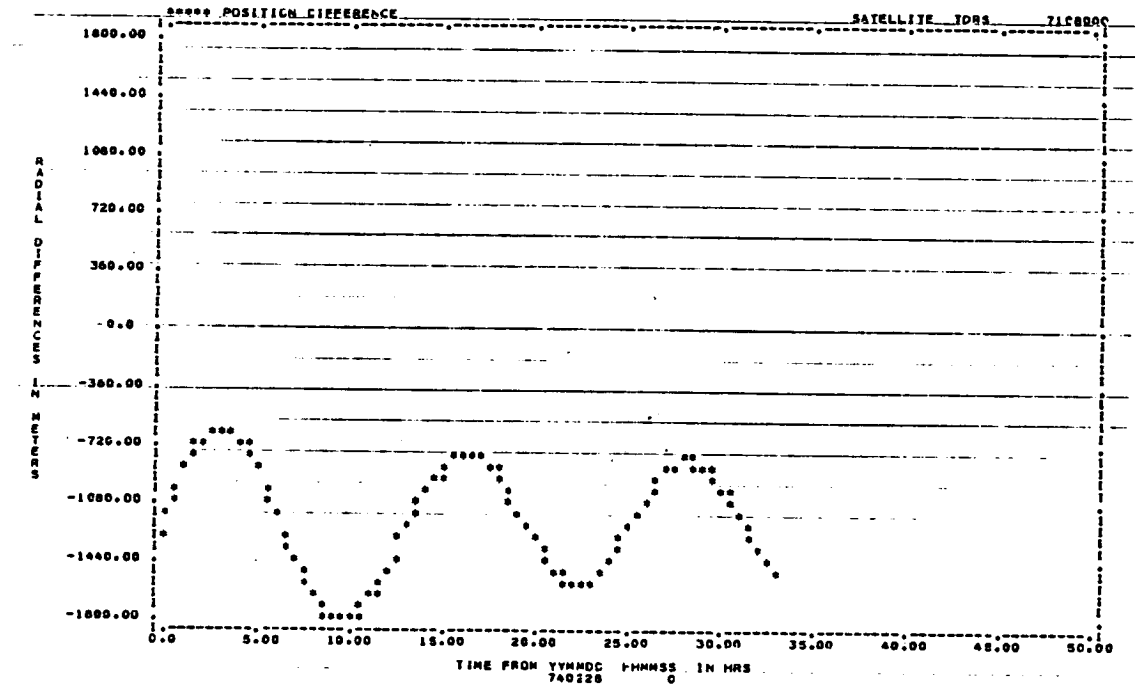

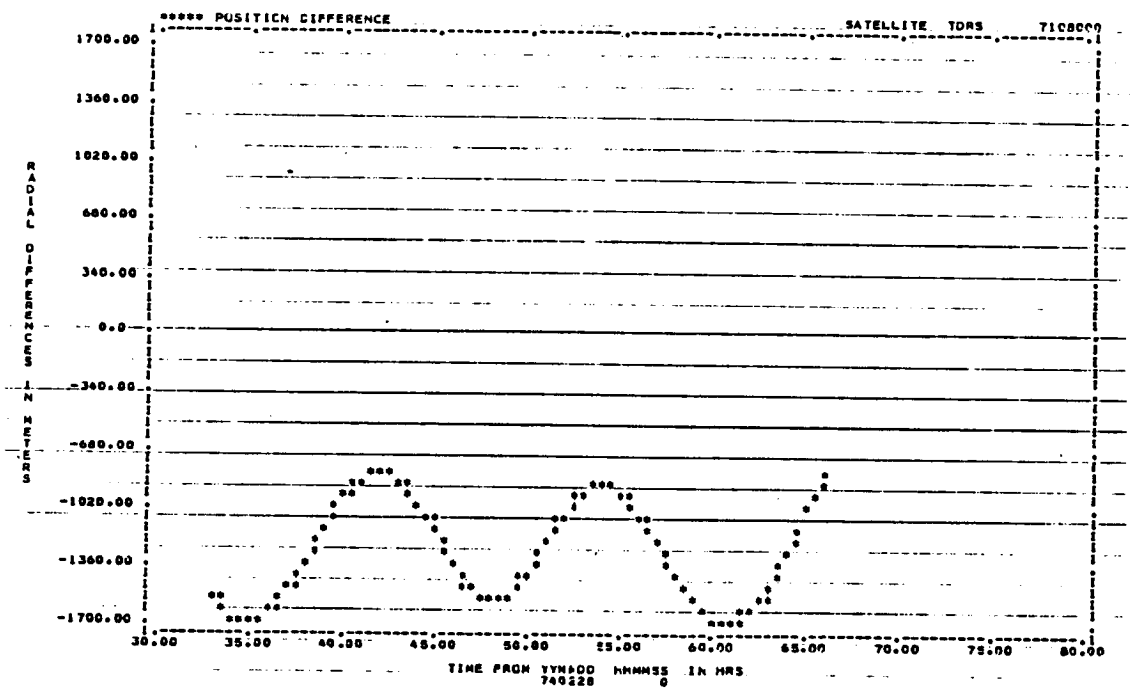

Figure 2-19. Difference Between the High-Precision and Mean Element Representations of the Radial Component of Position Using A Five-Point Lagrange Interpolator

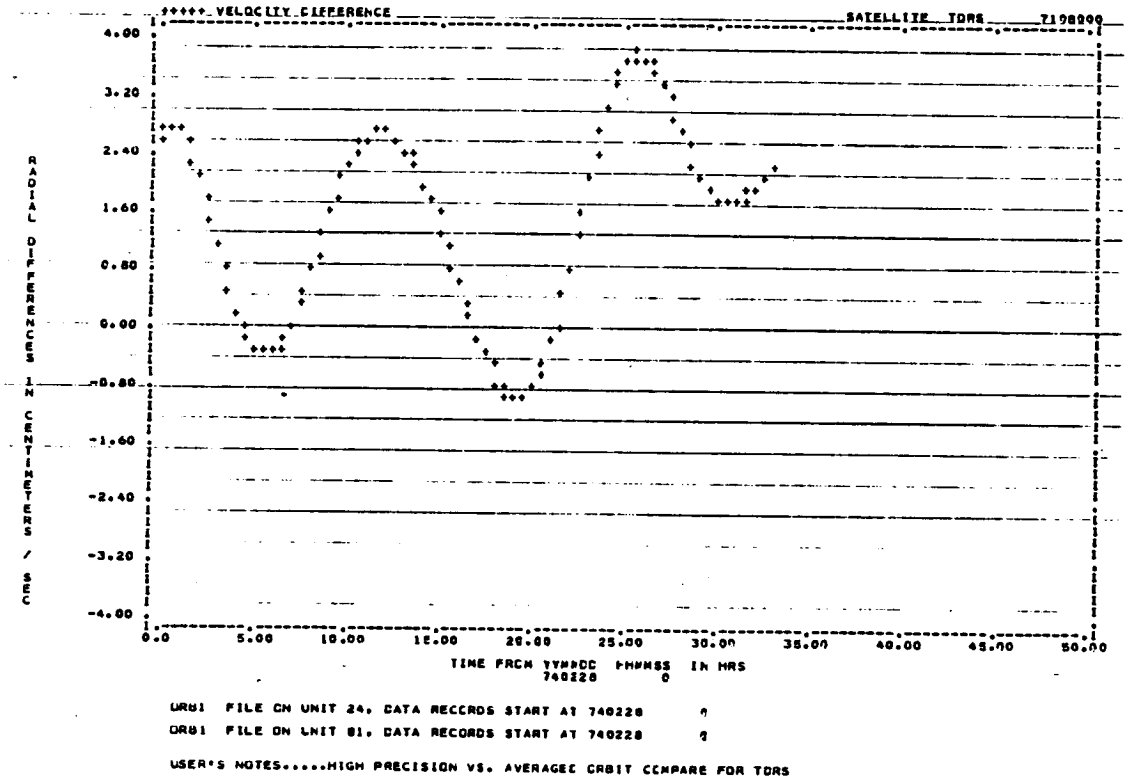

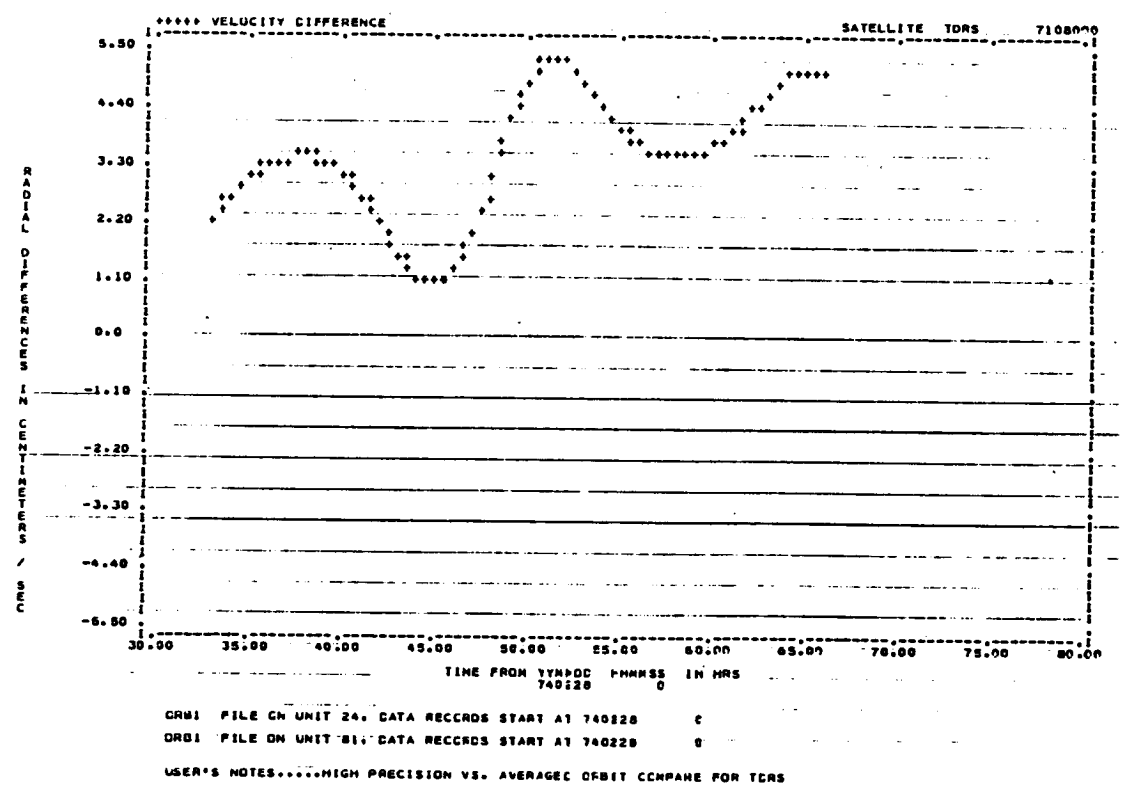

Figure 2-20. Difference Between the High-Precision and Mean Element Representations of the Radial Component of Velocity Using A Five-Point Lagrange Interpolator

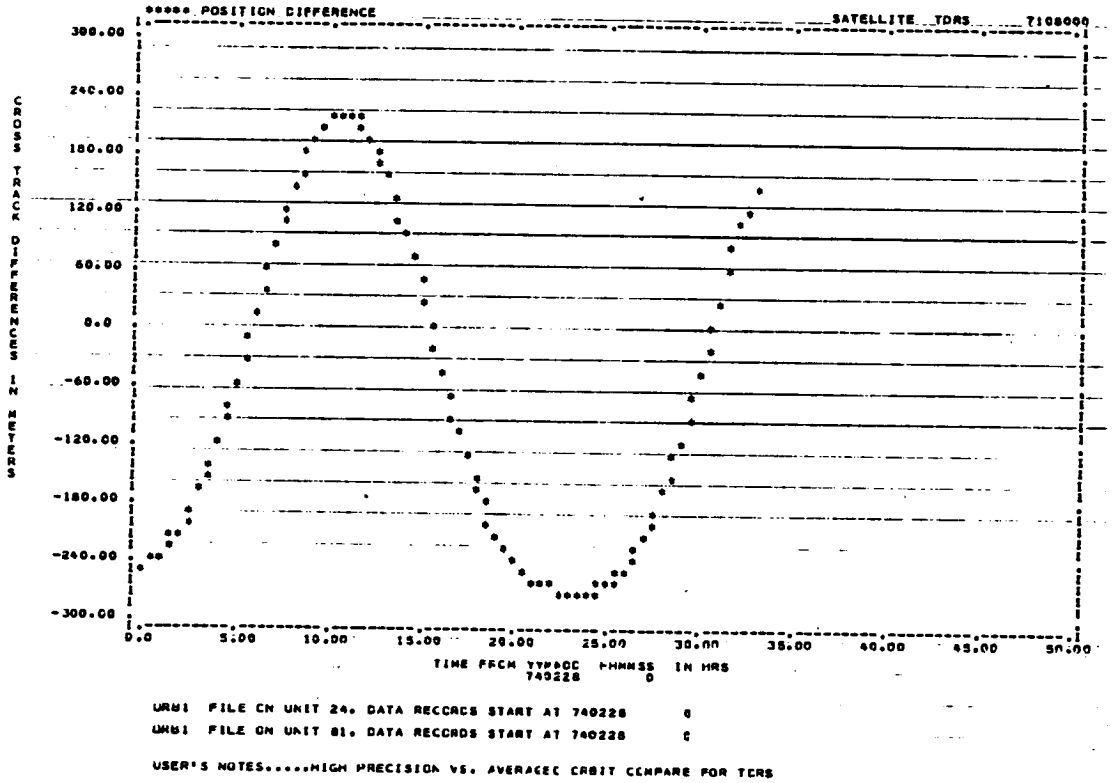

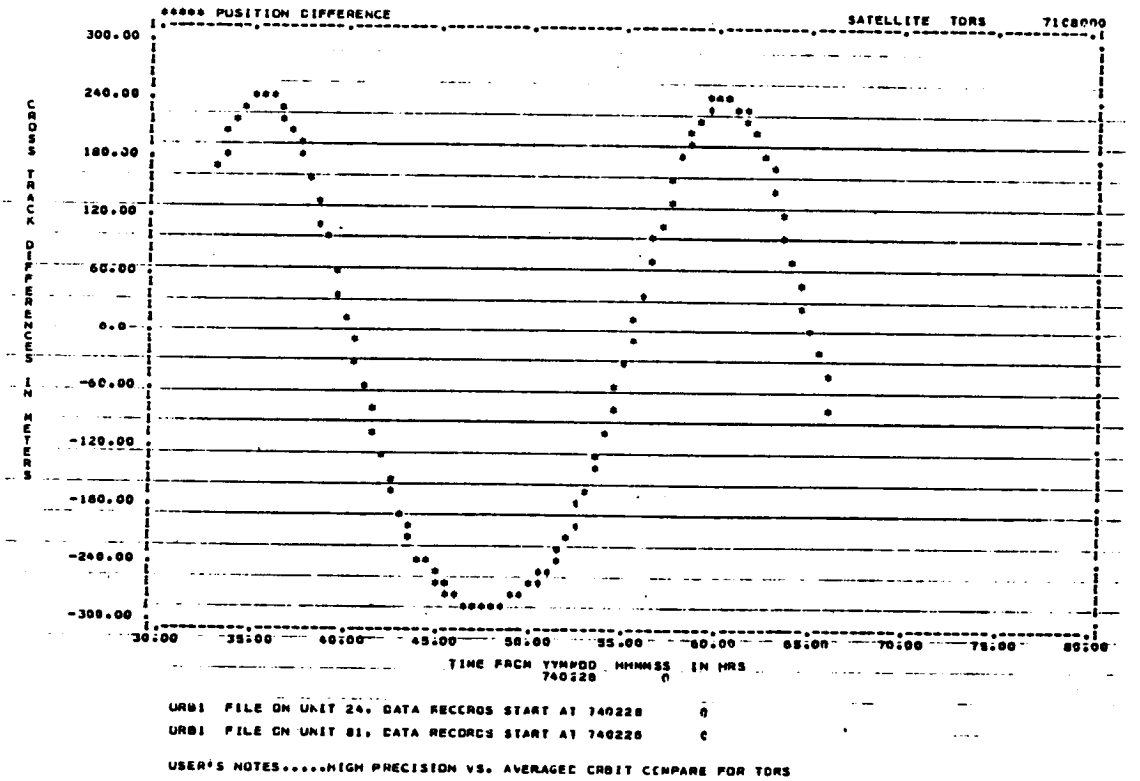

Figure 2-21. Difference Between the High-Precision and Mean Element Representations of the Cross-Track Component of Position Using a Five-Point Lagrange Interpolator

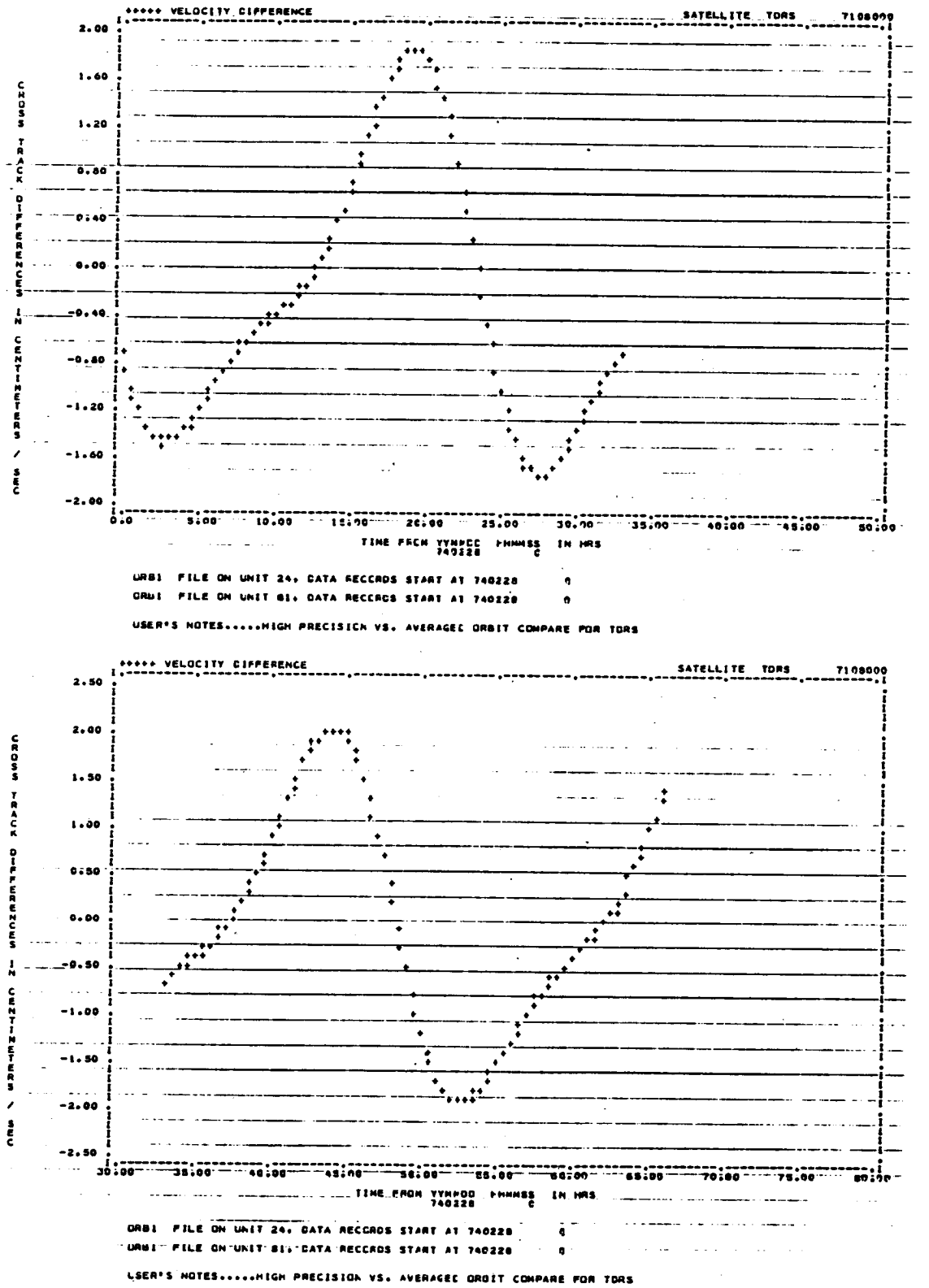

Figure 2-22. Difference Between the High-Precision and Mean Element Representations of the Cross-Track Component of Velocity Using a Five-Point Lagrange Interpolator

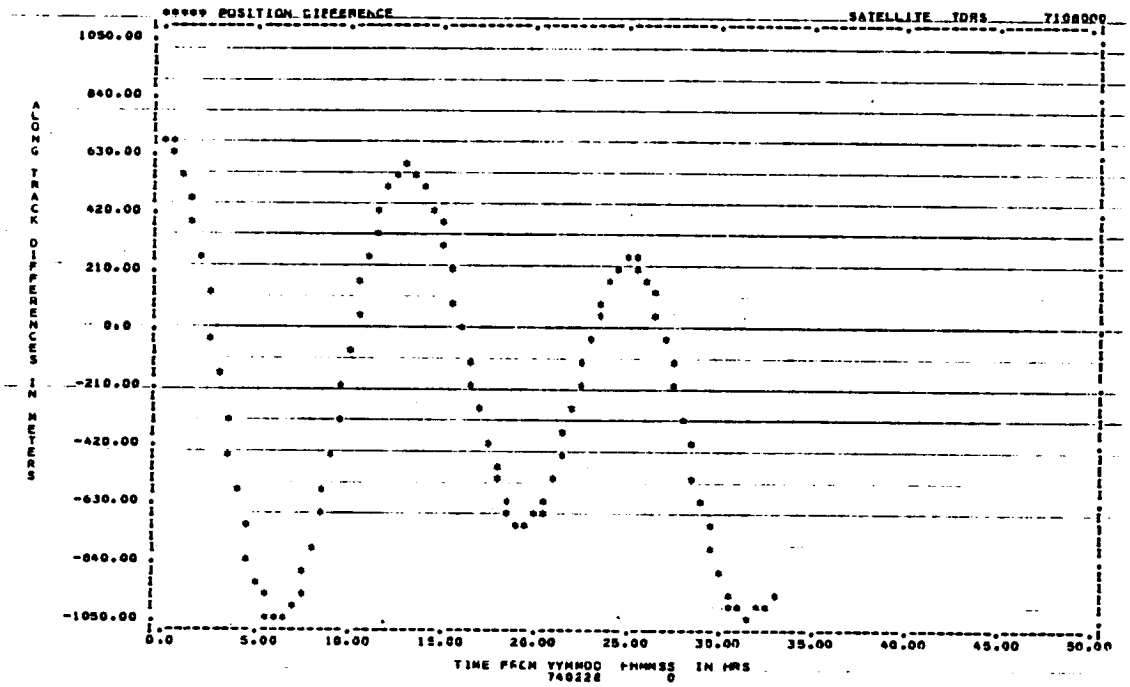

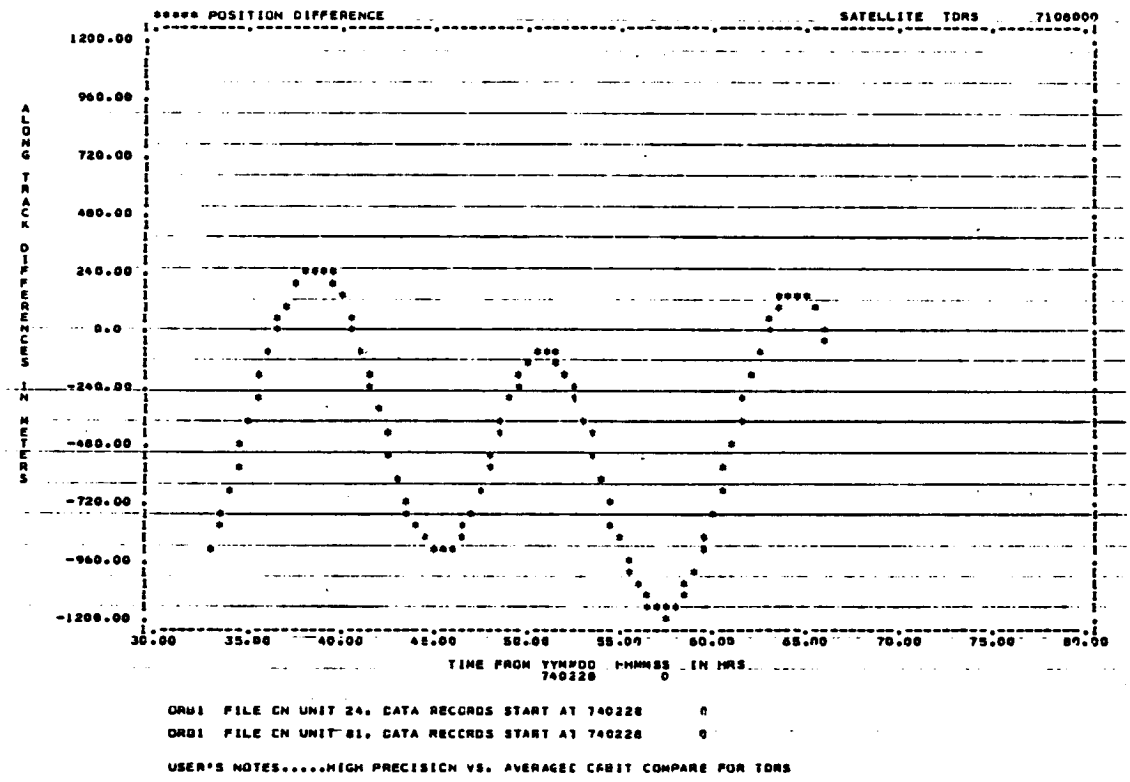

Figure 2-23. Difference Between the High-Precision and Mean Element Representations of the Along-Track Component of Velocity Using a Five-Point Lagrange Interpolator

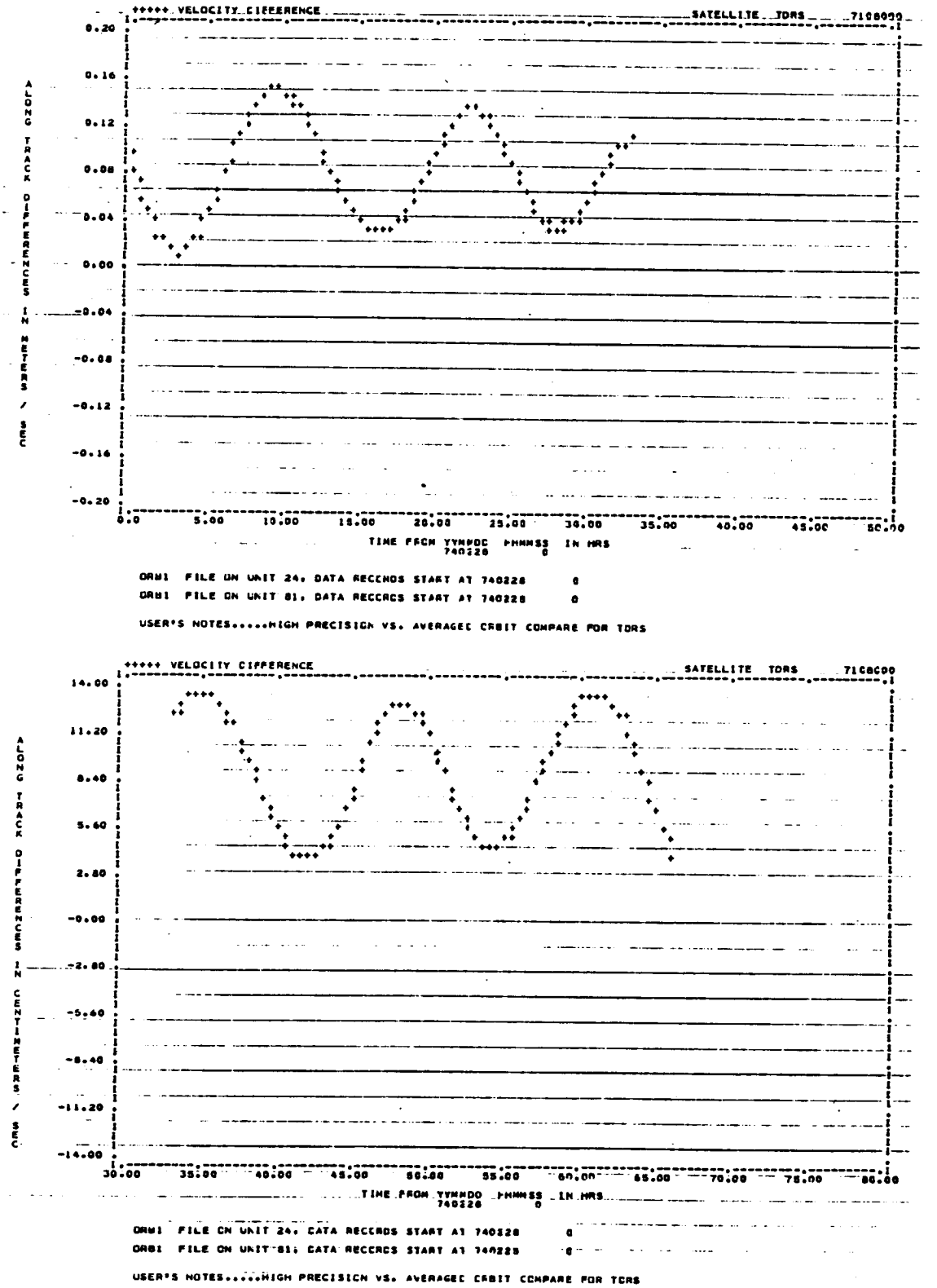

Figure 2-24. Difference Between the High-Precision and Mean Element Representations of the Along-Track Component of Position Using a Five-Point Lagrange Interpolator

SECTION 3 - FOURIER SERIES CARTESIAN COORDINATE REPRESENTATION

A representation of the form

$$\sum_{i=0}^{N} \sum_{j=0}^{M} \left[a_{ij} t^j \sin(i\omega t) + b_{ij} t^j \cos(i\omega t) \right] \tag{3-1}$$

where ω is the mean orbital frequency, was assumed for the Cartesian state variables. Such a representation is consistent with the theory of orbital dynamics. In practice, the series was used in the nested form (Reference 2)

$$\begin{aligned} f(x) = & \left\{ B_{00} + t\left[B_{01} + t\left(B_{02} + \cdots\right)\right)\cdots\right]\right\} \\ & + \left\{ A_{10} + t\left[A_{11} + t\left(A_{12} + \cdots\right)\right)\cdots\right]\right\} \sin(\omega t) \\ & + \left\{ B_{10} + t\left[B_{11} + t\left(B_{12} + \cdots\right)\right)\cdots\right]\right\} \cos(\omega t) \\ & + \left\{ A_{20} + t\left[A_{21} + t\left(A_{22} + \cdots\right)\right)\cdots\right]\right\} \sin^2(\omega t) \\ & + \left\{ B_{20} + t\left[B_{21} + t\left(B_{22} + \cdots\right)\right)\cdots\right]\right\} \sin(\omega t)\cos(\omega t) \\ & + \left\{ A_{30} + t\left[A_{31} + t\left(A_{32} + \cdots\right)\right)\cdots\right]\right\} \sin^3(\omega t) \\ & + \left\{ B_{30} + t\left[B_{31} + t\left(B_{32} + \cdots\right)\right)\cdots\right]\right\} \sin^2(\omega t)\cos(\omega t) \\ & + \cdots\cdots \end{aligned} \tag{3-2}$$

The coefficient in the preceding series are determined by a least-squares fit of each of the high-precision Cartesian state variables over a 3-day interval. The mean orbital frequency was computed from the mean semimajor axis, which was obtained from the numerical osculating-to-mean conversion procedure available in GTDS.

Three different subsets of the coefficients, viz,

- The 5-set: $\{B_{00}, A_{10}, B_{10}, A_{20}, B_{20}\}$
- The 7-set: $\{B_{00}, A_{10}, B_{10}, A_{20}, B_{20}, A_{30}, B_{30}\}$
- The 14-set: $\{B_{00}, A_{10}, B_{10}, A_{20}, B_{20}, A_{30}, B_{30}, B_{01}, A_{11}, B_{11}, A_{21}, B_{21}, A_{31}, B_{31}\}$

were evaluated at grid intervals of 50 minutes. It was found that while the 5-set is insufficient in terms of accuracy of the trajectory determination, the 7-set is optimum, since it is faster and almost as accurate as the 14-set. Using the optimal 7-set computed for grid intervals of 50, 100, and 150 minutes, the trigonometric series was evaluated at intervals of 20 minutes and the resulting trajectory compared with the high-precision file generated by the GTDS Cowell orbit generator.

The representation errors obtained using the 50-minute interval with the set of seven coefficients are given in Table 2-2. For this case, the rms position errors are 0.14 kilometers for the radial component, 0.16 kilometers for the cross-track component, and 0.34 kilometers for the along-track component. The rms velocity errors are 0.21×10^{-4} kilometers/second for the radial component, 0.11×10^{-4} kilometers/second for the cross-track component, and 0.18×10^{-4} kilometers/second for the along-track component. The minimum and maximum position differences in the 50-minute, 7-set case are 0.27×10^{-4} and 0.41 kilometers for the radial component, 0.63×10^{-3} and 0.48 kilometers for the cross-track component, and 0.20×10^{-2} and 0.63 kilometers for the along-track component.

A similar comparison was performed using the set of seven coefficients computed from data at 100-minute intervals. The errors, summarized in Table 2-2, are as follows: (1) the rms position errors are 0.14 kilometers for the radial component, 0.16 kilometers for the cross-track component, and

0.34 kilometers for the along-track component; (2) the rms velocity errors are 0.21×10^{-4} kilometers/second for the radial component, 0.11×10^{-4} kilometers/second for the cross-track component, and 0.18×10^{-4} kilometers/second for the along-track component; and (3) the minimum and maximum position differences are 0.19×10^{-3} and 0.39 kilometers for the radial component, 0.37×10^{-3} and 0.46 kilometers for the cross-track component, and 0.24×10^{-2} and 0.63 kilometers for the along-track component.

The results of a similar comparison performed using the set of seven coefficients computed from data at 150-minute intervals are as follows. The rms position errors are 0.14 kilometers for the radial component, 0.17 kilometers for the cross-track component, and 0.34 kilometers for the along-track component. The rms velocity errors are 0.21×10^{-4} kilometers/second for the radial component, 0.11×10^{-4} kilometers/second for the cross-track component, and 0.18×10^{-4} kilometers/second for the along-track component. The minimum and maximum position differences are 0.52×10^{-3} and 0.37 kilometers for the radial component, 0.34×10^{-3} and 0.56 kilometers for the cross-track component, and 0.95×10^{-1} and 0.63 kilometers for the along-track component.

The results of the comparison between the high-precision and the trigonometric series reconstruction of the trajectories are presented graphically in printer plots produced using the GTDS COMPARE Program. These plots are given in Figures 3-1 through 3-18.

A comparison of the results obtained with the trigonometric series using data at 50-, 100-, and 150-minute intervals, respectively, shows that there there is no significant difference in the position and velocity errors. In view of this fact, it is recommended that at least a 150-minute data interval be used to minimize the computational cost.

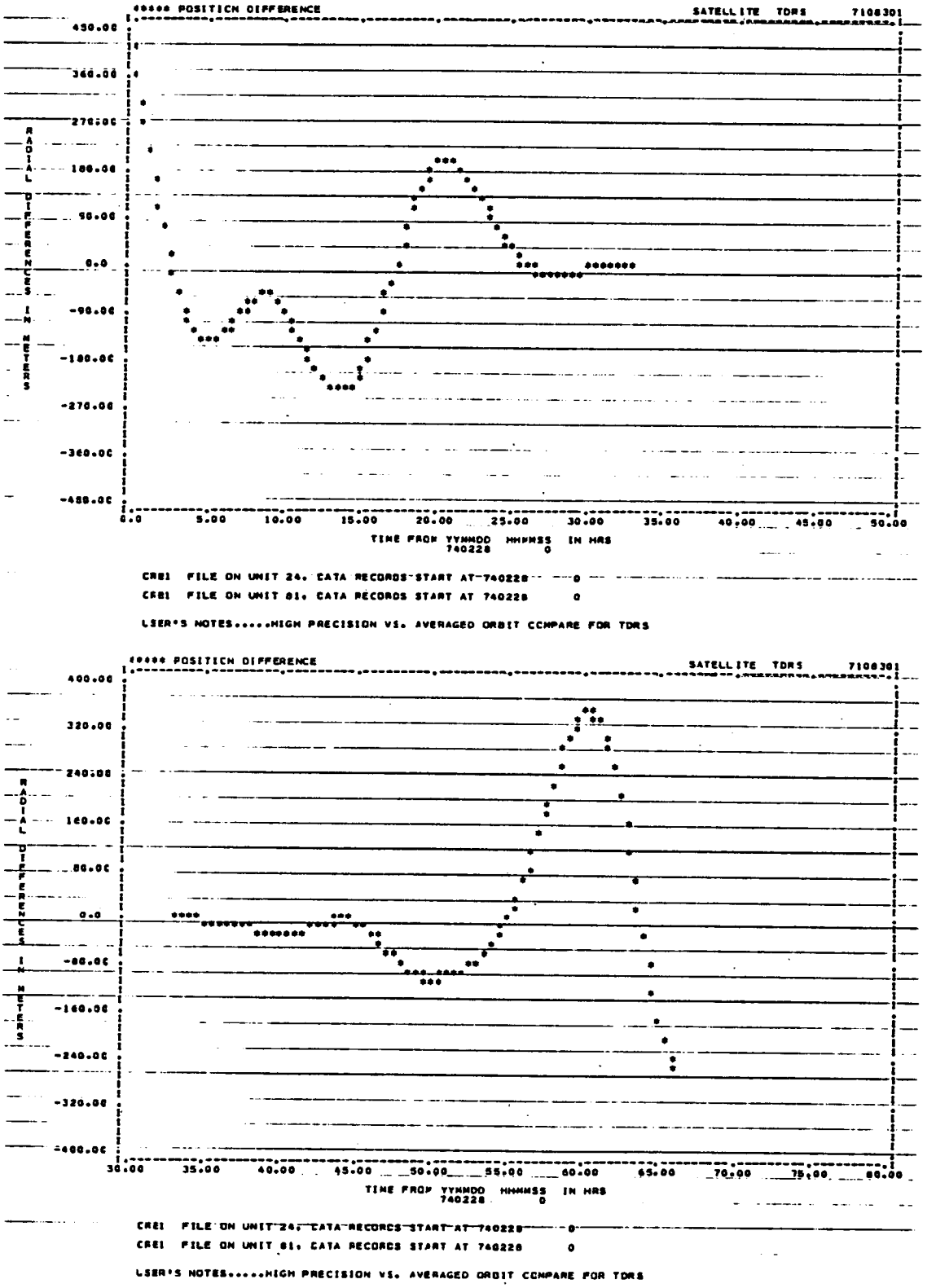

Figure 3-1. Difference Between the High-Precision and Cartesian/Fourier Representations of the Radial Component of Position Using a 50-Minute Grid Spacing

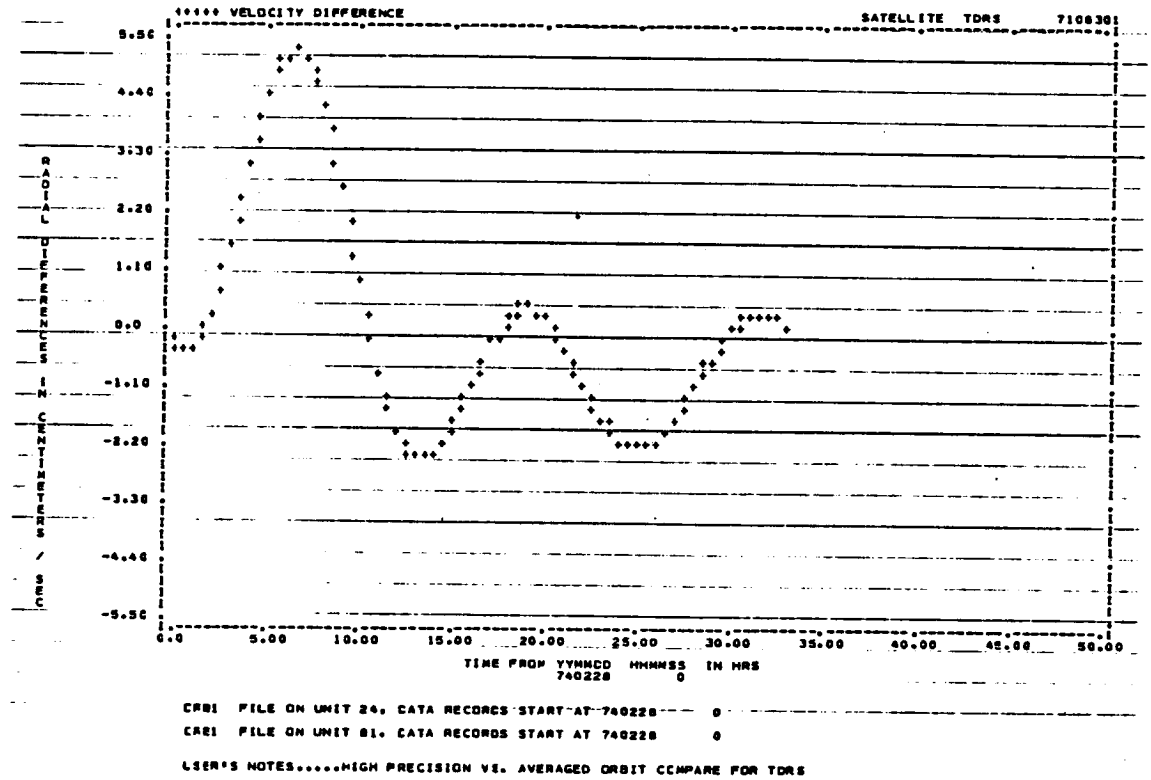

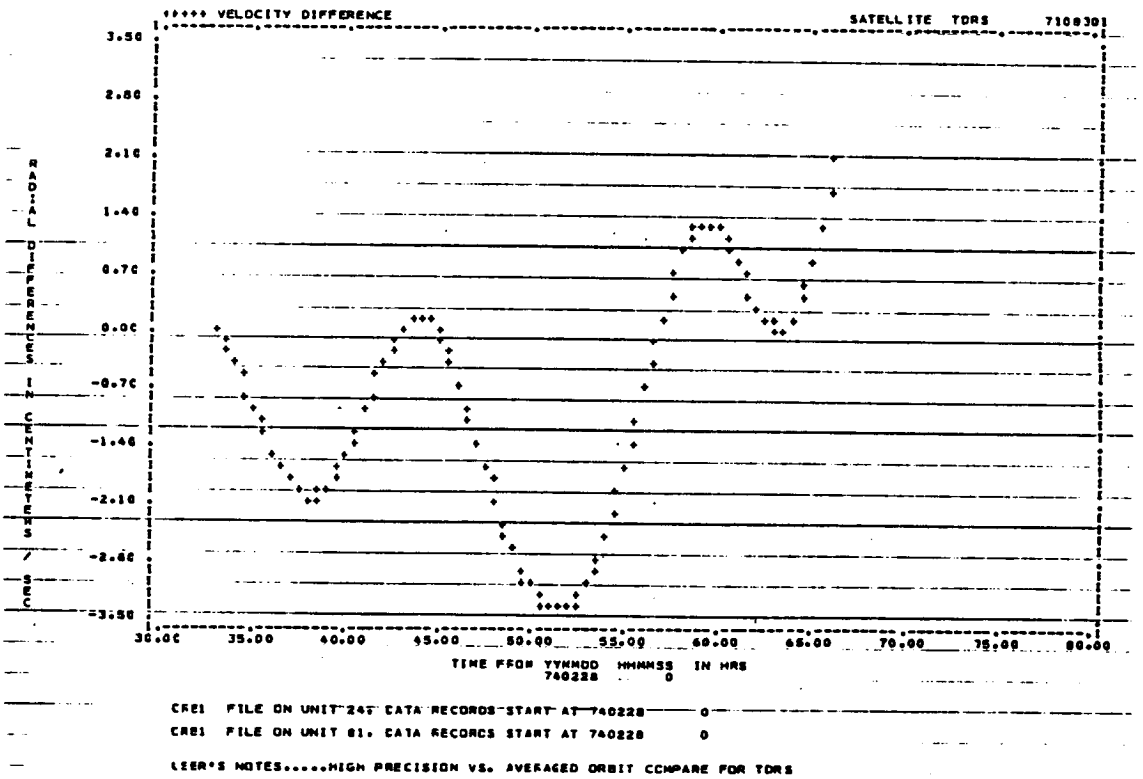

Figure 3-2. Difference Between the High-Precision and Cartesian/Fourier Representations of the Radial Component of Velocity Using a 50-Minute Grid Spacing

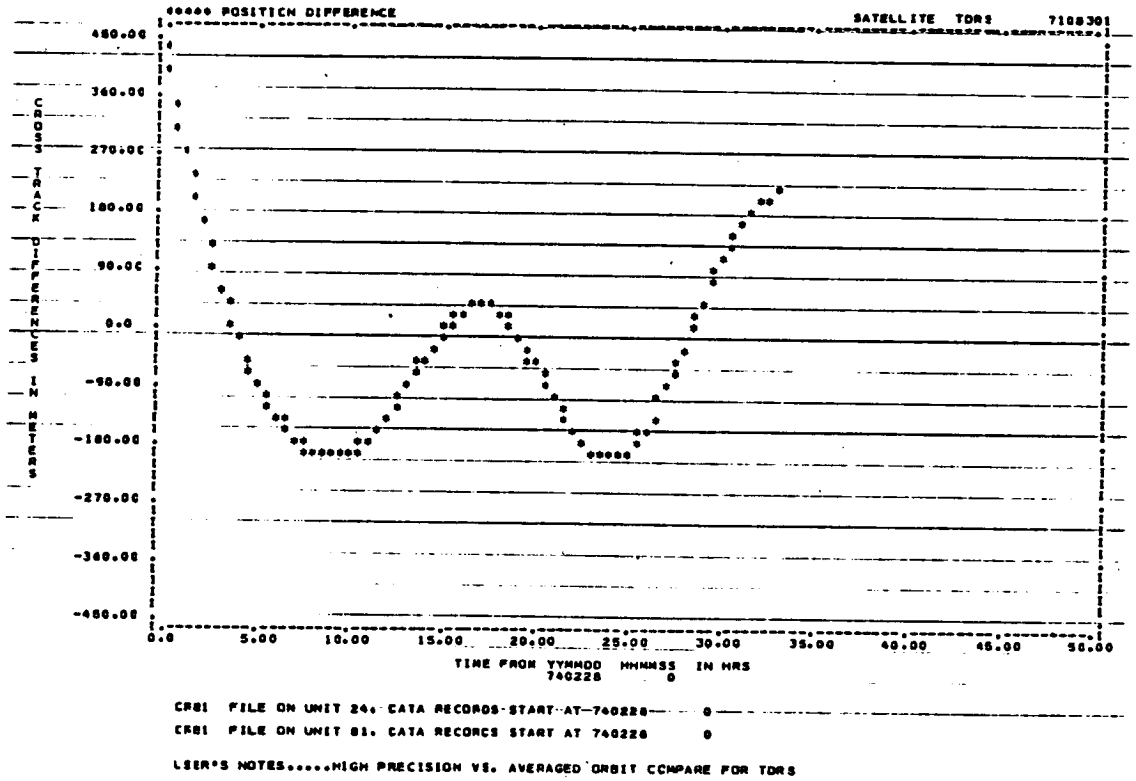

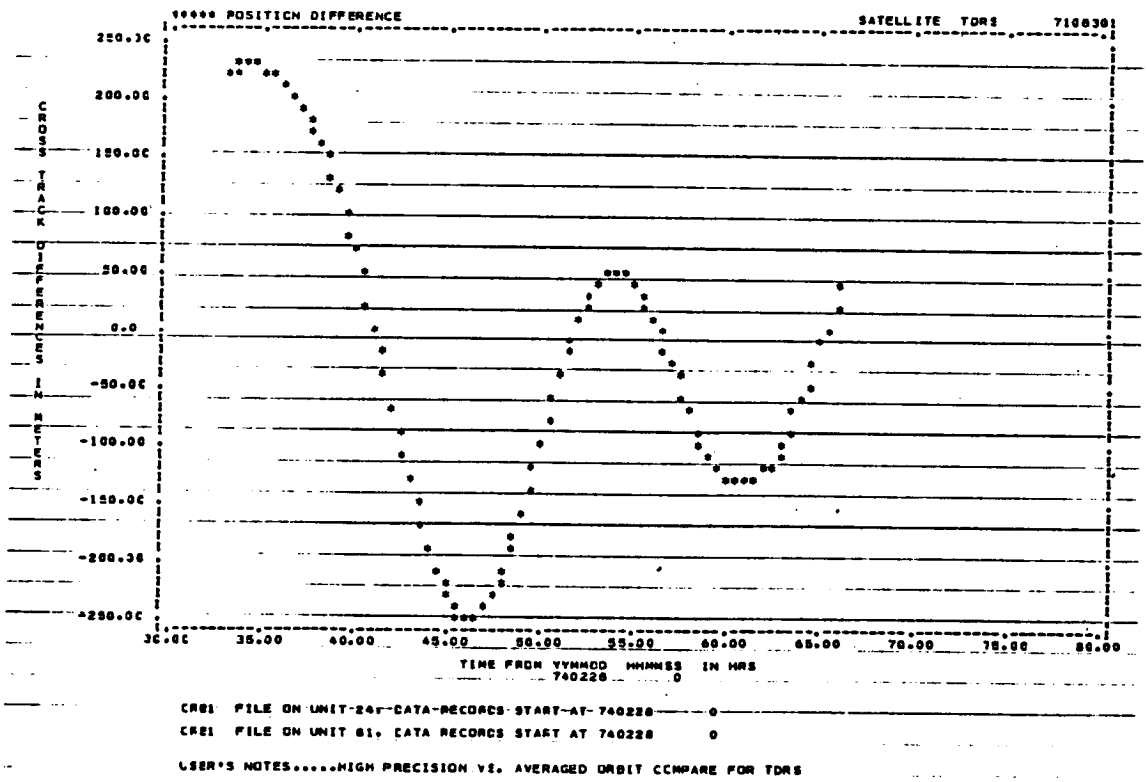

Figure 3-3. Difference Between the High-Precision and Cartesian/Fourier Representations of the Cross-Track Component of Position Using a 50-Minute Grid Spacing

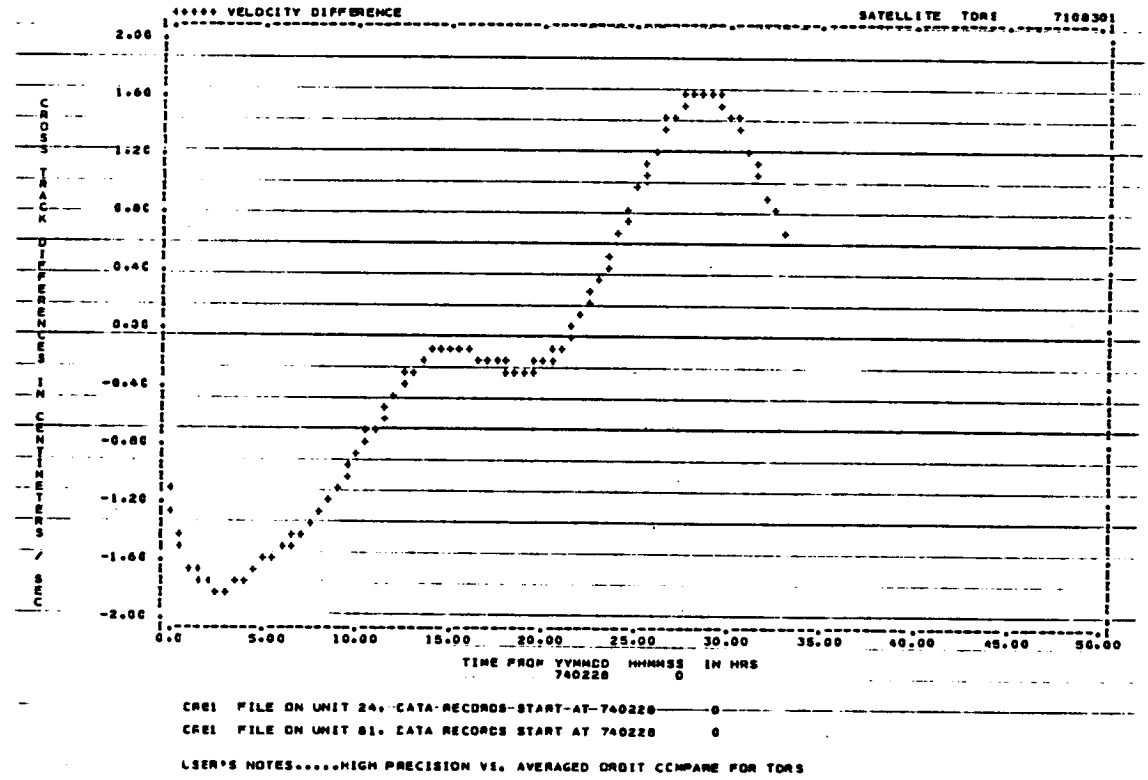

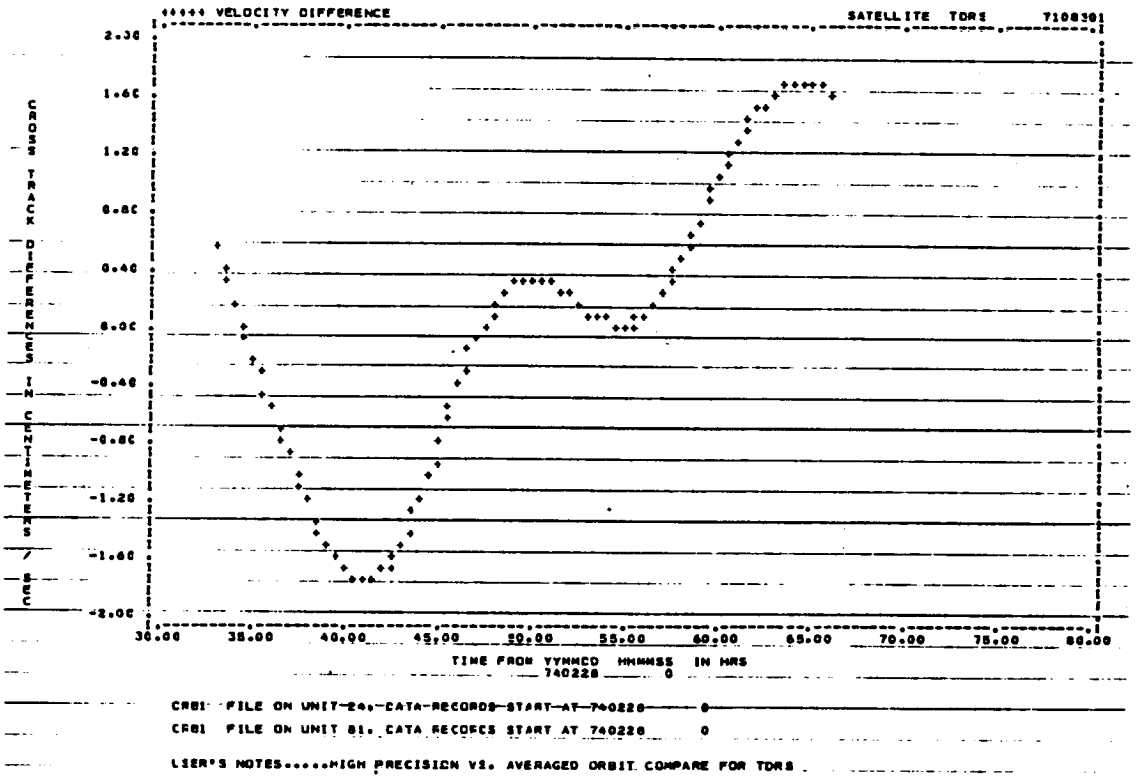

Figure 3-4. Difference Between the High-Precision and Cartesian/Fourier Representations of the Cross-Track Component of Velocity Using a 50-Minute Grid Spacing

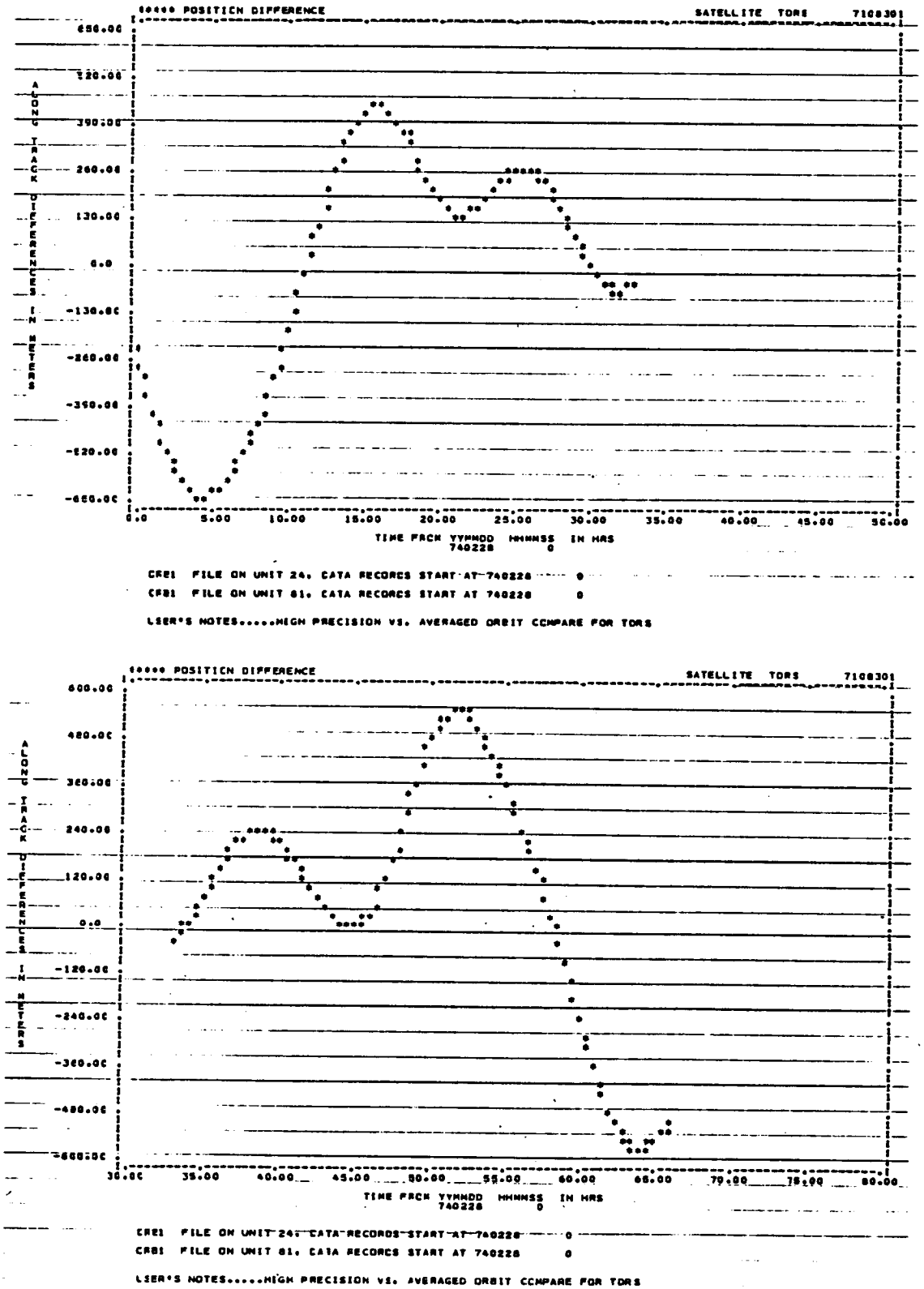

Figure 3-5. Difference Between the High-Precision and Cartesian/Fourier Representations of the Along-Track Component of Position Using a 50-Minute Grid Spacing

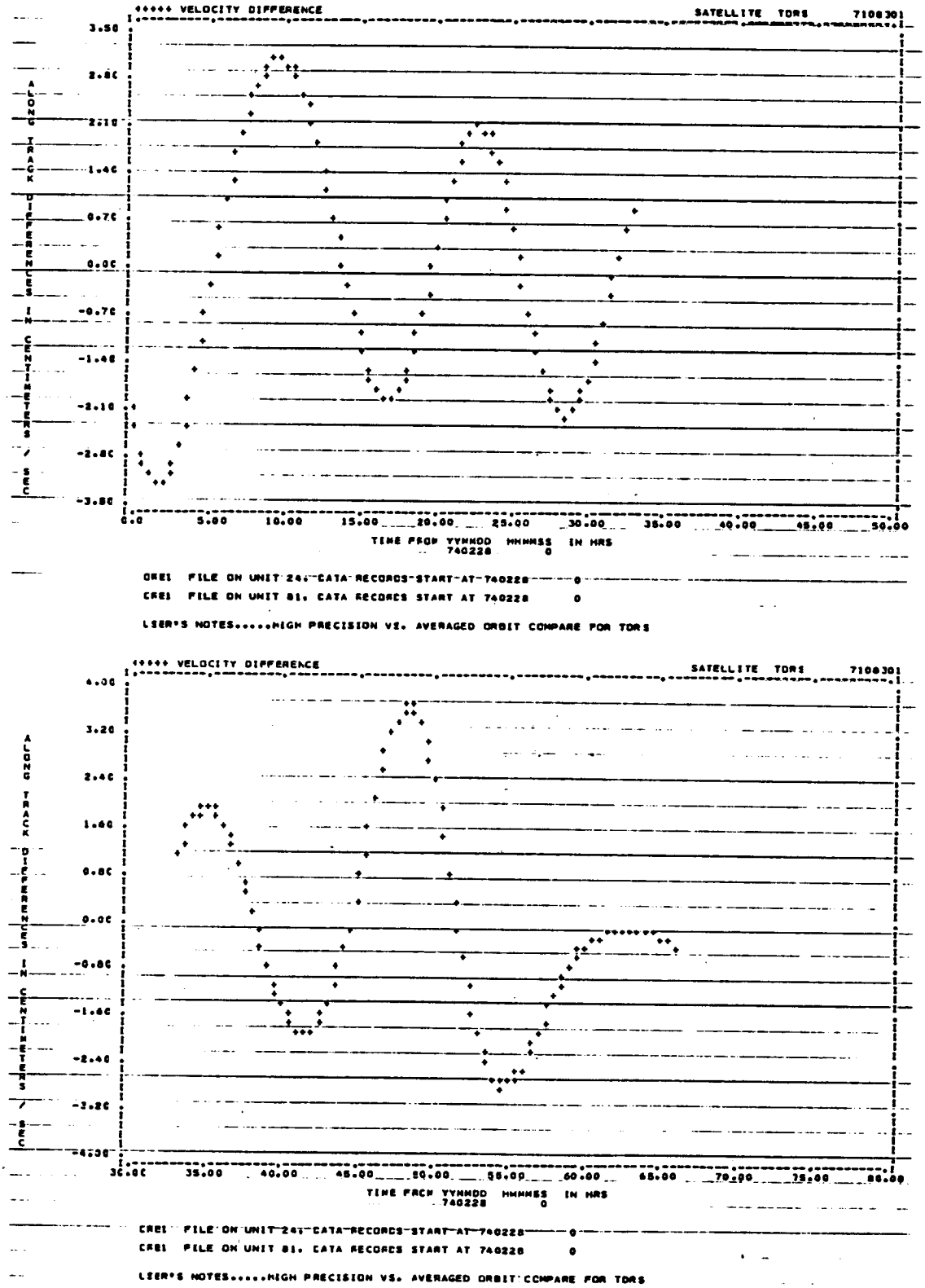

Figure 3-6. Difference Between the High-Precision and Cartesian/Fourier Representations of the Along-Track Component of Velocity Using a 50-Minute Grid Spacing

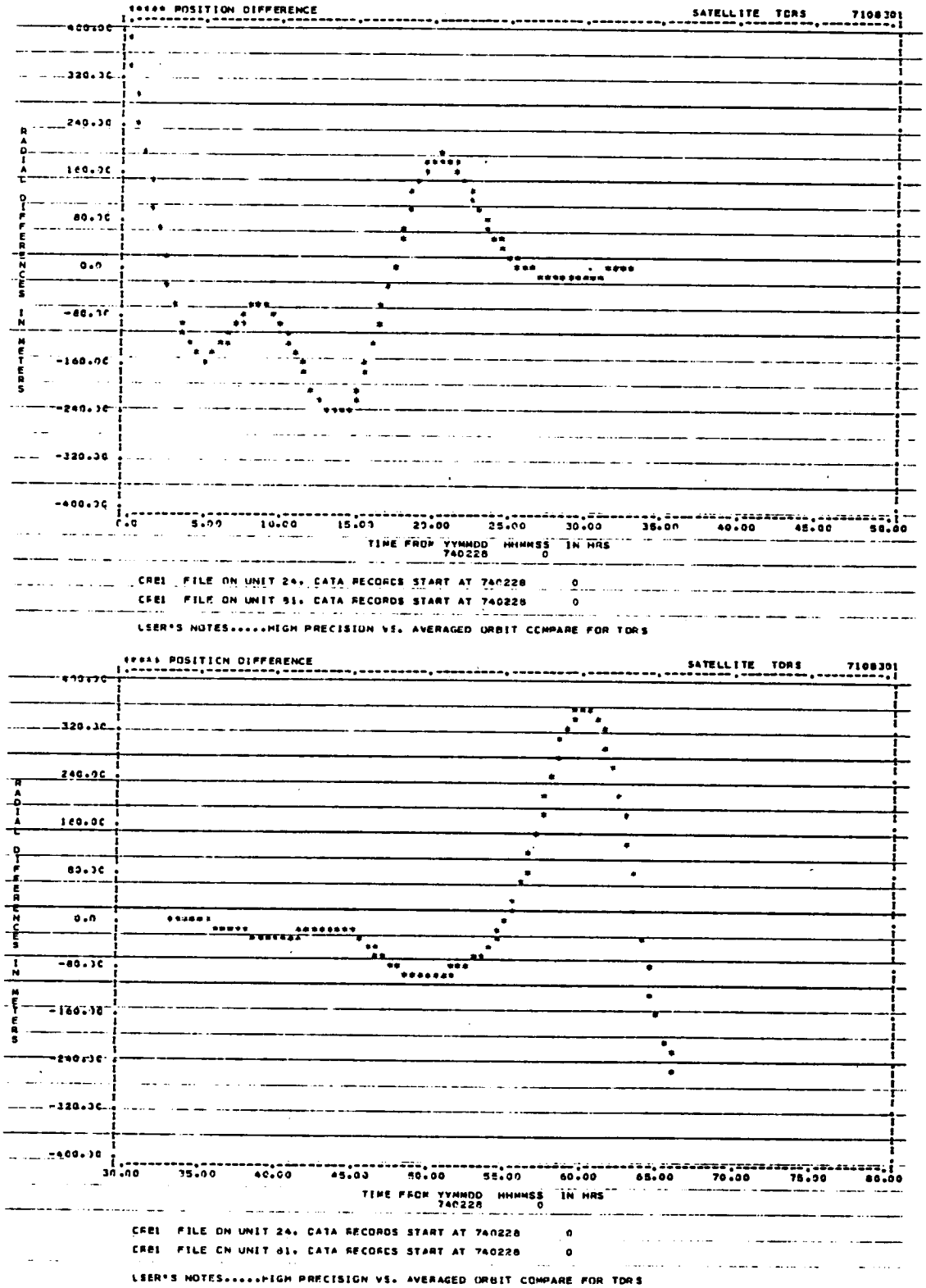

Figure 3-7. Difference Between the High-Precision and Cartesian/Fourier Representations of the Radial Component of Position Using a 100-Minute Grid Spacing

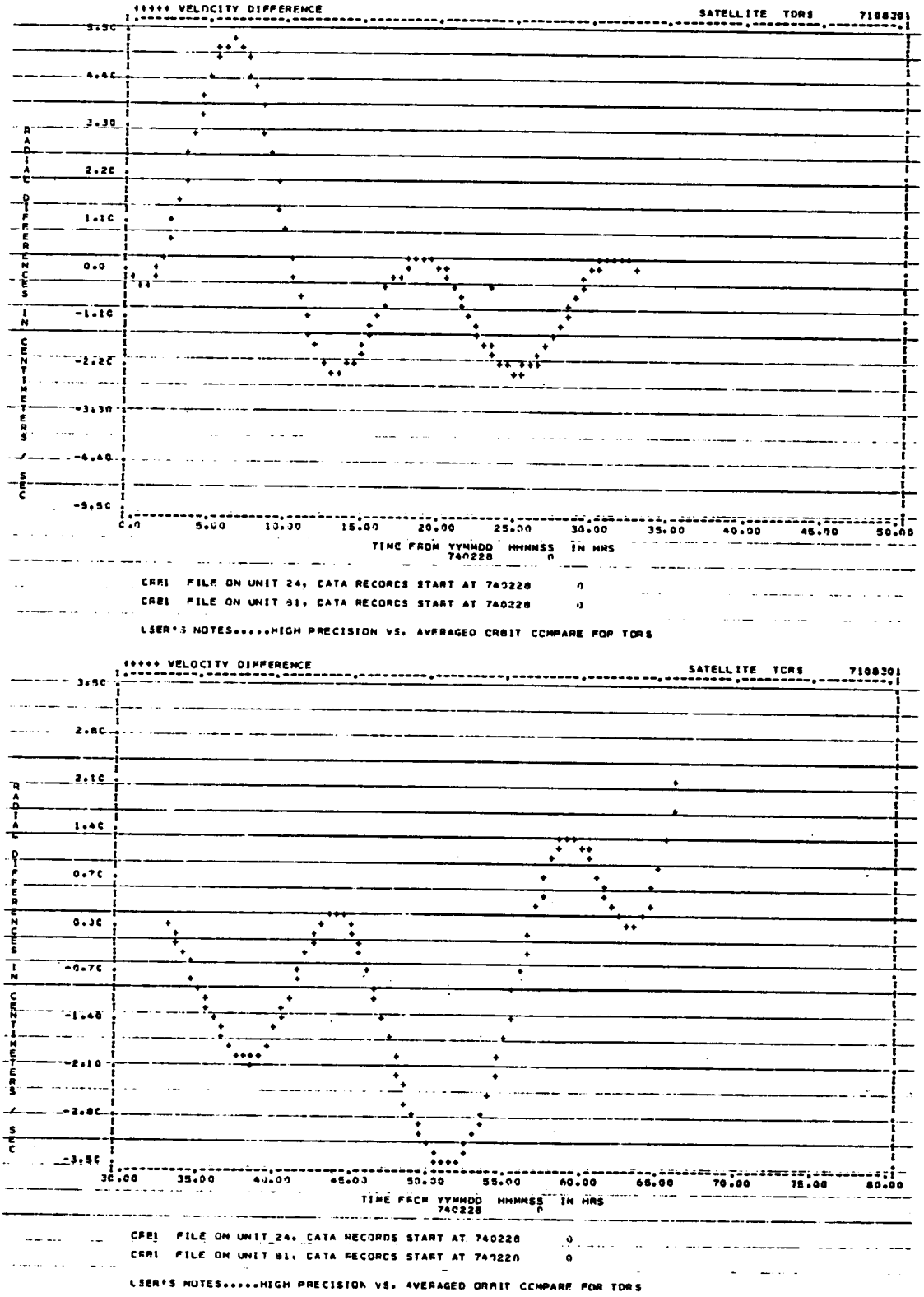

Figure 3-8. Difference Between the High-Precision and Cartesian/Fourier Representations of the Radial Component of Velocity Using a 100-Minute Grid Spacing

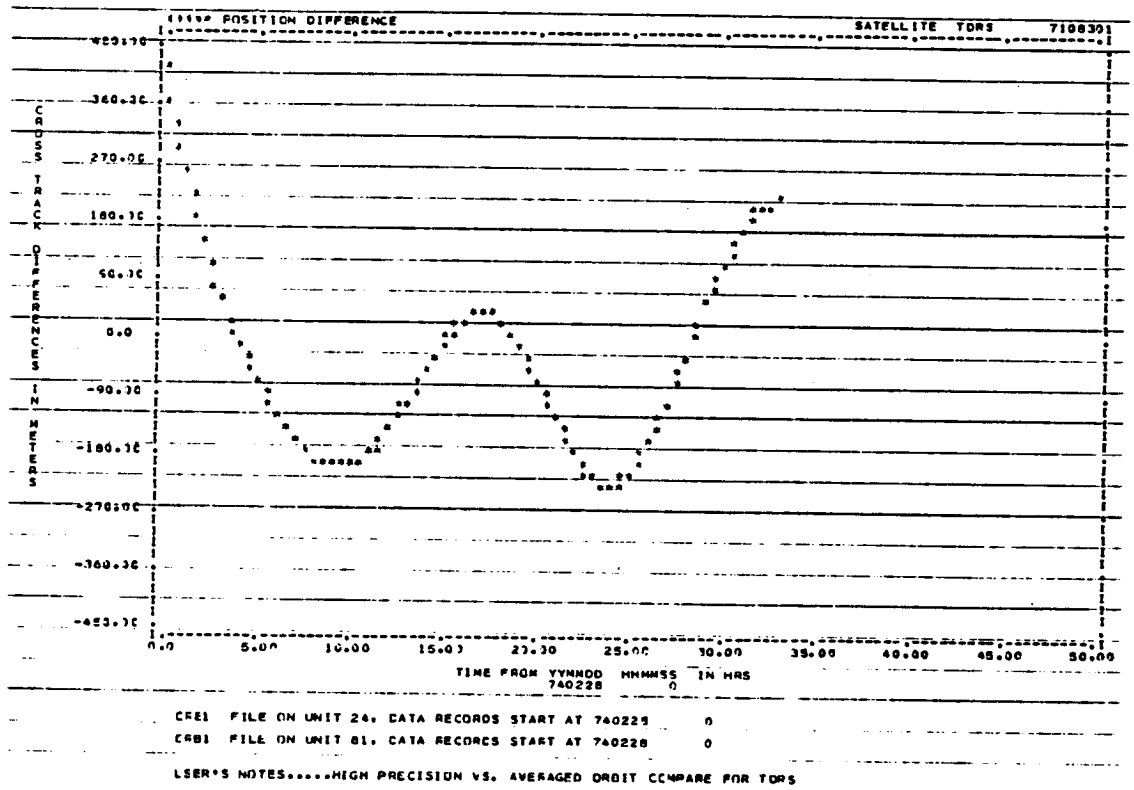

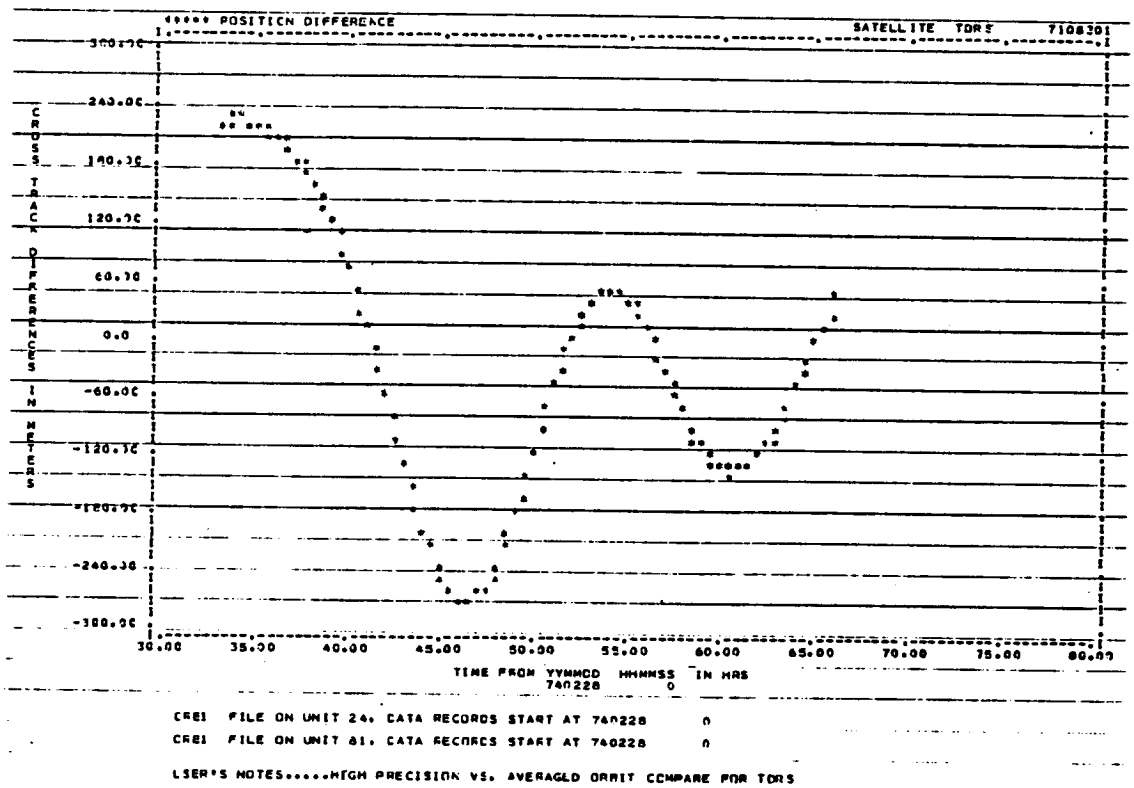

Figure 3-9. Difference Between the High-Precision and Cartesian/Fourier Representations of the Cross-Track Component of Position Using a 100-Minute Grid Spacing

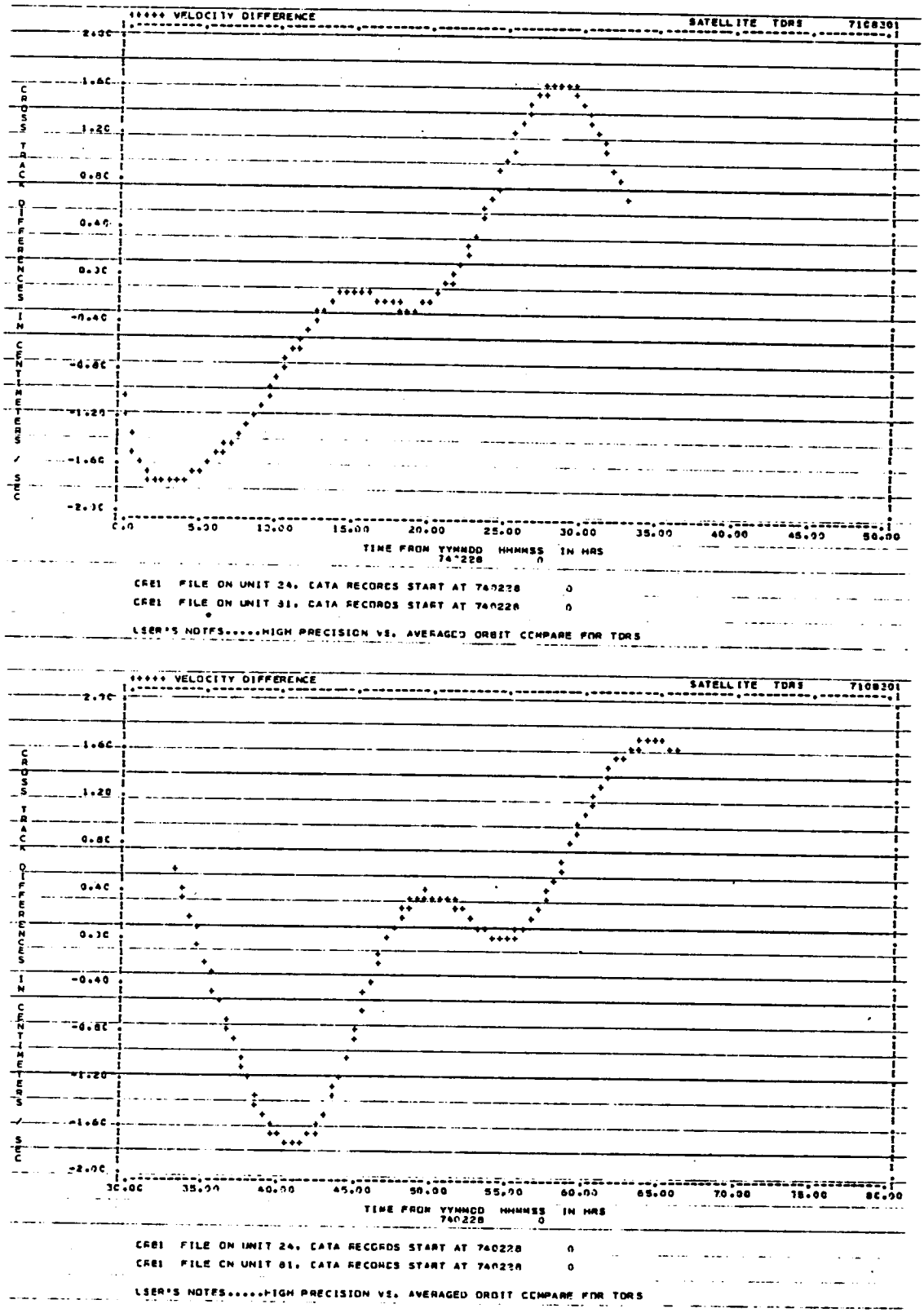

Figure 3-10. Difference Between the High-Precision and Cartesian/Fourier Representations of the Cross-Track Component of Velocity Using a 100-Minute Grid Spacing

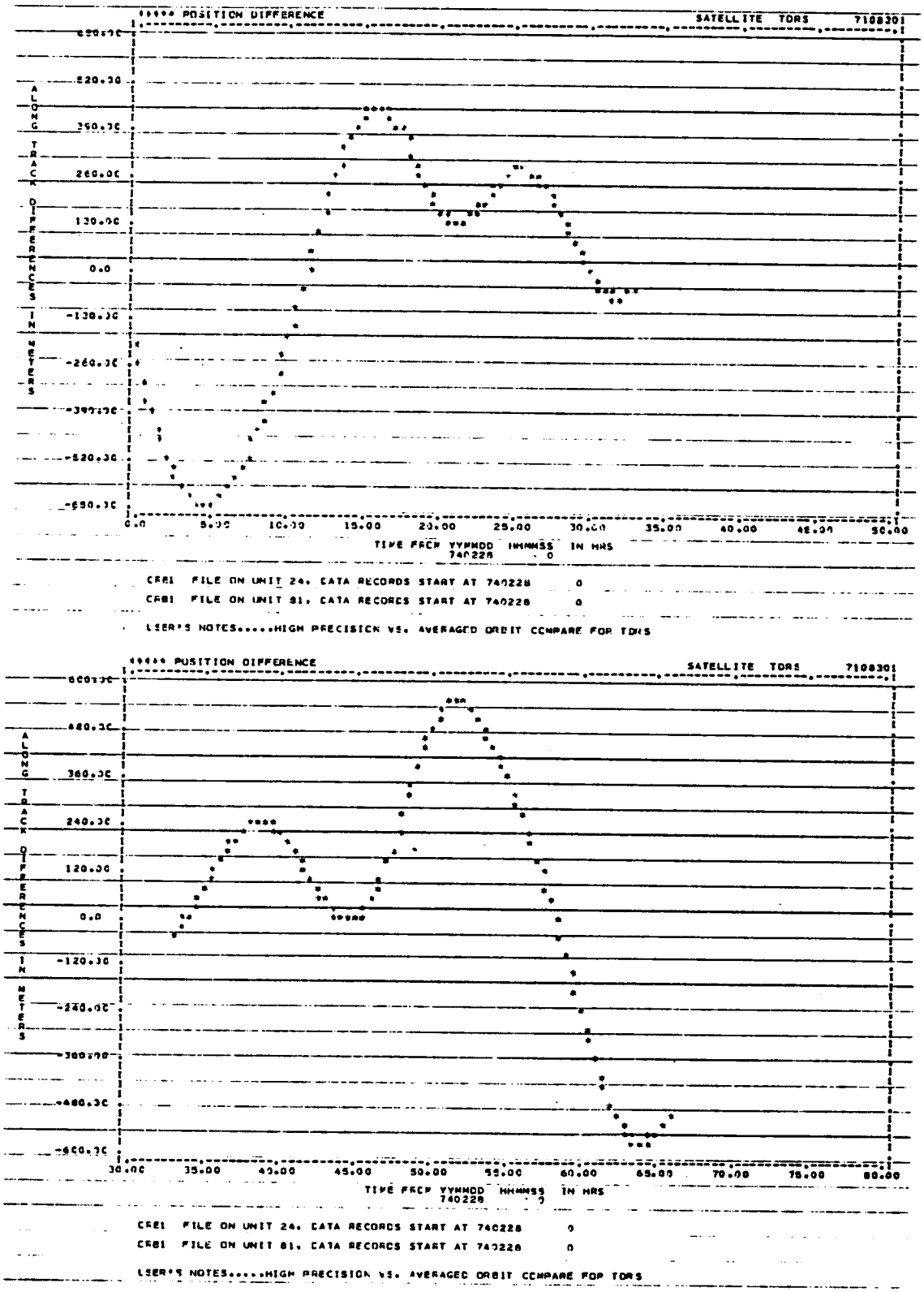

Figure 3-11. Difference Between the High-Precision and Cartesian/Fourier Representations of the Along-Track Component of Position Using a 100-Minute Grid Spacing

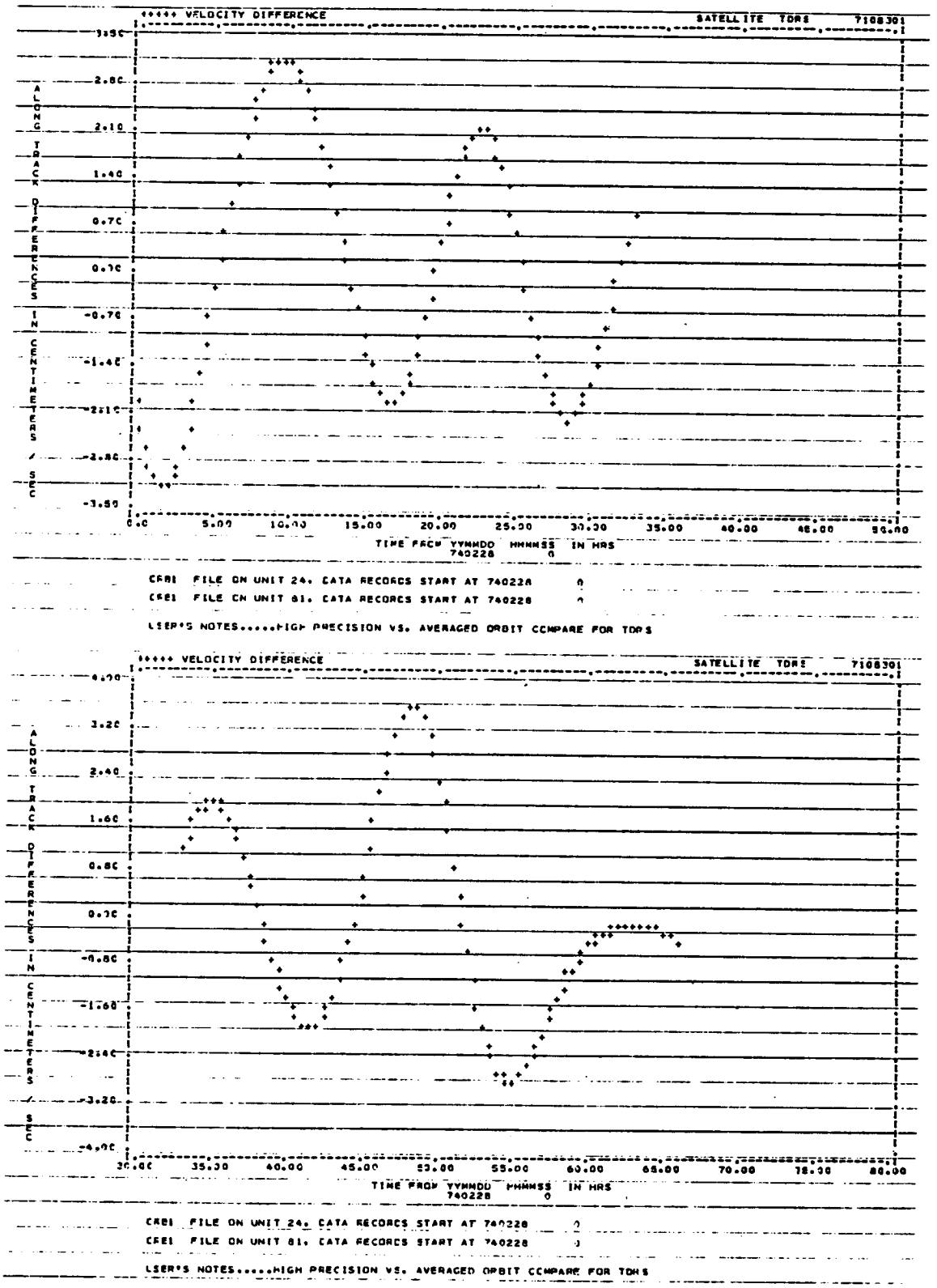

Figure 3-12. Difference Between the High-Precision and Cartesian/Fourier Representations of the Along-Track Component of Velocity Using a 100-Minute Grid Spacing

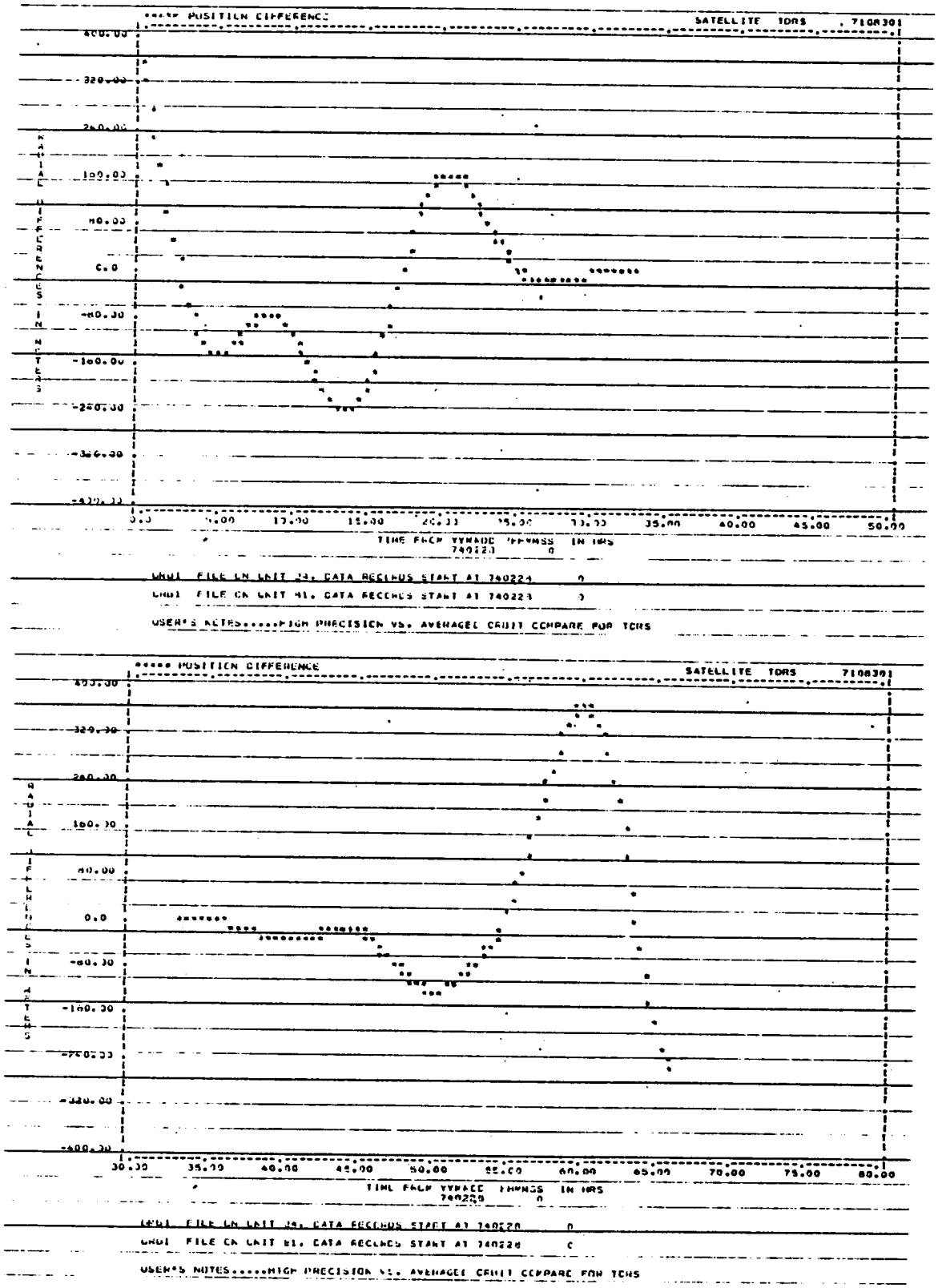

Figure 3-13. Difference Between the High-Precision and Cartesian/Fourier Representations of the Radial Component of Position Using a 150-Minute Grid Spacing

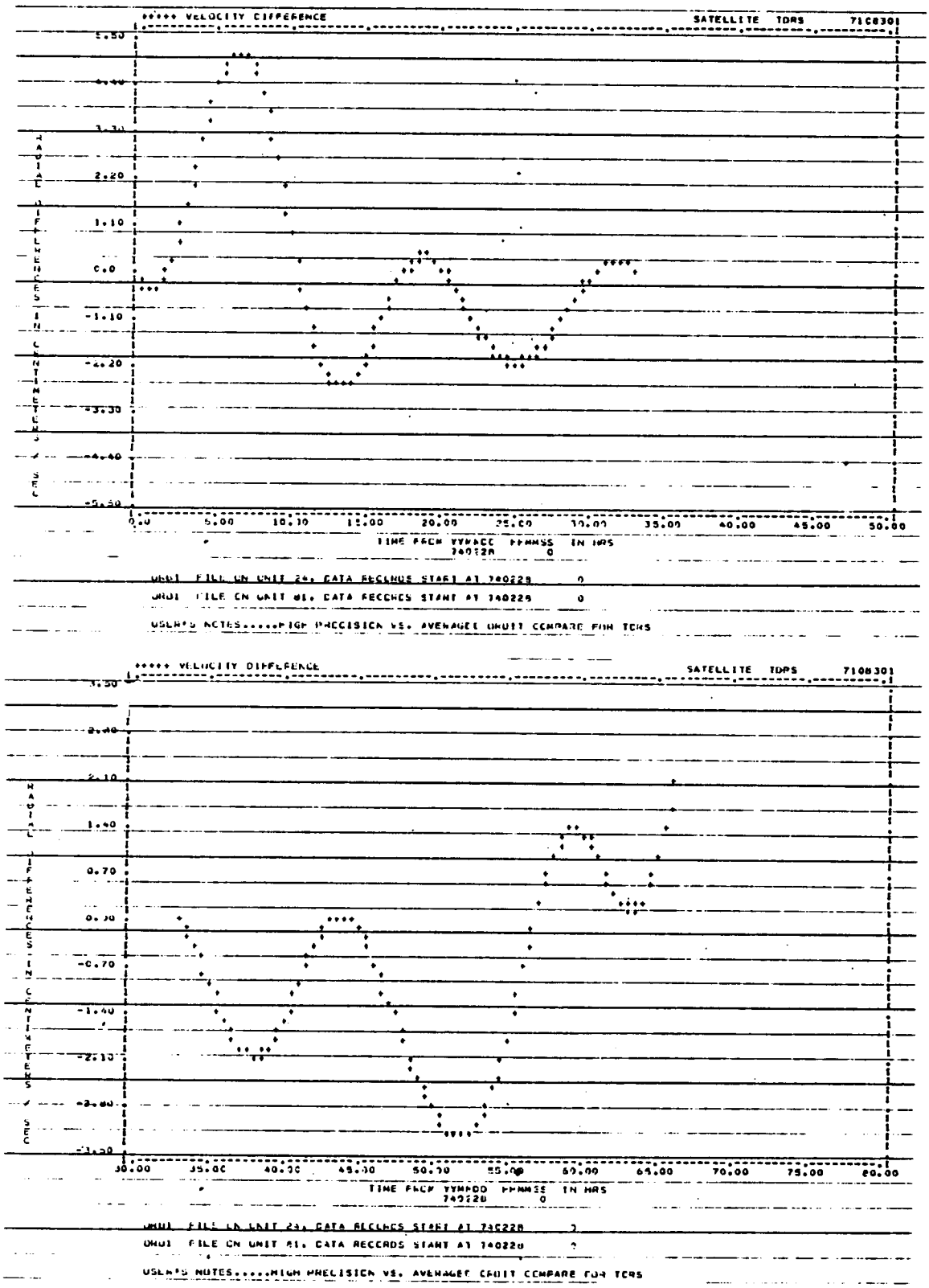

Figure 3-14. Difference Between the High-Precision and Cartesian/Fourier Representations of the Radial Component of Velocity Using a 150-Minute Grid Spacing

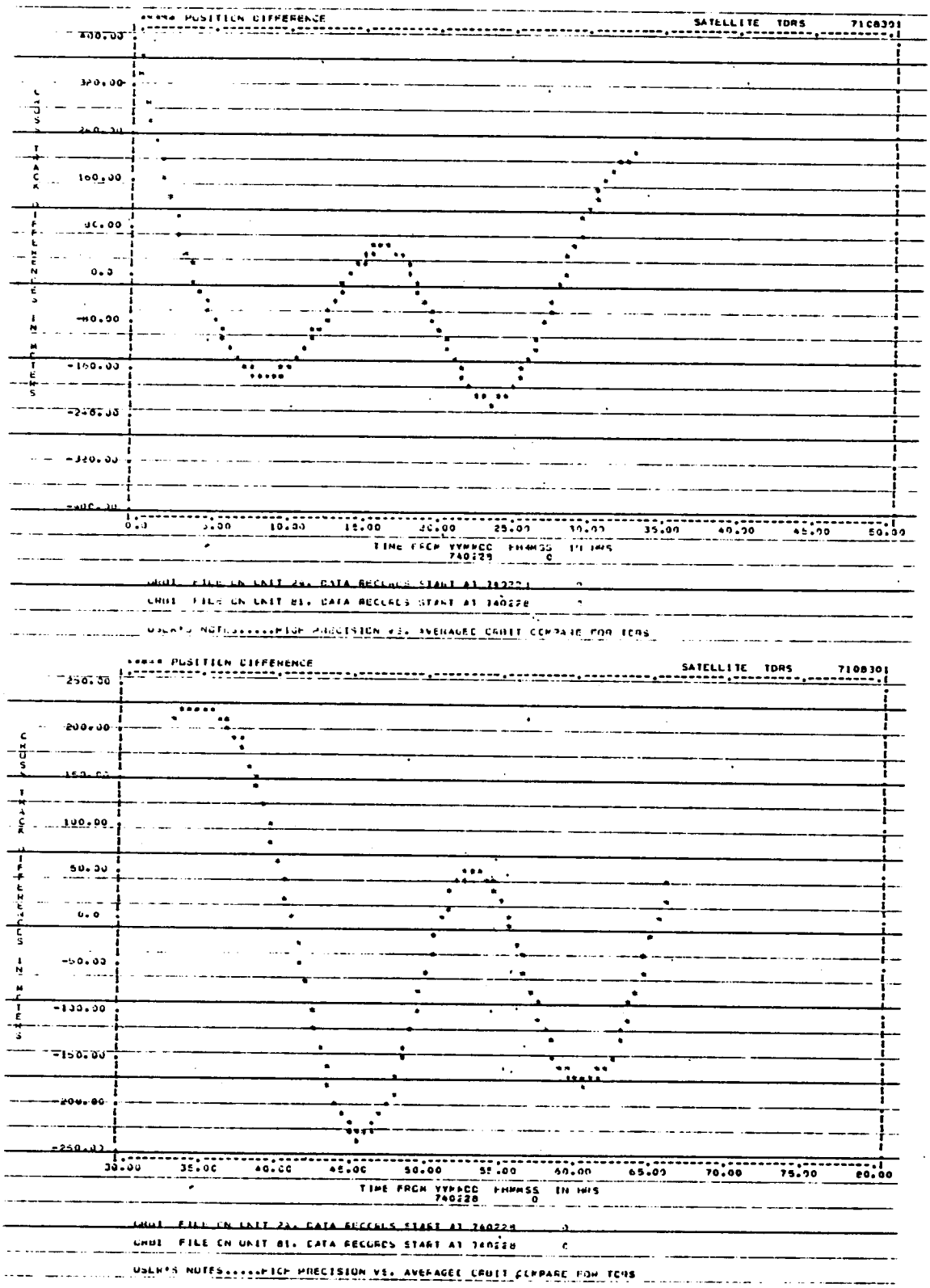

Figure 3-15. Difference Between the High-Precision and Cartesian/Fourier Representations of the Cross-Track Component of Position Using a 150-Minute Grid Spacing

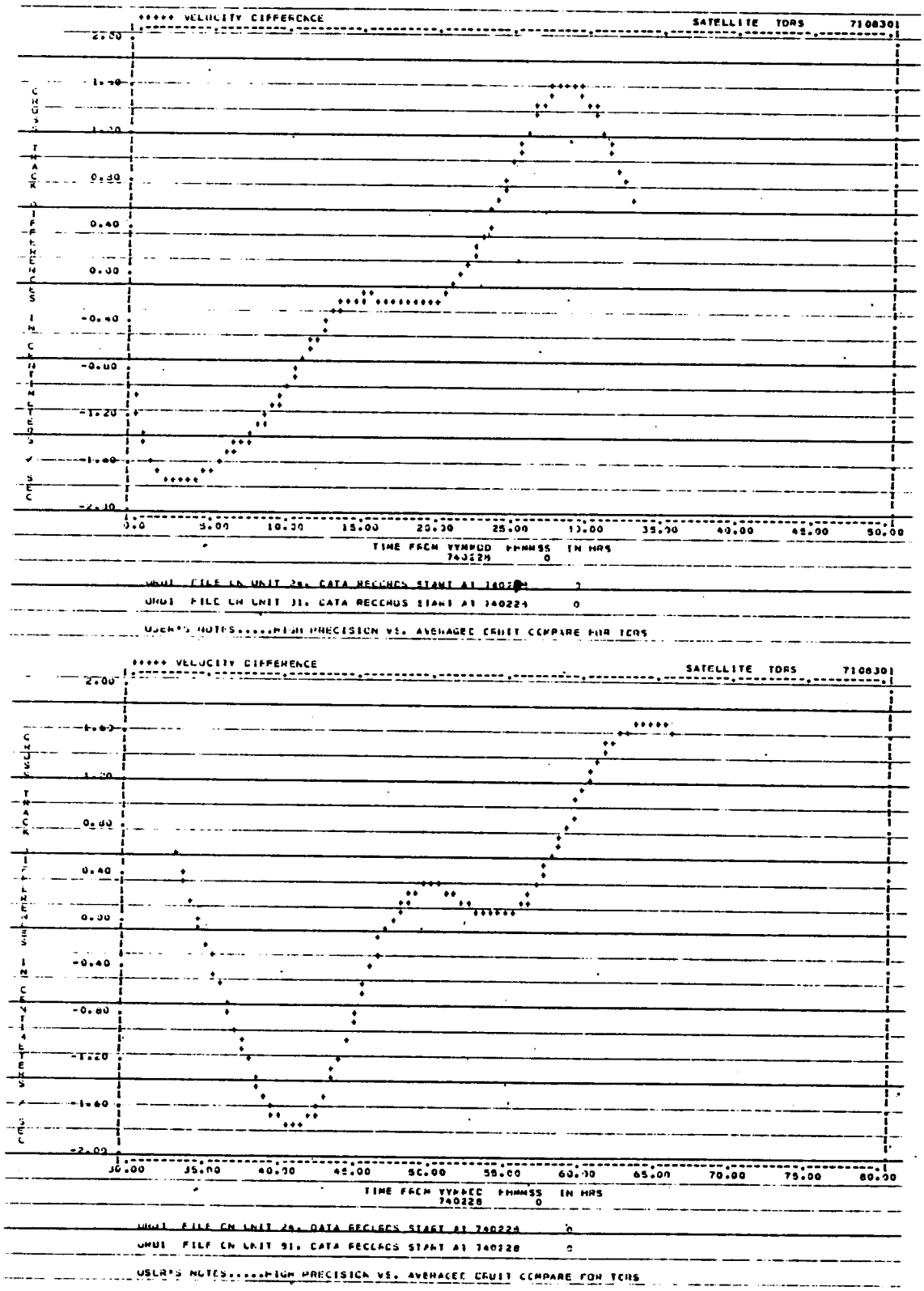

Figure 3-16. Difference Between the High-Precision and Cartesian/Fourier Representations of the Cross-Track Component of Velocity Using a 150-Minute Grid Spacing

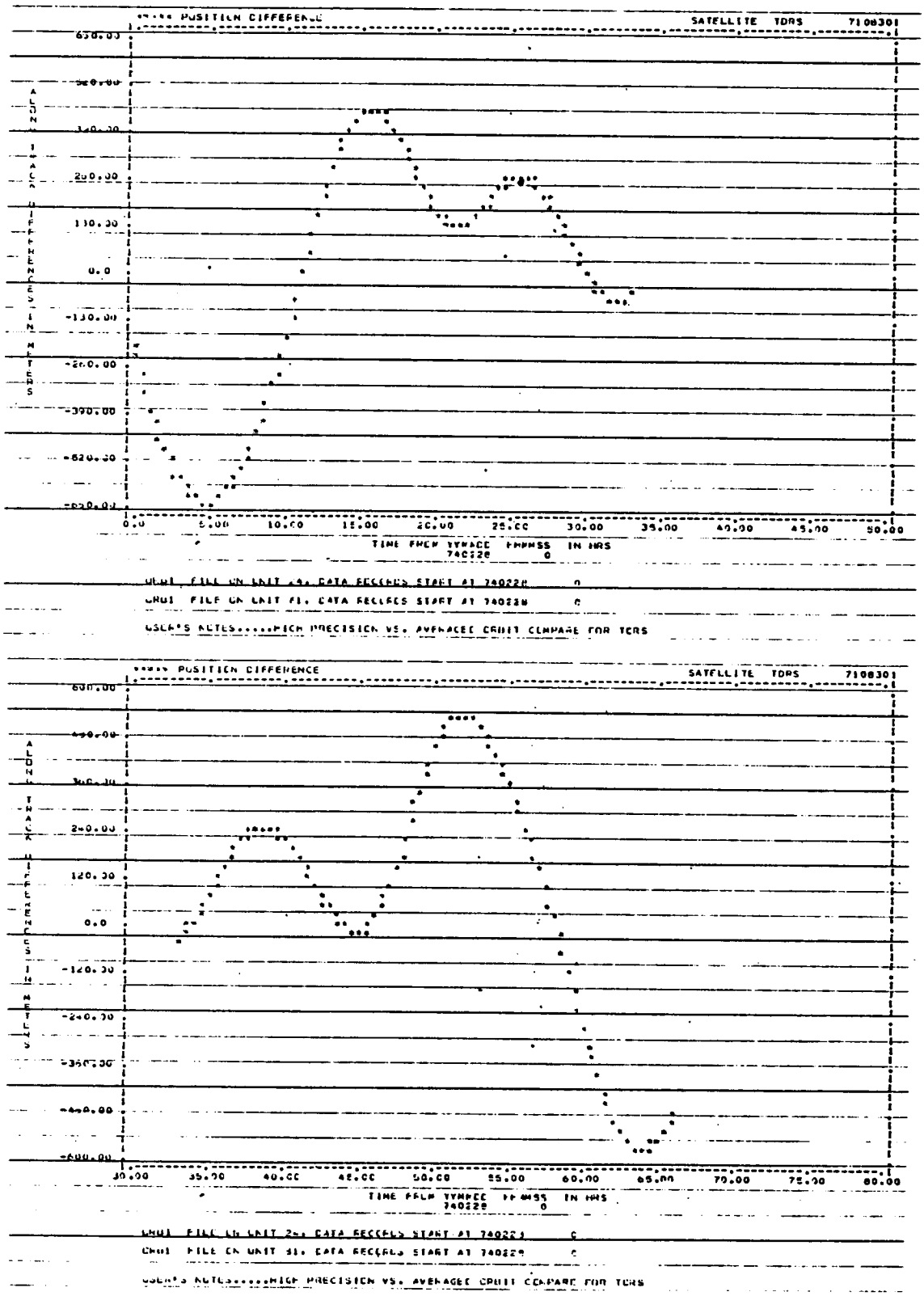

Figure 3-17. Difference Between the High-Precision and Cartesian/Fourier Representations of the Along-Track Component of Position Using a 150-Minute Grid Spacing

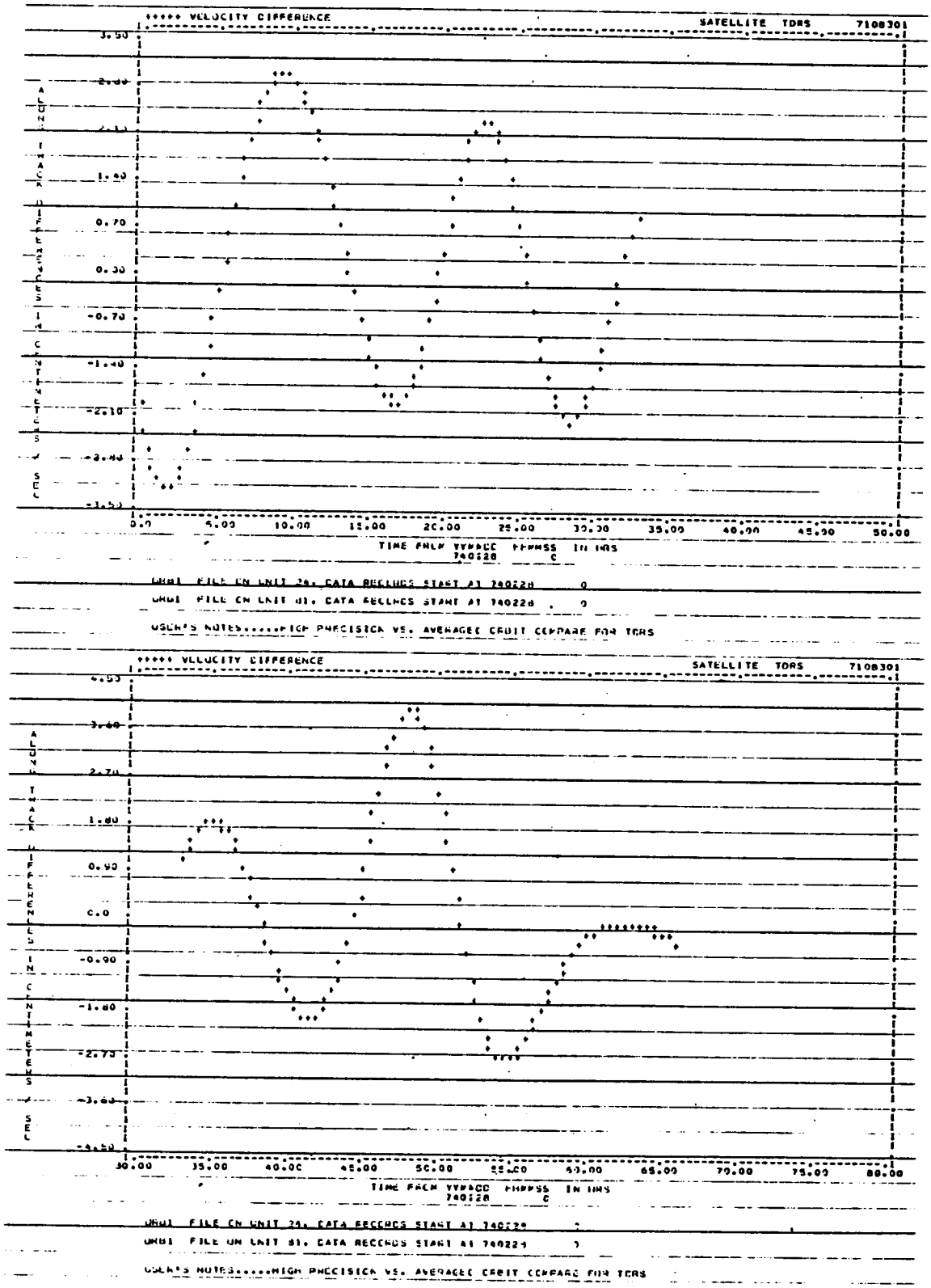

Figure 3-18. Difference Between the High-Precision and Cartesian/Fourier Representations of the Along-Track Component of Velocity Using a 150-Minute Grid Spacing

SECTION 4 - CONCLUSIONS

A summary of the results and conclusions is presented in this section.

4.1 SUMMARY OF REPRESENTATION ACCURACY RESULTS

Evaluation of the accuracy of several ephemeris representations for the Tracking and Data Relay Satellite System (TDRSS) was performed. Specifically, trigonometric series representations of the Cartesian state variables and mean element representations with Hermite and Lagrange interpolators were used. The following results were derived from this evaluation:

- Direct evaluation of a trigonometric series representation of the trajectory is accurate to better than 1 kilometer. Crucial to the success of this method is the choice of the number of coefficients in the original series. Seven coefficients appear to be optimal. Further, the accuracy of this representation trajectory is equivalent for coefficients computed using 150-, 100-, or 50-minute data.

- Use of a Hermite or Lagrange interpolation on mean elements is capable of achieving a 2-kilometer representation accuracy.

4.2 COMPARISON OF OBC TIME AND CORE REQUIREMENTS

The trigonometric series and mean element representations are compared in terms of onboard computer (OBC) computational cost and the length of the uplink data set. The following analysis is based on preliminary studies performed by Charles Shenitz of Computer Sciences Corporation (Reference 3). The cost of evaluating the trigonometric series is dependent on the number of terms in the series. It is found that if 36 coefficients are used, the evaluation of the series takes approximately 100 milliseconds. If 29 terms are used to evaluate a grid point, 85 milliseconds are needed for the procedure. Similarly, 22 terms require 70 milliseconds, 15 terms require 50 milliseconds, and an 8-term series requires 30 milliseconds. If an interpolator is used with the trigonometric

series, the series is evaluated once per grid interval. An additional 40 milliseconds is needed at each grid-point evaluation for computing new interpolation coefficients. Each interpolation call requires 20 milliseconds when interpolation coefficients are available.

Estimates of the uplink data set length and OBC timing requirements for the mean element and Cartesian representations are summarized in Table 4-1. Since the same set of interpolation coefficients holds over the entire 3-day arc in the case of the mean element representations, the interpolation coefficients could be uplinked rather than the element and element rates, thus saving their computation in the OBC.

From this comparison alone, it would appear that the mean element representation is more efficient both in terms of uplink data set length and interpolation cost. However, since position and velocity are required on board, the cost of conversion must be added to the mean element interpolation costs. This cost is not available for the SMM OBC; however, it is probably more expensive than the interpolation cost. Thus, the direct evaluation of the trigonometric series representation of Cartesian state variables appears to be an excellent choice, combining simplicity of algorithm with a reasonable, predictable timing cost.

Table 4-1. Comparison of Uplink Data Set Length and Onboard Computer (OBC) Timing Requirements

Representation	Interpolator	Interpolation Interval	RMS Accuracy Over 1 Day (km)	Uplink Data Set	Uplink Data Set Length†	Time/ Grid Point (msec)	Time/ Coefficient Evaluation (msec)	Time/ Interpolation (msec)	Average Cost at 1-Min. Rate (msec)	Maximum Cost/ Computation (msec)
Mean elements	2-point Hermite	3 days	1.5	Elements + rates	24	-	30*	15*	15*	45*
Mean elements	2-point Hermite	3 days	1.5	Coefficients	24	-	-	15*	15*	15*
Mean elements	3-point Hermite	2 days	1.5	Elements + rates	36	-	40	20	20	60
Mean elements	3-point Hermite	2 days	1.5	Coefficients	36	-	-	20	20	20
Mean elements	5-point Lagrange	1 day	1.5	Elements	30	-	40*	20*	20*	60*
Mean elements	5-point Lagrange	1 day	1.5	Coefficients	30	-	-	20*	20*	20*
Cartesian/ Fourier	3-point Hermite	100 minutes	0.5*	7 coefficients	42	30	40	20	21	90
Cartesian/ Fourier	None	-	0.5	7 coefficients	42	30	-	-	30	30

† Double-precision onboard computer (OBC) words

* Estimated

REFERENCES

1. Computer Sciences Corporation, CSC/TM-76/6074, Evaluation of Ephemeris Representations for the Multimission Modular Spacecraft, P. S. Desai and A. C. Long, August 1976

2. ---, CSC/SD-77/6078, Systems Description of the Orbit Representation Program, C. Shenitz, July 1977

3. C. Shenitz, Computer Sciences Corporation, private communication